`

BIOCHEMICAL CHARACTERIZATION OF NIEMANN-PICK C:
A DISEASE OF CHOLESTEROL TRANSPORT

APPROVED BY SUPERVISORY COMMITTEE

Michael S. Brown, M.D. (Supervisor) _____

Joseph L. Goldstein, M.D. (Supervisor) _____

Zhijian Chen, Ph.D. (Chair) _____

Xiaodong Wang, M.D., Ph.D. _____

George DeMartino, Ph.D. _____

Russell DeBose-Boyd, Ph.D. _____

DEDICATION

This is dedicated to my son, Jacob Elwood Infante.

He is an inspiration to my life and work

BIOCHEMICAL CHARACTERIZATION OF NIEMANN-PICK C: A DISEASE OF CHOLESTEROL TRANSPORT

by

RODNEY ELWOOD INFANTE

DISSERTATION

Presented to the Faculty of the Graduate School of Biomedical Sciences

The University of Texas Southwestern Medical Center at Dallas

In Partial Fulfillment of the Requirements

For the Degree of

DOCTOR OF PHILOSOPHY

The University of Texas Southwestern Medical Center at Dallas

Dallas, Texas

July, 2008

BIOCHEMICAL CHARACTERIZATION OF NIEMANN-PICK C:
A DISEASE OF CHOLESTEROL TRANSPORT

Publication No. _____

Rodney Elwood Infante, Ph.D.

The University of Texas Southwestern Medical Center at Dallas, 2008

Supervising Professors: Michael S. Brown, M.D. and Joseph L. Goldstein, M.D.

Despite intense scientific interest, the mechanism by which cholesterol is transported between membrane compartments in animal cells remains obscure. One transport pathway begins in lysosomes where cholesterol is liberated from plasma lipoproteins that have entered the cell through receptor-mediated endocytosis. This cholesterol is transported from the lysosome to other cellular membranes to perform structural and regulatory roles. A clue to the mechanism of this cholesterol movement comes from observations in cells from patients with Niemann-Pick Type C (NPC) disease. These individuals accumulate large amounts of cholesterol throughout the body caused by mutations in either one of two genes encoding the

lysosomal proteins NPC1 and NPC2. Unlike the membrane protein NPC1, evidence suggests that the soluble protein NPC2 is a cholesterol binding protein.

In the course of isolating a cholesterol-homeostasis membrane protein that binds sterols, we encountered NPC1. Using rabbit membranes, an integral membrane protein that bound sterols was isolated with a 14,000-fold purification while maintaining 8% final yield. Mass spectrometry identified the protein to be NPC1. Recombinant human NPC1 was expressed, purified, and confirmed to be a high affinity sterol receptor. NPC1's sterol binding domain was localized to it's N-terminal luminal soluble domain, which can be prepared as a soluble protein of 240 amino acids, NPC1(NTD), that is secreted by cells. The binding properties of NPC1(NTD) binds cholesterol similar to NPC2 with a K_d of ~130nM. Cross-competition studies between purified NPC1(NTD) and the soluble NPC2 protein revealed differences in sterol specificity depicting the different parts of the cholesterol moiety the NPC proteins bind.

Finally, an *in vitro* assay was established to measure transfer of [^{3}H]cholesterol between the two NPC proteins and phosphatidylcholine liposomes. NPC1(NTD) donates or accepts cholesterol from liposomes very slowly, whereas NPC2 acts quickly. NPC2 stimulates the bidirectional transfer of cholesterol between NPC1(NTD) and liposomes. A naturally-occurring human mutant of NPC2 (Pro120Ser) failed to facilitate the movement of cholesterol from NPC1(NTD) to lipid bilayers. These studies directly link both proteins to the cholesterol egress process from lysosomes, explaining how mutations in either protein produce similar clinical phenotypes.

ACKNOWLEDGEMENTS

This section provides me the opportunity to acknowledge all of the faculty, students, technicians, and family that made my work possible.

Before entering the graduate school I believed I comprehended Sir Isaac Newton's famous saying, "If I have seen further it is by standing on the shoulder of giants." Having the opportunity to research under the guidance of Drs. Michael Brown and Joseph Goldstein completely clarified my understanding of Newton's vision. The intellectual support and encouragement provided by my mentors laid the very foundation of my research. I am forever grateful and will always use them as the model that all physician scientists should strive towards.

The members of my thesis committee have always been helpful when needed. Fortunately, all members are exemplary scientist in their respective fields providing critical insight into my project. Therefore, I would like to acknowledge Zhijian Chen, Xiaodong Wang, Russell Debose-Boyd, and George DeMartino.

Furthermore, the help of students and postdoctoral fellows were critical for the progression of my project. Specifically, Dr. Arun Radhakrishnan, Michael Wang, and Lina Abi-Mosleh were essential for any success attributed to this research. As well, the technical staff of the Department of Molecular Genetics served to be another crucial force in my project. Lisa Beatty, Dorothy Goddard, Shomanike Head, Richard Gibson, and Debbie Morgan provided impeccable technical support.

Lastly, my family has always provided me the platform to pursue my medical career. My parents instilled the importance of education and sought every opportunity for my career goals. My wife, Marissa Infante, sacrifices everyday so I can work that much more in the laboratory. This selfless attitude towards my career has been and will remain instrumental for past and future accomplishments. As mentioned above, this work is dedicated to my son Jacob Elwood Infante. My dream is that he too will pursue a career that is driven by altruism rather than profit.

TABLE OF CONTENTS

PRIOR PUBLICATIONS

Infante RE, Wang ML, Radhakrishnan A, Kwon HJ, Brown MS, Goldstein JL. (2008). NPC2 facilitates bidirectional transfer of cholesterol between NPC1 and lipid bilayers, a step in cholesterol egress from lysosomes. *Proc Natl Acad Sci* USA. In Press.

Infante RE, Radhakrishnan A, Abi-Mosleh L, Kinch LN, Wang ML, Grishin NV, Goldstein JL, Brown MS. (2008). Purified NPC1 Protein II. LOCALIZATION OF STEROL BINDING TO A 240-AMINO ACID SOLUBLE LUMINAL LOOP. *J Biol Chem*. **283(2),** 1064-1075.

Infante RE,, Abi-Mosleh L, Radhakrishnan A, Dale JD, Brown MS, Goldstein JL. (2008). Purified NPC1 Protein I.BINDING OF CHOLESTEROL AND OXYSTEROLS TO A 1278-AMINO ACID MEMBRANE PROTEIN. *J Biol Chem.* **283(2),** 1052-1063.

LIST OF FIGURES AND TABLES

INTRODUCTION

CHAPTER 1

CHAPTER 2

CHAPTER 3

CONCLUSION AND PERSPECTIVE

LIST OF ABBREVIATIONS

ACAT, acyl-CoA:cholesterol acyl-transferase

ALLN, N-acetyl-Leu-Leu-norleucinal

BSA, bovine serum albumin

CHAPS, 3-[(3-cholamidopropyl)dimethylammonio]-1-propane-sulfonic acid

CHO, Chinese hamster ovary

CMC, critical micellar concentration

CMV, cytomegalovirus

DDM, n-dodecyl-β-D-maltopyranoside

DHPC, 1,2-diheptanoyl-sn-glycero-3-phosphocholine

DMEM, Dulbecco's modified Eagle's medium

DTT, dithiothreitol

EndoH, endogylcosidase H

ER, endoplasmic reticulum

FCS, fetal calf serum

HMG CoA, 3-hydroxy-3-methylglutaryl coenzyme A

HSV, herpes simplex virus

PBS, phosphate-buffered saline

LDL, low density lipoprotein

LPDS, lipoprotein-deficient serum

MES, 4-morpholineethanesulfonic acid

MOBP, membrane-bound oxysterol binding protein

Ni-NTA, nickel-nitrilotriacetic acid

NP-40, nonidet P-40

NPC, Niemann-Pick Type C

NPC1, Niemann-Pick Type C1 disease protein

NPC1(NTD), N-terminal soluble domain of NPC1 protein (amino acids 25-264)

NPC2, Niemann-Pick Type C2 disease protein

NTD, N-terminal domain

OSBP, oxysterol-binding protein

PC, Egg Yolk L-α-phosphatidylcholine

SCAP, SREBP cleavage-activating protein

SREBP, sterol regulatory element-binding protein

hTERT, catalytic subunit of human telomerase

Texas Red dye, Texas Red 1,2,-dihexadecanoyl-sn-glycero-3-phosphoethanolamine

β-VLDL, β-migrating very low density lipoprotein

25-HC, 25-hydroxycholesterol

INTRODUCTION

NIEMANN-PICK C DISEASE

Through studies of humans with inborn errors of metabolism, scientists have uncovered many aspects of lipid biochemistry (6,27,37). One disorder that remains puzzling is the complex disease known as Niemann-Pick Type C (NPC), which is caused by loss-of-function mutations in one of two different genes, *NPC1* and *NPC2* (53). The clinical spectrum in patients with this lipid storage disorder is wide. Most subjects manifest in childhood with a devastating syndrome that includes enlargement of liver and spleen, lung disease, and neurological degeneration manifested by ataxia, dysarthria, gaze palsies, and progressive dementia, usually resulting in death before age 20 (63). The liver and spleen accumulate unesterified cholesterol, sphingomyelin, and a variety of phospholipids and glycosphingolipids. Brain tissue does not contain a gross excess of cholesterol or sphingomyelin, but there is a distinct elevation of glycosphingolipids (63). Recent studies of a mouse model of NPC1 disease indicate that neurons may accumulate excess cholesterol, but this accumulation is masked at a gross level by a decline in the amount of cholesterol in myelin (68).

Despite the wide variety of lipid abnormalities in organs of these patients, the functional abnormality in cultured fibroblasts is surprisingly simple (51). These cells exhibit a striking defect in the disposal of cholesterol that has entered the cell through receptor-mediated endocytosis initiated by binding to low density lipoprotein (LDL) receptors. After uptake in coated vesicles, ingested low density lipoprotein (LDL) particles are delivered to

lysosomes where the cholesteryl esters, which constitute the bulk of its cholesterol, are hydrolyzed. The unesterified cholesterol exits the lysosome and is transported to other organelles, including the endoplasmic reticulum (ER), where the cholesterol exerts two regulatory actions that maintain cholesterol homeostasis: 1) it blocks the ER exit and subsequent proteolytic activation of sterol regulatory element-binding proteins (SREBPs), which are transcription factors that increase cholesterol synthesis (29), and 2) it activates acyl CoA: cholesterol acyltransferase (ACAT), an enzyme that re-esterifies cholesterol for storage as cytoplasmic cholesteryl ester droplets (7,13). In fibroblasts from NPC patients, LDL enters cells normally, and the cholesteryl esters are hydrolyzed in lysosomes, but the liberated cholesterol remains trapped as free cholesterol in lysosomes. As a result of this exit block, LDL-derived cholesterol fails to inhibit SREBP processing (32), and it fails to activate ACAT (51,41). A similar defect occurs in fibroblasts from BALB/*c* npc^{nih} mice, a line of mice with an NPC phenotype (43), and in CT60 cells, a line of cultured Chinese hamster ovary (CHO) cells that were mutagenized and selected to have a defect in cholesterol release from lysosomes (10).

A major advance in understanding of NPC disease occurred when the first defective gene was identified by positional cloning (11). This gene encodes a 1278-amino acid integral membrane protein, now known as NPC1, that resides in late endosomes and lysosomes of cultured cells. Mutations in the murine version of NPC1 are responsible for the defect in BALB/*c* npc^{nih} mice, and the hamster version is defective in CT60 cells.

Evidence indicates that NPC1 is a polytopic membrane protein with 13 membrane-spanning helices (19). As depicted in Figure 1, the protein has a cleaved NH_2-terminal signal

sequence that targets the protein for insertion into membranes, three large luminal domains, and a cytoplasmic COOH-terminal segment that includes a dileucine sequence that targets the protein to lysosomes (65). Helices 3-7 of mature NPC1 bear sequence homology to a sterol-sensing sequence that was found initially in Scap, a sterol-sensing polytopic membrane protein of the ER (47). Scap transports SREBPs from the ER to the Golgi, a process that is required for the subsequent activation of the SREBPs (30). Similar sequences are found in the ER enzyme 3-hydroxy-3-methylglutaryl coenzyme A reductase, the rate-controlling enzyme in cholesterol synthesis (31), and in Patched, a receptor for Hedgehog, a protein morphogen that bears a covalently attached cholesterol moiety (45,47). In Scap, this sequence has been shown to bind cholesterol (54,55), and it has been called the sterol-sensing domain (47). Whether this sequence binds cholesterol in NPC1, HMG CoA reductase, or Patched has not yet been determined.

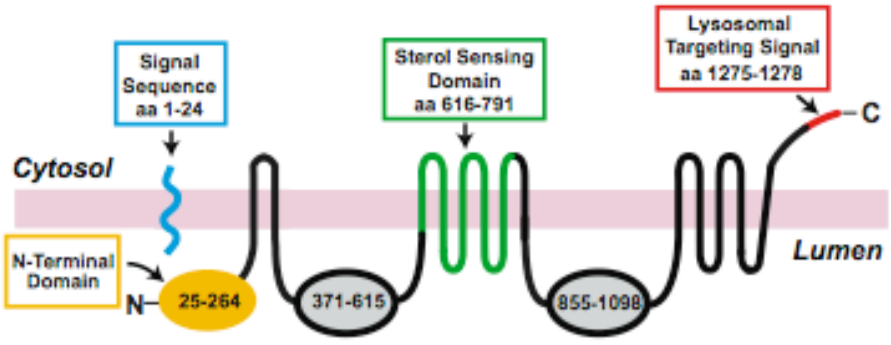

Figure 1: Predicted topology of full-length NPC1. The domain structure of NPC1 is discussed in the Introduction. Adapted from Davies, J. P. and Ioannou, Y. A. (2000).

Approximately 5-10% of patients with NPC disease have a mutation in NPC2, a soluble protein (containing 132 amino acids) that is partially sequestered in lysosomes, and partially secreted by cells (46). Cultured cells from subjects with NPC2 deficiency have the same defect in release of lysosomal cholesterol as do cells with an NPC1 mutation (24). NPC2 has been demonstrated to bind cholesterol (16,23,36,49), and a crystal structure of NPC2 with bound cholesterol sulfate has been solved (70). The similarity in phenotypes between NPC1 and NPC2 mutations strongly suggests that the two proteins function sequentially in a pathway that releases cholesterol from lysosomes, but the order of their actions has not been determined (59).

In the only previous study of cholesterol binding to NPC1, Ohgami, *et al*. (48) used a photoactivated analog of cholesterol (7,7-azocholestanol). They added a radiolabeled version of this compound to intact cells and observed crosslinking to NPC1. There was a marked reduction in crosslinking when the cells expressed a loss-of-function mutant of NPC1 with a substitution in the sterol-sensing domain. Whether this crosslinking was caused by direct binding to the sterol-sensing domain, or whether this domain played a permissive role, could not be determined from these studies. The sterol specificity of the crosslinking in terms of whether or not the cholesterol interaction was competed by oxygenated metabolites of cholesterol, oxysterols, was also not determined.

Lipoprotein-derived Cholesterol Transport and the Putative Role of NPC Proteins

Although much has been learned about the regulation of cellular cholesterol metabolism, a major question remains: How does lipoprotein-derived cholesterol transfer

from its entry point in endosomes/lysosomes to the endoplasmic reticulum (ER) where it performs regulatory functions or to the plasma membrane where it plays a crucial structural role? Despite intense scientific interest, the mechanism by which cholesterol is transported from one membrane compartment to another in animal cells remains obscure. A major source of cellular cholesterol comes from plasma LDL, which enter cells by receptor-mediated endocytosis after binding to cell surface LDL receptors (7). After internalization in coated pits and vesicles, LDL particles are delivered to endosomes and lysosomes. On average, each LDL particle contains 1500 molecules of cholesteryl esters. The esters are hydrolyzed in lysosomes by lysosomal acid lipase (26), and the resulting free cholesterol somehow leaves the lysosome and arrives at the ER, plasma membrane, and other membranes. This cholesterol that is transported from the lysosome to the endoplasmic reticulum (ER) performs vital regulatory functions by inhibiting the proteolytic processing of SREBPs, and where the excess cholesterol is stored by conversion to cholesteryl esters through the action of the ER enzyme ACAT.

A major clue to the mechanism of cholesterol exit from lysosomes was supplied by discoveries in cells from patients with autosomal recessive NPC disease (53). In affected individuals, unesterified cholesterol, sphingomyelin, and other lipids accumulate in endosomes and lysosomes of many organs, including the brain.

As mentioned above, the defect in NPC disease has been traced to mutations in either one of two genes, both of whose products are required for cholesterol export from lysosomes. One gene, *NPC1*, encodes a polytopic membrane protein that is located on membranes of late endosomes and lysosomes (11). The second gene, *NPC2*, encodes a soluble protein that is

concentrated in lysosomes and is also excreted in seminal fluid and milk (46). Homozygous loss-of-function mutations in either gene produce the same NPC phenotype, suggesting that both genes function in the same pathway for lysosomal cholesterol export (51). However, direct interaction of NPC1 and NPC2 has never been shown.

NPC1 has never been purified from native membranes, and recombinant forms of the protein have never been studied *in vitro*. Unlike NPC2, the ability of NPC1 to directly bind cholesterol and other sterols with high affinity remains elusive. It would seem highly probable that NPC1, like NPC2, would need to bind directly to cholesterol during the process of transporting this molecule out of the lysosome. Furthermore, the mechanism by which NPC1 and NPC2 facilitate lipoprotein-derived cholesterol transport out of the lysosome into membranes still remains a mystery.

CHAPTER ONE

BINDING OF STEROLS TO THE MEMBRANE PROTEIN NIEMANN-PICK C1

SUMMARY

The Niemann-Pick C1 protein (NPC1) is required for the transport of lipoprotein-derived cholesterol from lysosomes to endoplasmic reticulum (ER). The 1278-amino acid, polytopic membrane protein has not been purified, and its mechanism of action is unknown. Unexpectedly, we encountered NPC1 in a search for a membrane protein that binds 25-hydroxycholesterol (25-HC) and other oxysterols. A 25-HC binding protein was purified more than 14,000-fold from rabbit liver membranes and identified as NPC1 by mass spectroscopy. We prepared recombinant human NPC1 and confirmed its ability to bind oxysterols, including those with a hydroxyl group on the 24, 25, or 27 positions. Hydroxyl groups on the 7, 19, or 20 positions failed to confer binding. Recombinant human NPC1 also bound [^{3}H]cholesterol in a reaction inhibited by Nonidet P-40 above its critical micellar concentration. Low concentrations of unlabeled 25-HC abolished binding of [^{3}H]cholesterol, but the converse was not true, i.e., unlabeled cholesterol, even at high concentrations, did not abolish binding of [^{3}H]25-HC. NPC1 is not required for the known regulatory actions of oxysterols. Thus, in NPC1-deficient fibroblasts 25-HC blocked the processing of sterol regulatory element-binding proteins and activated acyl-CoA: cholesterol acyltransferase in a

normal fashion. The availability of assays to measure NPC1 binding *in vitro* may further the understanding of ways in which sterols regulate intracellular lipid transport.

INTRODUCTION

.

This chapter describes the purification of a membrane-bound protein that binds 25-hydroxycholesterol (25-HC). 25-HC belongs to a class of sterols called oxysterols because they contain, in addition to the hydroxyl group on the 3-position, another hydroxyl group, usually on the iso-octyl side chain. We were searching for such a protein because 25-HC and related oxysterols mimic the regulatory actions of cholesterol in the ER of animal cells. Thus, 25-HC blocks the ER-to-Golgi transport of sterol regulatory element-binding proteins (SREBPs), which are transcriptional activators for synthesis of cholesterol and other lipids (1); it accelerates the degradation of HMA CoA reductase (25); and it activates ACAT (8).

Working with membranes from rabbit liver, we purified a protein that binds 25-HC with high affinity. We designated this protein as "membrane-bound oxysterol-binding protein" (MOBP) to distinguish it from the "soluble oxysterol-binding protein" (OSBP-1), which was purified and its cDNA cloned in our laboratory 20 years ago (20, 21). Peptide sequencing by mass spectroscopy identified MOBP as NPC1. We purified recombinant human NPC1 and confirmed that it binds 25-HC. We also found that the recombinant protein binds cholesterol, but only when the detergent is reduced to submicellar concentrations. We here describe the initial purification of rabbit NPC1 and an analysis of the sterol binding properties of the rabbit and human proteins. This work provides a beginning for the eventual analysis of the mechanism by which NPC1 transports cholesterol from lysosomes to ER

EXPERIMENTAL PROCEDURES

Materials – We obtained [26,27-^{3}H]25-hydroxycholesterol (75-80 Ci/mmol), [1,2,6,7-^{3}H]cholesterol (60 Ci/mmol), [3β-^{3}H]7,7-azocholestan-3β,25-diol (20 Ci/mmol) (photo [^{3}H]25-HC), and [1-^{14}C]oleic acid (54.6 mCi/mmol) from American Radiolabeled Chemicals; Fos-Choline 13 from Anatrace; anti-Flag M2-Agarose affinity beads and 6-methylcholesterol from Sigma; all other sterols from Steraloids; FuGENE 6 and Nonidet P-40 (NP-40) from Roche Applied Sciences; and Hybond C nitrocellulose filters and all chromatography products (unless otherwise mentioned) from GE Healthcare Biosciences. Rabbit β-migrating very low density lipoproteins (β-VLDL) (d < 1.006) (38) and human and newborn calf lipoprotein-deficient serum (LPDS, d > 1.215 g/ml) (31) were prepared by ultracentrifugation as described in the indicated reference. Solutions of compactin and sodium mevalonate were prepared as previously described (9,35). Recombinant hamster His_{10}-Scap(TM1-8) was produced in Sf9 cells and purified as previously described (55).

Buffers – Buffer A contains 50 mM Tris-chloride at pH 7.4, 50 mM KCl, 10% (v/v) glycerol, 5 mM dithiothreitol (DTT), 1 mM sodium EDTA, and protease inhibitor mixture (1 μg/ml pepstatin A, 2 μg/ml aprotinin, 10 μg/ml leupeptin, and 200 μM phenylmethysulfonyl fluoride). Buffer B contains 50 mM Tris-chloride at pH 7.4, 10% (w/v) NP-40, 1 mM EDTA, and 0.1 mM DTT. Buffer C contains 50 mM Tris-chloride at pH 7.4, 1% NP-40, 1 mM EDTA, and 0.1 mM DTT. Buffer D contains 50 mM MES-chloride at pH 5.5, 1% NP-

40, 1 mM EDTA, and 0.1 mM DTT. Buffer E contains 10 mM sodium phosphate at pH 7.4, 1% NP-40, 150 mM KCl, 1 mM EDTA, and 0.1 mM DTT. Buffer F contains 50 mM Tris-chloride at pH 7.4, 1% NP-40, and 150 mM KCl. Buffer G contains 50 mM Tris-chloride at pH 7.4, 1% NP-40, and 100 mM KCl. Buffer H contains 50 mM Tris-chloride at pH 7.4, 0.1% (w/v) Fos-Choline 13, and 100 mM NaCl. Buffer I contains 50 mM Tris-chloride at pH 7.4, 0.004% NP-40, and 150 mM NaC1.

Plasmid Construction – pCMV-NPC1-His_8-Flag encodes wild-type human NPC1 followed sequentially by eight-histidines and a Flag tag under control of the cytomegalovirus (CMV) promoter. This plasmid was constructed from pCMV-NPC1 (Origene Technologies) by site-directed mutagenesis (QuickChange II XL kit, Stratagene). The coding region of pCMV-NPC1-His_8-Flag was sequenced to ensure integrity of the construct.

Solubilization of Sterols in Detergent or Ethanol – For solubilization of sterols in detergent, an ethanol solution containing 4-5 nmol of [^{3}H]25-hydroxycholesterol ([^{3}H]25-HC) at 75-80 Ci/mmol was evaporated to dryness on the sides of a microcentrifuge tube in a SpeedVac concentrator. Detergent-containing buffer G or buffer H (0.5 ml) was then added to the tube, after which it was agitated for 4 h on a vortex mixer and centrifuged at 20,000*g* for 30 min at room temperature. As determined by scintillation counting, the concentration of solubilized [^{3}H]25-HC in the supernatant ranged from 0.4-1.5 μM. Stock solutions of [^{3}H]cholesterol at 60 Ci/mmol were prepared in a similar manner. Saturated solutions of unlabeled sterols in buffer G or buffer H were prepared by evaporating an ethanolic solution of each sterol (50 μg) in a microcentrifuge tube in a SpeedVac concentrator. The dried sterol was solubilized by the same procedure as above. The recovery was estimated by adding

tracer amounts of [^{3}H]25-HC or [^{3}H]cholesterol, which allowed calculation of the concentrations of various sterol solutions. The choice of the labeled tracer sterol was based on structural similarity to the bulk sterol.

Sterols not solubilized in detergent were dissolved in 100% ethanol and delivered to reaction mixtures at a final ethanol concentration of 1-4%. In a given experiment, all reactions received the same amount of ethanol.

Filter Assay for [^{3}H]25-HC Binding – Each reaction, in a final volume of 120 µl of buffer C, contained 50 nM [^{3}H]25-HC (165-180 dpm/fmol) delivered in ethanol and the indicated amount of liver extract, column fraction, or purified protein. After incubation for 2 h at 4°C, the mixture was loaded onto a pretreated glass-fiber filter (G4, Fisher) placed on a vacuum apparatus that contained 1 ml of buffer F. The filter was pretreated by soaking in 0.3% (w/v) polyethyleneimine for at least 1 h. After application of the vacuum, the free [^{3}H]25-HC was removed by washing with 2.5 ml of buffer F. The filter was then dried and immersed in 8 ml of scintillation fluid (3a70B, Research Product International). Bound [^{3}H]25-HC was measured by scintillation counting. Nonspecific binding was determined by incubating a duplicate reaction with 10 µM unlabeled 25-HC delivered in ethanol.

Ni-NTA Agarose Assay for [^{3}H]Sterol Binding – Each reaction was carried out in a final volume of 80-140 µl of buffer G, buffer H, or buffer I containing the indicated amount of purified NPC1-His$_8$-Flag and 10-400 nM [^{3}H]25-HC (165-180 dpm/fmol) or [^{3}H]cholesterol (130 dpm/fmol) delivered in buffer G, buffer H, or ethanol. After incubation for 3 h at 4°C, the mixture was loaded onto a column packed with 0.3 ml of Ni-NTA agarose beads (Qiagen). Each column was washed for ~15 min with 6 ml of buffer G. The protein-

bound ^{3}H-sterol was eluted with 200 mM imidazole in buffer G and quantified by scintillation counting as previously described (55). For competition experiments with unlabeled sterols, the standard assays were carried out in the presence of buffer G, buffer H, or ethanol containing the indicated unlabeled sterol (0-10 μM).

Solubilization of MOBP from Rabbit Liver Membranes – All operations were carried out on ice or at 4°C. Frozen rabbit liver (200-300 grams, Pel-Freez Biologicals) was thawed in 300 ml of cold buffer A supplemented with 25 μg/ml N-acetyl-leucinal-leucinal-norleucinal (ALLN). The thawed tissue was shredded into small pieces in an Oster blender, homogenized with a Polytron homogenizer, and filtered through a triple-layered cheese cloth. The filtrate was again homogenized with a 100-ml Dounce homogenizer and then centrifuged at 100,000*g* for 1 h. The resulting 100,000*g* pellet was washed in three sequential steps, each followed by centrifugation at 100,000*g*. The first and third steps employed 300 ml of buffer A supplemented with 450 mM KCl and protease inhibitors; the second step employed 300 ml of 100 mM Na_2CO_3 (pH 11.3) and protease inhibitors. The final washed membrane pellet was resuspended in 300 ml of buffer C containing the protease inhibitor mixture. Protein concentration was measured using a BCA kit (Pierce), and the final detergent (NP-40) to protein ratio was adjusted to 4.5 (w/w) with buffer B. This mixture was rotated overnight at 4°C and centrifuged at 100,000*g* for 30 min, after which the supernatant was collected.

Purification of MOBP from Detergent-solubilized Rabbit Liver – All operations were carried out at 4°C. The filter binding assay described above was used to follow [^{3}H]25-HC binding activity through each of the seven steps in the purification (Table 1-1). The content of OSBP-1 was followed by immunoblotting. A solubilized extract of rabbit liver

membranes was prepared as described above (*Step 1*). As described in Figure 1-1, the soluble extract was loaded onto a 20-ml Q-Sepharose ion-exchange column (Hi Prep 16/10 Q FF, pH 7.4) (Table 1-1, *Step 2*). Active fractions that were devoid of immunoblot reactivity for OSBP were pooled from multiple runs and frozen at -80°C. Pooled material was thawed and dialyzed against buffer D for 6-12 h and then loaded onto a 20-ml SP-Sepharose ion-exchange column (Hi Prep 16/10 SP FF) pre-equilibrated with buffer D (*Step 3*). The flow-through was collected and loaded onto a 5-ml Q-Sepharose ion exchange column (HiTrap Q HP, pH 5.5) pre-equilibrated with buffer D (*Step 4*). The column was washed with 8 column volumes of buffer D, and bound proteins were eluted with a continuous KCl gradient (0-500 mM) in buffer D. The fractions containing binding activity were dialyzed against buffer E for 6-12 h. The dialyzed material was loaded onto 5 to 10 2-ml RCA Lectin columns (EY Laboratories) pre-equilibrated with buffer E (*Step 5*). Each column was washed with 3 column volumes of buffer E, and proteins were eluted with buffer E plus 250 mM α-Lactose. The eluted fractions containing binding activity were pooled, dialyzed into buffer C, and concentrated by loading onto a 1-ml Mono-Q ion-exchange column pre-equilibrated in buffer C. The column was washed with 8 column volumes of buffer C and eluted with a continuous KCl gradient (0-500 mM). The fractions containing binding activity were loaded onto a 320-ml Sephacryl 300 gel filtration column (HiPrep 26/60 S-300) pre-equilibrated with buffer C containing 100 mM KCl (*Step 6*). The fractions eluting between 112 and 140 ml (containing peak binding activity) were pooled and mixed with an equal volume of buffer C to decrease the salt concentration. The diluted fractions (containing ~50 mM KCl) were concentrated over a 1-ml Mono-Q ion-exchange column. After washing with 8 column volumes of buffer

C, proteins were eluted with a continuous KCl gradient (0-500 mM). The eluted fractions containing 25-HC binding activity were pooled and loaded onto a 2-ml Reactive Blue Dye 72 column (Sigma) that was pre-equilibrated with buffer C (*Step 7*). The column was washed with 4 column volumes of buffer C, and the bound protein was eluted with a step KCl gradient (100, 250, and 500 mM KCl) in buffer C. Binding activity was found primarily in the 250-mM KCl fraction.

Photoaffinity Labeling of MOBP – All experiments were performed in the dark. Each reaction, in a final volume of 3 ml, contained 0.133 mg of purified protein (fraction eluting from Reactive Blue 72 column (Table 1-1) and 500 nM of photo [^{3}H]25-HC in the absence or presence of 10 µM unlabeled 25-HC. After overnight incubation at 4°C, each reaction was subjected to 20 min of UV irradiation (1) and loaded onto a 1-ml Mono-Q ion-exchange column pre-equilibrated with buffer C. After washing with 12 column volumes of buffer C, bound protein was eluted with a salt gradient (0-500 mM KCl). Radioactivity of each fraction was quantified by applying 20-µl aliquots into a scintillation vial filled with 8 ml of scintillation fluid 3a70b. Samples with the highest radioactivity were subjected to 8% SDS-PAGE. Individual gel lanes were cut into 3-mm slices and placed into scintillation vials. Two ml of tissue solubilizer (TS-2, Research Product International) were added to each vial. After incubation overnight at 50°C, each sample received 400 µl of glacial acetic acid, after which it was shaken and then filled with 8 ml of scintillation fluid. The vials were stored in the dark for 6 h before radioactivity was measured.

LC-MS/MS Analysis of Photo [^{3}H]25-HC Labeled Proteins – Protein samples were separated by SDS-PAGE and then subjected to in-gel tryptic digestion followed by HPLC/tandem mass spectrometry analysis as previously described (14).

Purification of Epitope-tagged NPC1 from Transfected CHO Cells – Stock cultures of CHO-K1 cells were grown in monolayer at 37°C in an atmosphere of 8-9% CO_2 and maintained in medium A (1:1 mixture of Ham's F-12 medium and Dulbecco's modified Eagle's medium, 100 units/ml penicillin and 100 μg/ml streptomycin sulfate) containing 5% (v/v) fetal calf serum (FCS). On day 0, CHO-K1 cells were set up for experiments in medium A containing 5% FCS at $6x10^5$ cells/100-mm dish. On day 2, each dish was transfected with 4-5 μg of pCMV-NPC1-His_8-Flag in medium A with 5% FCS, using FuGENE 6 reagent as described (56). After incubation at 37°C for 24 h, the cells were harvested, washed, and resuspended in ice-cold buffer A containing 25 μg/ml ALLN. Cells were homogenized with a 15-ml or 40-ml Dounce homogenizer, and then subjected to 100,000*g* centrifugation for 30 min at 4°C. The membrane pellet was resuspended by Dounce homogenization in buffer C containing the protease inhibitor mixture and 25 μg/ml ALLN (4 dishes of cells per 1 ml of buffer), incubated overnight at 4°C to solubilize membrane proteins, and centrifuged at 100,000*g* for 30 min. The resulting 100,000*g* supernatant (containing detergent-solubilized membranes) was dialyzed against buffer G for 6-12 h at 4°C, after which imidazole was added at a final concentration of 20 mM. This material was then loaded onto a 1-ml His Trap HP nickel column pre-equilibrated with buffer G. The column was washed sequentially with 10 column volumes of buffer G, 10 column volumes of buffer G plus 25 mM imidazole, and 20 column volumes of buffer G plus 50 mM

imidazole. Bound protein was eluted in 1.5-ml fractions with buffer G plus 200 mM imidazole. The eluted fractions containing anti-Flag (NPC1) immunoblot reactivity were then loaded onto a column containing 1-ml Anti-Flag M2-Agarose beads (Sigma), which had been pre-equilibrated with buffer G. The column was washed with either 10 column volumes of buffer G (1% NP-40) or 25 column volumes of buffer H (0.1% Fos-Choline 13). Bound protein was eluted with 0.1 mg/ml of Flag peptide in 9 column volumes of either buffer G or buffer H. Protein concentration of purified NPC1 was estimated by silver staining and densitometric scanning of an 8% SDS-PAGE gel in which known amounts (50 to 400 ng) of bovine serum albumin (Pierce) was used as a reference.

Preparation of Epitope-tagged NPC1 at Low Detergent Concentration - The fractions containing eluted protein (in 1% NP-40) from the His Trap HP nickel column as described in the above section were loaded onto a 1-ml anti-Flag M2-Agarose affinity column and then washed with 6 column volumes of buffer I (in 0.004% NP-40). Bound protein was eluted with 0.1 mg/ml of Flag peptide in 9 column volumes of buffer I.

SREBP-2 Processing in Cultured Cells – Skin fibroblasts from a normal subject and a patient with NPC1 disease (obtained from American Type Culture Collection, ATTC No. GM3123) were immortalized with the catalytic subunit of telomerase (hTERT) by retroviral infection of the cells with the Babepuro-hTERT vector as previously described (50,67). The resulting immortalized cell lines are designated hTERT-Control and hTERT-NPC1. The cells were grown in monolayer at 37°C in 5% CO_2 and maintained in medium B (Dulbecco's modified Eagle's medium containing 100 units/ml penicillin and 100 μg/ml streptomycin sulfate) supplemented with 10% FCS. On day 0, hTERT-Control and hTERT-NPC1

fibroblasts were set up in medium B containing 10% FCS at $6x10^4$ and $7x10^4$ cells/60-mm dish, respectively. On day 2, cells were washed once with phosphate-buffered saline and switched to medium B containing 5% human LPDS. On day 4, cells were switched to medium C (medium B containing 50 μM compactin, 50 μM sodium mevalonate) supplemented with 10% human LPDS and various concentrations of 25-HC or β-VLDL. After incubation for 5 h, cells were treated with 25 μg/ml ALLN for 1 h and then harvested. Six dishes for each condition were pooled for preparation of nuclear extract and membrane fractions, which were analyzed by immunoblotting for SREBP (described below).

Primary fibroblast cultures from a wild type BALB/c mouse and a mutant BALB/c *npc*^{nih} mouse (43) were established from explants of skin taken at 7 to 8 weeks of age (66). Cells were cultured and set up for experiments as described above for the human fibroblasts except that the density for plating was 4 x 10^4 cells/60-mm dish. The wild type and mutant mice were obtained from Drs. Stephen Turley and John Dietschy (UT Southwestern Medical Center, Dallas, TX).

Immunoblot Analysis – Column fractions from liver purification of MOBP and nuclear extract and membrane fractions from cultured cells were subjected to 8% or 12% SDS-PAGE, after which the proteins were transferred to nitrocellulose filters. The immunoblots were performed at room temperature using the following primary antibodies: 1 μg/ml of a rabbit polyclonal antibody against human NPC1 (Novus); 5 μg/ml of a mouse monoclonal anti-Flag (IgG fraction; Sigma); 4 μg/ml of monoclonal IgG-11H9 directed against rabbit OSBP (IgG fraction) (20); 8 μg/ml of a rabbit polyclonal antibody (IgG-R139) directed against hamster Scap (57); and 10 μg/ml of a rabbit polyclonal antibody (IgG-1819)

directed against amino acids 1-100 of human SREBP-2. The latter antibody was raised by injecting rabbits with a His_8-tagged recombinant version of the antigen. Bound antibodies were visualized by chemiluminescence (SuperSignal Substrate; Pierce) using a 1:5000 dilution of anti-mouse IgG (Jackson Immunoresearch Laboratories, Inc.) or a 1:2000 dilution of anti-rabbit IgG conjugated to horseradish peroxidase (Amersham Biosciences). The filters were exposed to Kodak X-Omat Blue XB-1 film at room temperature.

ACAT Assay – The rate of incorporation of [^{14}C]oleate into cholesteryl [^{14}C]oleate and [^{14}C]triglycerides by intact cell monolayers was measured as described previously (28).

RESULTS

Purification and Sterol Binding Characteristics of MOBP from Rabbit Livers – In an attempt to isolate a membrane-bound oxysterol binding protein (MOBP), we carried out a biochemical purification of MOBP from rabbit liver membranes as described in "Experimental Procedures." MOBP activity was followed during each step of the purification by a filter assay for [^{3}H]25-HC binding as described in "Experimental Procedures." The overall scheme and enrichment of MOBP through the various purification steps is shown in Table 2-1. Figure 1-1A shows the result of Q-Sepharose chromatography of detergent-solubilized liver membranes (*Step 2* of the purification scheme in Table 2-1). The [^{3}H]25-HC binding activity separated into two discrete peaks (*filled circles*). As shown by the immunoblot in *Inset*, the second peak (fractions 39-51) co-eluted with OSBP-1, a soluble protein with nanomolar affinity for 25-HC (21). The fractions comprising the first peak (fractions 30-35) do not contain OSBP-1 immunoreactivity and were postulated to contain a novel MOBP, which then became the focus of all subsequent purification steps. Gel filtration studies were consistent with a molecular mass of ~440 kDa for this MOBP•detergent complex (Figure 1-1*B*). Fractions 30-35 from several Q-Sepharose chromatography runs were combined, and the 25-HC binding activity was further purified through 5 additional chromatography steps as described in "Experimental Procedures" and Table 1-1, resulting in an overall enrichment of ~14,000-fold and an 8% recovery of activity relative to the starting solubilized membrane fraction (i.e., *Step 1* in Table 2-1).

Purified MOBP from *Steps 4* and *5* (see *Table 2-1*) was used to define the specificity of sterol binding. We tested 13 sterols (listed in Figure 1-2*B*) with modifications either to the tetracyclic sterol nucleus or the iso-octyl side chain for their ability to compete for binding of 50 nM [^{3}H]25-HC to MOBP. These assays were carried out in micellar concentrations of NP-40 (1%). As shown in Figures 1-2*C* – *1*-2*E*, sterols 1-3 showed complete competition at 10 μM, whereas sterols 4-13 competed only weakly at 10 μM. Thus, under these assay conditions the presence of a hydroxyl group on the iso-octyl side chain is crucial for sterol binding to MOBP.

Identification of MOBP as NPC1 – The final purified MOBP fraction from *Step 7* contained 5-8 proteins that could be visualized on silver-stained SDS-PAGE gels. In order to determine which of these bands accounted for the [^{3}H]25-HC binding activity, we carried out cross-linking studies with photo [^{3}H]25-HC. When photo [^{3}H]25-HC is activated by UV light, the diazirine ring is cleaved, generating a carbene radical that crosslinks covalently to interacting proteins (1). The eluate from *Step 7* was incubated with photo [^{3}H]25-HC in the absence or presence of unlabeled 25-HC, exposed to UV light, and then subjected to Mono-Q chromatography. As shown in Figure 1-3*A*, the eluate showed a distinct peak of radioactivity (*closed circles*), which was diminished by 86% when the incubation was conducted in the presence of unlabeled 25-HC (*open circles*). The peak fraction (number 32) in Figure 1-3*A* was subjected to 8% SDS/PAGE. As shown in the top panel of Figure 1-3*B*, silver staining of the gel revealed 3 distinct and 2 faintly visible protein bands, labeled *Band 1-5*. A duplicate gel lane was cut into 18 equal slices, each of which was assayed for radioactivity (see "Experimental Procedures"). The radioactivity from the crosslinked photo [^{3}H]25-HC

localized almost exclusively to *Band 1* (*filled circles*). Mass spectrometry analysis of *Band 1* yielded sequences of 19 peptides, 17 of which corresponded to NPC1 (Table 1-2). The other 2 peptides corresponded to sialoadhesin. A complete summary of the mass spectrometry results for *Band 1* and *Bands 2-5* can be found in Table 1-2. NPC1 was chosen for further studies because of its abundance and because it contains a putative sterol-sensing domain, which is found in other proteins involved in cholesterol homeostasis, i.e., Scap and HMG CoA reductase (30,45,47).

Purification of Recombinant Human NPC1 and Demonstration of Oxysterol Binding in Presence of 1% NP-40 – To confirm that NPC1 binds oxysterols, we used CHO-K1 cells to express recombinant human NPC1 with a tandem His_8-tag and Flag-tag at the COOH-terminus. The recombinant protein, designated NPC1-His_8-Flag, was solubilized with 1% NP-40 from the 100,000*g* pellet of CHO-K1 membranes. The solubilized NPC1-His_8-Flag was purified to near homogeneity using Ni-chromatography (Figure 1-4*A*), followed by Flag affinity chromatography (Figure 1-4*B*). Oxysterol binding activity was measured by the aforementioned filter assay (*closed circles*), and protein concentration was measured with the BCA method (*open circles*). The [^{3}H]25-HC binding activity co-eluted with NPC1 on both columns as judged by immunoblots in Figure 1-4*A* and 1-4*B*. Silver-stained gels of the final purified product subjected to 8% and 12% SDS/PAGE are shown in Figures 1-4*C* and 1-4*D*, respectively. The major protein (indicated by *asterisks*) migrated near the 250-kDa marker. This protein reacted with anti-Flag antibody (see immunoblots in Figures 1-4*A* and 1-4*B*) and was confirmed to be NPC1 by mass spectrometry. The less intense band above the 250-kDa marker (denoted by arrows in Figure 1-4*C*) also stained with anti-Flag antibody; it most

likely represents an oligomerized form of NPC1 that is resistant to SDS denaturation. The faint band between 37-50 kDa is non-muscle γ-actin as indicated by mass spectrometry (data not shown); it likely represents contamination by this abundant cellular protein.

Binding of 25-HC but not Cholesterol to Recombinant NPC1 in Presence of 1% NP-40 or 0.1% Fos-Choline 13 – We used an assay developed in earlier work on Scap (55) with slight modification to investigate the binding of ^{3}H-labeled sterols to NPC1-His$_8$-Flag. ^{3}H-Sterols were solubilized in NP-40, the same detergent used for the solubilization and purification of NPC1-His$_8$-Flag. Free and NPC1-bound ^{3}H-sterols were separated using a column packed with nickel beads. Figure 1-5*A* shows a saturation curve for binding of [^{3}H]25-HC to NPC1-His$_8$-Flag. The binding was saturable and was diminished in the presence of excess unlabeled 25-HC. Under the conditions of this assay, [^{3}H]cholesterol did not bind to NPC1-His$_8$-Flag in a saturable fashion (Figure 1-5*B*). Consistent with these results, unlabeled 25-HC but not unlabeled cholesterol competed for binding of [^{3}H]25-HC to NPC1 (Figure 1-5*C*).

In previous studies, we showed that [^{3}H]cholesterol binds with high affinity and specificity to solubilized Scap (54,55). Scap resembles NPC1 in that both proteins contain a sterol-sensing domain (45,47). The binding studies with Scap were carried out in Fos-Choline 13 detergent, whereas the studies with NPC1 used NP-40. In order to assess the possibility that [^{3}H]cholesterol is not delivered efficiently to NPC1 in NP-40, we exchanged NPC1-His$_8$-Flag into Fos-Choline 13 detergent. Gel filtration studies showed that NPC1 in Fos-Choline 13 detergent was not aggregated and migrated as a ~350 to 400-kDa species (data not shown). We also dissolved [^{3}H]cholesterol, [^{3}H]25-HC, and their unlabeled

versions in Fos-Choline 13 as described in "Experimental Procedures." Figure 1-5*D* shows that NPC1 solubilized in Fos-Choline 13 bound [^{3}H]25-HC with high affinity, but not [^{3}H]cholesterol. Under the same detergent conditions Scap bound [^{3}H]cholesterol with high affinity, but not [^{3}H]25-HC (Figure 1-5*E*).

Sterol Specificity for Purified Recombinant NPC1 in Presence of 1% NP-40 – We tested the binding specificity of NPC1-His$_8$-Flag by measuring the ability of unlabeled oxysterols and cholesterol to compete for binding of 100 nM [^{3}H]25-HC (Figures 1-6*A* and 1-6*B*). As shown in Figures 1-6*C* and 1-6*D*, sterols with hydroxyl groups at positions 24, 25, or 27 competed with [^{3}H]25-HC for binding to NPC1-His$_8$-Flag. On the other hand, sterols with a hydroxyl group on the 19 or 20 position did not compete for [^{3}H]25-HC binding to NPC1-His$_8$-Flag. We also tested the ability of various sterol precursors in the cholesterol synthesis pathway, analogs of cholesterol, and other sterols to compete for binding of [^{3}H]25-HC, when added at a 50-fold excess concentration. Under the conditions of this *in vitro* assay, none of these precursor sterols, cholesterol analogs, or other sterols competed effectively for binding of [^{3}H]25-HC to NPC1-His$_8$-Flag (Figure 1-6*E*).

Binding of Cholesterol to Recombinant NPC1 in Low Concentrations of Detergent – The failure of NPC1 to bind [^{3}H]cholesterol *in vitro* was surprising since NPC1 functions in cholesterol transport and since photoactivated cholesterol binds to NPC1 when added to living cells (48). We speculated that the failure of binding *in vitro* may have been due to the presence of high concentrations of detergent in the assay. Previous studies of cholesterol binding to Scap showed that high concentrations of detergent slowed the binding reaction, but they did not abolish it (55). To lower the concentration of detergent, we solubilized

doubly-tagged recombinant human NPC1 and purified the protein on nickel agarose in the standard way in the presence of 1% NP-40. We then bound the protein to anti-FLAG beads, washed the beads extensively in a solution containing 0.004% NP-40, and then eluted the protein in 0.004% NP-0. The NPC1 remained in solution at this low detergent concentration. On gel filtration the protein emerged with an apparent molecular mass of ~400 kDa, which was the same as its apparent molecular mass in 1% NP-40 (Figure 1-7*A*).

To measure cholesterol binding in low detergent concentrations, we added various concentrations of [^{3}H]cholesterol in ethanol to the isolated NPC1 in the presence of 0.004% NP-40. Under these conditions recombinant NPC1 bound [^{3}H]cholesterol with saturation kinetics, an apparent K_d of ~100 nM, and a B_{max} of 0.5 fmol of [^{3}H]cholesterol bound per fmol of NPC1 dimer (Figure 1-7*B*, *left panel*). In 0.004% NP-40, the K_d for [^{3}H]25-HC was ~10 nM, and the B_{max} was 0.5 fmol of [^{3}H]25-HC bound per fmol of NPC1 dimer. In the low detergent concentration (0.004%), recombinant NPC1 bound [^{3}H]25-HC with a higher affinity than at a higher detergent concentration (1%) where the K_d was ~80 nM (compare Figure 1-7*B*, *right panel*, with Figure 1-5*A*).

Competition studies indicated that binding of [^{3}H]cholesterol was inhibited by 25-HC and by 27-HC, but not by epicholesterol, which has a 3α-hydroxyl group, or by androstenol, which lacks a side chain (Figure 1-7*C, left panel*). Binding of [^{3}H]25-HC was competed by 25-HC and by 27-HC (Figure 1-7*C, right panel*). Remarkably, binding of [^{3}H]25-HC was not inhibited by cholesterol, even though 25-HC potently inhibited the binding of [^{3}H]cholesterol. Binding of [^{3}H]25-HC was also not inhibited by epicholesterol or androstenol.

To explore the relation between micellar concentrations of NP-40 and [^{3}H]cholesterol binding, we first determined the critical micellar concentration (CMC) for NP-40 at 4°C in the buffer solution used for assays. Using a dye encapsulation assay (22), we estimated the CMC for NP-40 to be ~0.0015% (data not shown). We then measured [^{3}H]cholesterol binding to recombinant NPC1 at detergent concentrations ranging between 0.0007% and 0.01% (Figure 1-8*A*). Binding of [^{3}H]cholesterol remained constant up to 0.002% NP-40 which roughly matches the CMC. Binding declined precipitously as the detergent exceeded the threshold for micelle formation. Figure 1-8*B* shows that the binding of [^{3}H]25-HC was not decreased by NP-40 at concentrations up to 0.1%, which greatly exceeded the CMC.

NPC1 Not Required for Oxysterol-mediated Inhibition of SREBP-2 Processing – Oxysterols such as 25-HC are potent inhibitors of SREBP-2 processing in mammalian cells (1). To test whether NPC1 is required for this processing event, we analyzed the proteolytic processing of SREBP-2 in mutant fibroblasts that lack functional NPC1. The first set of experiments was performed with telomerase-immortalized human fibroblasts from an individual with NPC1 disease (GM3123). Previous studies have shown that NPC1 is required for the export of lipoprotein-derived cholesterol from the lysosome to the ER where the cholesterol activates ACAT, thereby causing an increase in the incorporation of radiolabeled fatty acids into cholesteryl esters (53,41). However, NPC1 is not required for the stimulation of cholesterol esterification by 25-HC (41). To deliver lipoprotein cholesterol to cells, we used cholesterol-rich rabbit β-VLDL, which binds with high affinity to human LDL receptors (62) and reaches lysosomes through receptor-mediated endocytosis. We tested the ability of increasing concentrations of β-VLDL to stimulate the incorporation of

[^{14}C]oleate into cellular cholesteryl [^{14}C]oleate. As shown in Figure 1-9*A* (*left panel*), β-VLDL markedly increased the amount of cholesteryl [^{14}C]oleate formed in control fibroblasts, but not in NPC1 fibroblasts. On the other hand, 25-HC increased cholesteryl [^{14}C]oleate formation in both control and NPC1 cells (*right panel*).

If NPC1 is required for the oxysterol-mediated inhibition of the proteolytic processing of SREBPs, then the telomerase-immortalized NPC1 fibroblasts should show a decreased nuclear accumulation of the cleaved form of SREBP. Figure 1-9*B* shows an immunoblot analysis of SREBP-2 processing in control and mutant fibroblasts. As a positive control for NPC1 function, we added β-VLDL, which inhibited cleavage in control cells (lanes *2-4*), but not in NPC1 cells that fail to transport lipoprotein-derived cholesterol to the ER (lanes *9-11*). In contrast, 25-HC blocked the generation of nuclear SREBP-2 at 0.3-1 μg/ml both in control (lanes *5- 7*) and NPC1 (lanes *12-14*) cells.

To verify the above result in another cell culture system, we carried out similar studies of SREBP-2 processing in fibroblasts from a mouse homozygous for a nonfunctional *NPC1* gene (43). Figure 1-9*C* shows that the mouse NPC1 cells responded similarly to the control cells in terms of inhibition of SREBP-2 processing by 25-HC (lanes *2-4, 9-11*), but not in terms of their response to β-VLDL (lanes *5-7, 12-14*).

TABLE 1-1

Purification of MOBP from rabbit liver

Step	Fraction	Protein[a] (mg)	Specific Activity (pmol/mg)	Total Activity (pmol)	Purification (fold)	Recovery (%)
1	Solubilized Membranes[b]	29,008	0.01	300	----------	100
2	Q-Sepharose (pH 7.4)	1,727	0.19	332	19 (74)[c]	110
3	SP-Sepharose	846	0.35	295	34 (135)	98
4	Q-Sepharose (pH 5.5)	92	1.6	144	150 (601)	48
5	RCA Lectin	9	3.6	31	347 (1388)	10
6	S-300 Gel Filtration	9	3.2	29	309 (1237)	10
7	Reactive Blue 72	0.7	37.4	25	3618 (14471)	8

[^{3}H]25-HC binding activity was assayed under standard conditions in the presence of 50 nM [^{3}H]25-HC. Incubations were carried out for 90 min at 4°C as described under "Experimental Procedures."

[a]Protein concentration of the various fractions was determined as described under "Experimental Procedures."

[b]This starting fraction contains two proteins that bind [^{3}H]25-HC: MOBP (~25% of total binding) and OSBP-1 (~75% of total binding).

[c]Numbers in parenthesis denote the *fold*-purification of MOBP when the contribution of OSBP-1 binding in the starting fraction is subtracted.

TABLE 1-2

Sequence of tryptic peptides of silver-stained bands from purified rabbit liver

Band	Protein Name	GenInfo Identifier	Peptide Sequence	Residue # in NPC1 cDNA Sequence
1	Niemann-Pick type C1 disease protein	6581072	DNLQLPLQFLSR	94-105
			TNVKELQYYIGQR	148-160
			ELQYYIGQR	152-160
			DVEAPSSNDK	171-180
			NNGQAPFTITPIFSDLPVR	206-224
			VTTNPIDLWSAPSSQAR	382-398
			APHTNKHTYQPYPSGADVPFGPPLDK	421-446
			HTYQPYPSGADVPFGPPLDK	427-446
			FLVDSK	657-662
			LQGETLDQQLGR	724-735
			GAEAGTSIQASESYLFR	812-828
			NSYSPLLLK	832-840
			CRPLTPEGK	988-996
			QRPQGEDFMR	997-1006
			FLPMFLSDNPNPK	1007-1019
			AFTVSGK	1182-1188
			AEEALAHMGSSVFSGITLTK	1195-1214
	Siloadhesin	557250	ATANSLQLEVR	-
			DLKPEDSGTYNFR	-
2	Niemann-Pick type C1 disease protein	6581072	LQGETLDQQLGR	724-735
			FLPMFLSDNPNPK	1007-1019
	Prostaglandin F2 receptor, negative regulator	41152506	MYQTQVSDAGLYR	-
			SVLALTHEGR	-
3	Niemann-Pick type C1 disease protein	6581072	LQGETLDQQLGR	724-735
			FLPMFLSDNPNPK	1007-1019
	Prostaglandin F2 receptor, negative regulator	41152506	MYQTQVSDAGLYR	-
			SDLSLER	-
			SVLALTHEGR	-
			SYHLLVR	-
			VQEDEFR	-

TABLE 1-2 (cont'd)

Band	Protein Name	GenInfo Identifier	Peptide Sequence	Residue # in NPC1 cDNA Sequence
4	Predicted:similar to CD166 antigen precursor (Activated leukocyte-cell adhesion molecule) (ALCAM)	74002506	APFLETEQLKK	-
			ESLTLIVEGKPQIK	-
			LDVPQNLMFGK	-
			SVQYDDVPEYK	-
			SVQYDDVPEYKDR	-
			VFKQPSKPEIVSK	-
	CD166 Antigen (Activated leukocyte cell adhesion molecule) (ALCAM)	47605370	ADIQTPFTCSITYYGPSGQK	-
			CSLIDK	-
			CSLIDKK	-
			HVNKDLGNMEENK	-
			LGDCISR	-
			SVQYDDVPEYK	-
			SVQYDDVPEYKDR	-
			VFKQPSKPEIVSK	-
			VLQPLEGAVVIIFK	-
	Niemann-Pick type C1 disease protein	6581072	LQGETLDQQLGR	724-735
			CRPLTPEGK	988-996
			FLPMFLSDNPNPK	1007-1019
	Predicted:similar to Prostaglandin F2 receptor, negative regulator precursor	73981186	FRPGPGYEQR	-
			MYQTQVSDAGLYR	-
	Glycogen Phosphorylase	73983205	DYYFALAHTVR	-
			GLAGVENVTELKK	-
5	γ-Glutamyltranspeptidase 1	121150	DSEEGGLSVAVPGEIR	-
			LFQPSIQLAR	-

FIGURE 1-1: Representative steps in purification of rabbit MOBP.

A, separation of MOBP from OSBP-1 by Q-Sepharose chromatography**.** The 100,000*g* supernatant of NP-40 solubilized membrane proteins from rabbit liver (181 mg) was applied to a 20-ml Q-Sepharose column pre-equilibrated with buffer C. The column was washed with 5 column volumes of buffer C, and bound proteins were eluted with a continuous gradient of 0-500 mM KCl in buffer C. Fractions (5-ml) were collected and assayed for [^{3}H]25-HC binding activity (●) and protein concentration (○) using the filter assay and BCA method, respectively. Fractions 26-54 were also subjected to SDS/PAGE and OSBP-1 immunoblot analysis using monoclonal antibody 11H9 as described under "Experimental Procedures." *B*, estimation of molecular mass of MOBP by gel filtration. Partially purified MOBP (Q-Sepharose fraction, 5 mg protein), which was devoid of detectable OSBP-1 immunoblot reactivity, was loaded onto a 320-ml Sephacryl 300 gel filtration column pre-equilibrated with buffer C containing 100 mM KCl. Fractions (2-ml) were collected and assayed for [^{3}H]25-HC binding activity (●) and protein concentration (○) as described in (*A*). Standard molecular weight markers (thyroglobulin, 670 kDa; γ-globulin, 158; ovalbumin, 44; and myoglobulin, 17) were chromatographed on the same column under identical buffer conditions. The apparent molecular mass of MOBP is ~440 kDa.

FIGURE 1-1

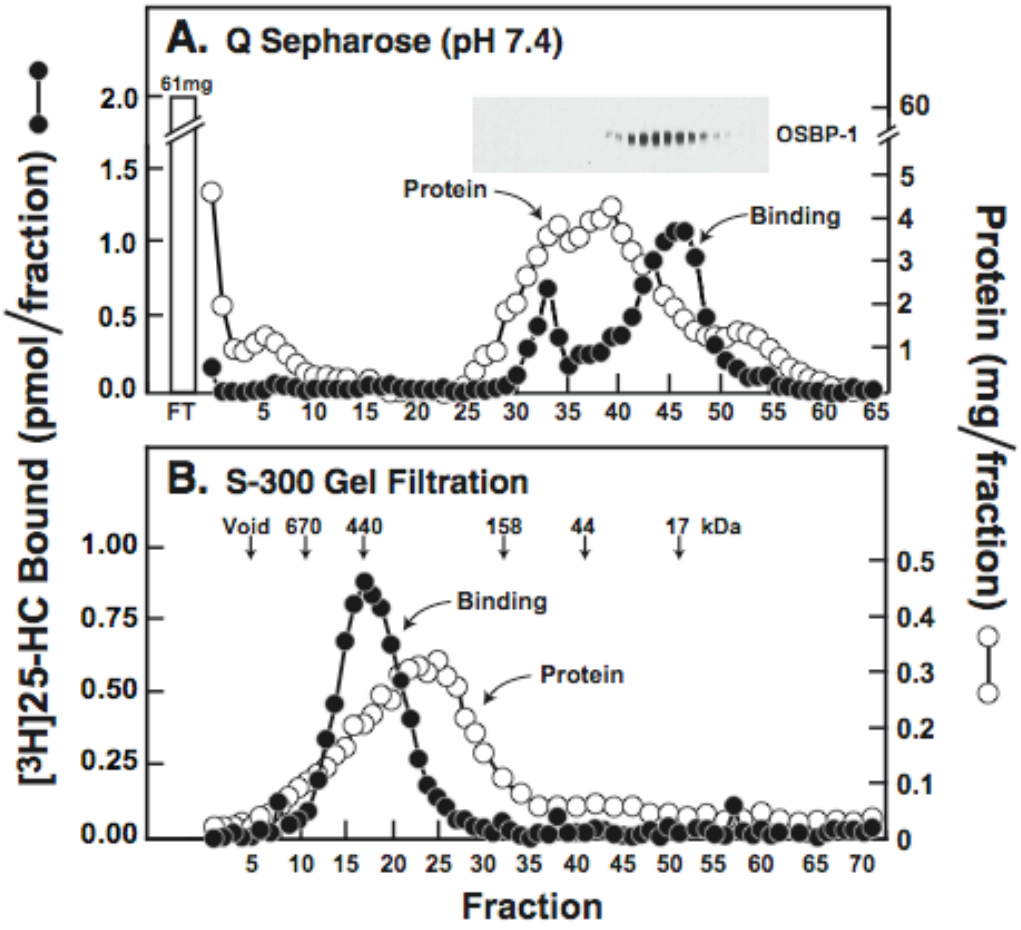
A. Q Sepharose (pH 7.4)
61mg
OSBP-1
Protein
Binding
FT
B. S-300 Gel Filtration
Void 670 440 158 44 17 kDa
Binding
Protein
[3H]25-HC Bound (pmol/fraction)
Protein (mg/fraction)
Fraction

FIGURE 1-2: Specificity of sterol binding to partially purified rabbit MOBP.

A, chemical structure of cholesterol. *B*, list of unlabeled sterols tested for their ability to compete with binding of [^{3}H]25-HC to MOBP. Blue and red colored sterols denote those that compete and those that do not compete for [^{3}H]25-HC binding, respectively. *C*, each assay tube, in a final volume of 120 µl of buffer C, contained partially purified MOBP (Q-Sepharose (pH 5.5) fraction), 50 nM of [^{3}H]25-HC delivered in ethanol, and varying concentrations of the indicated unlabeled competitor sterol, delivered in ethanol. After incubation for 2 h at 4°C, the amount of [^{3}H]25-HC binding was measured by the filter assay. The "100% of control" value in tubes with no unlabeled sterol was 50 fmol/filter. Blank values of 3.3 fmol (obtained in parallel assays of tubes containing no protein) were subtracted from each point. Each value is the average of triplicate incubations. *D* and *E*, each assay was performed as in (*C*) except that a different partially purified preparation of MOBP was used (RCA lectin fraction). The "100% of control" value in tubes with no unlabeled sterol was 71 fmol/filter for both (*D*) and (*E*). Blank values of 1.4 (*D*) and 2.5 (*E*) fmol were subtracted from each point. Each value in (*D*) is the average of triplicate incubations; each value in (*E*) represents a single incubation.

FIGURE 1-2

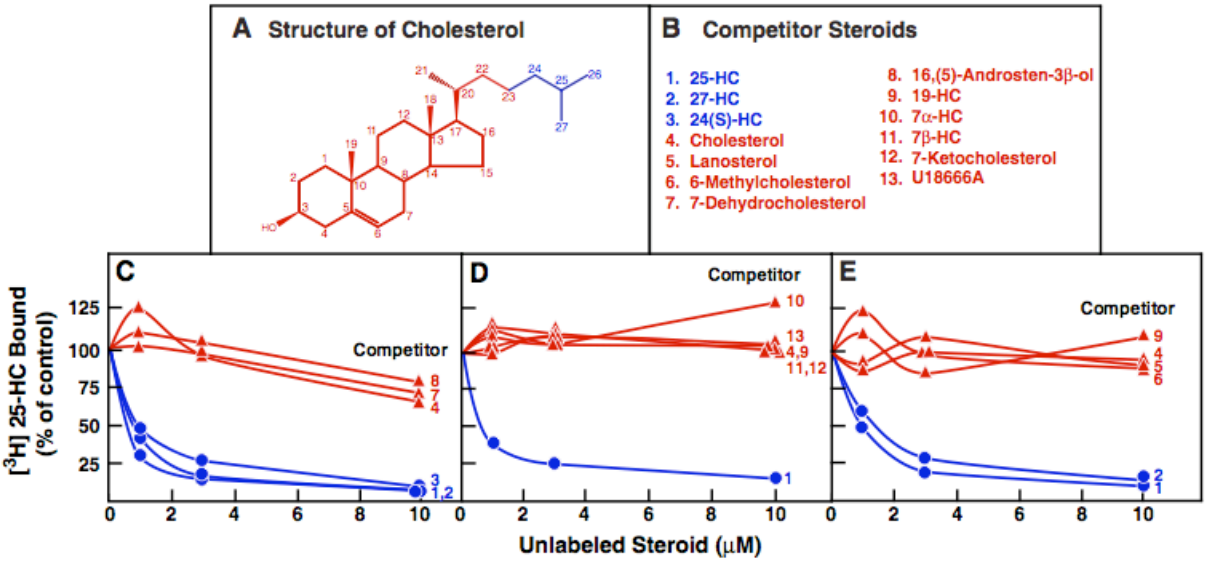
A Structure of Cholesterol
B Competitor Steroids
1. 25-HC
2. 27-HC
3. 24(S)-HC
4. Cholesterol
5. Lanosterol
6. 6-Methylcholesterol
7. 7-Dehydrocholesterol
8. 16,(5)-Androsten-3β-ol
9. 19-HC
10. 7α-HC
11. 7β-HC
12. 7-Ketocholesterol
13. U18666A
C
D
E
Competitor
[3H] 25-HC Bound (% of control)
Unlabeled Steroid (μM)

FIGURE 1-3: Photolabeling and SDS-PAGE of purified rabbit MOBP.

A, Mono-Q chromatography of photolabeled MOBP. Highly purified rabbit MOBP (0.13 mg of the Reactive Blue Dye 72 fraction) was incubated in a final volume of 3 ml with 500 nM of photo [^{3}H]25-HC in the absence (●) or presence (○) of 10 μM unlabeled 25-HC. After overnight incubation at 4ºC, the photo crosslinking group was activated by UV irradiation for 20 min. Each sample was loaded onto a 1-ml Mono-Q ion exchange column, washed, and eluted with a salt gradient. Radioactivity was determined by direct counting of each fraction. *B*, SDS-PAGE of Mono-Q purified material. Fractions 32 (with and without unlabeled 25-HC) from (*A*) were subjected to 8% SDS-PAGE, after which the gel was cut into 18 slices (3-mm each) that were then subjected to scintillation counting as described under "Experimental Procedures." A silver-stained gel (done in parallel with the cut gel) is shown at the top.

FIGURE 1-3

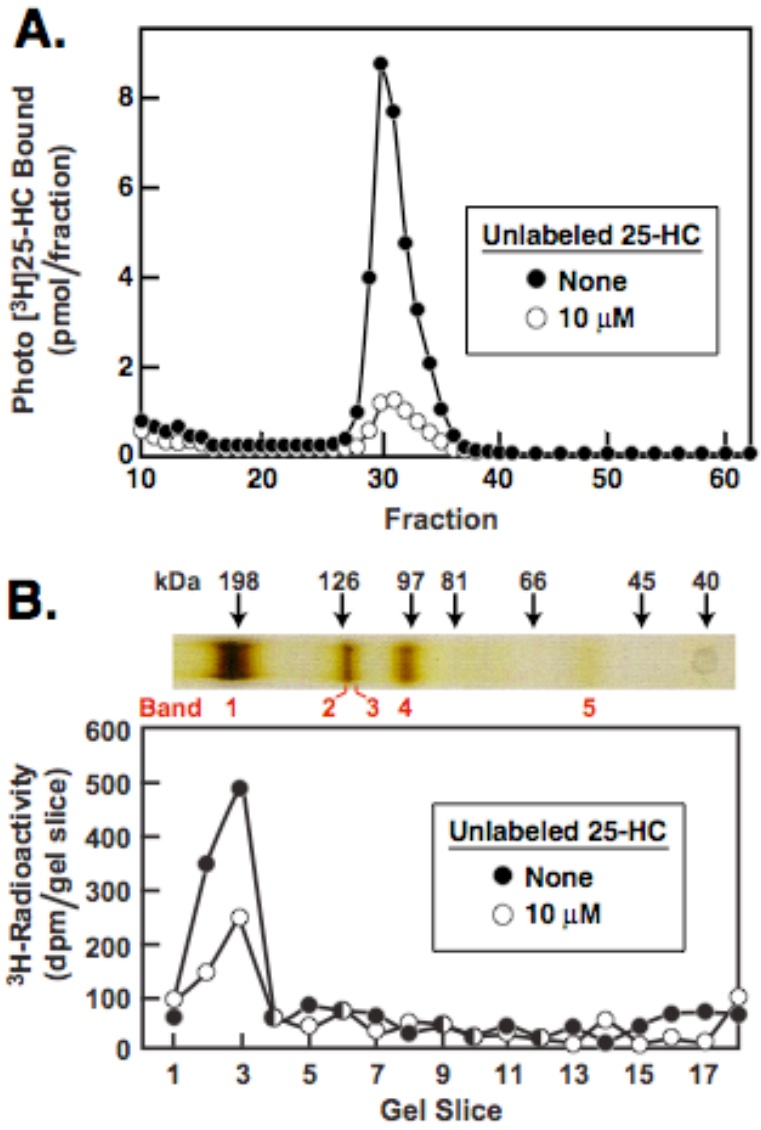
A.
Photo [3H]25-HC Bound (pmol/fraction)
Unlabeled 25-HC
None
10 μM
Fraction
B.
kDa 198 126 97 81 66 45 40
Band 1 2 3 4 5
3H-Radioactivity (dpm/gel slice)
Gel Slice

FIGURE 1-4: Purification of recombinant human NPC1 from transfected CHO-K1 cells.

A, nickel column chromatography. CHO-K1 cells (50 100-mm dishes) were transfected with 5 μg/dish of human NPC1-His_8-Flag as described under "Experimental Procedures." Detergent-solubilized membranes (100,000*g* fraction, 22 mg protein in buffer G containing 20 mM imidazole) was loaded onto a 1-ml His Trap HP nickel column pre-equilibrated with buffer G and eluted stepwise with 4 imidazole washes (25, 50, 200, 300 mM) as indicated. Fractions (1.5 ml) were tested for protein concentration (○), [^{3}H]25-HC binding activity (●), and immunoblot analysis with monoclonal Flag antibody (shown below fraction numbers). *B*, anti-Flag chromatography. Fractions 27 and 28 from (*A*) were pooled, loaded onto a 1-ml M2 anti-Flag M2-Agarose affinity column, washed with buffer G, and eluted with 0.1 mg/ml of Flag peptide in buffer G. Fractions (1 ml) were tested for protein concentration (○), [^{3}H]25-HC binding activity (●), and immunoblot analysis with monoclonal anti-Flag antibody. Protein measurements for fractions 14-21 are not shown since they contain the eluted Flag peptide. *C* and *D,* SDS-PAGE of purified recombinant NPC1. An aliquot of fraction 15 from the anti-Flag M2-Agarose column in (*B*) was subjected to 8% (*C*) and 12% (*D*) SDS-PAGE along with bovine serum albumin (BSA) standards and then stained with silver. The two bands at the top of the 8% gel (*C*) in the lane designated "Flag Peak" (~200 kDa and > 250 kDa) were shown by mass spectrometry to be NPC1.

FIGURE 1-4

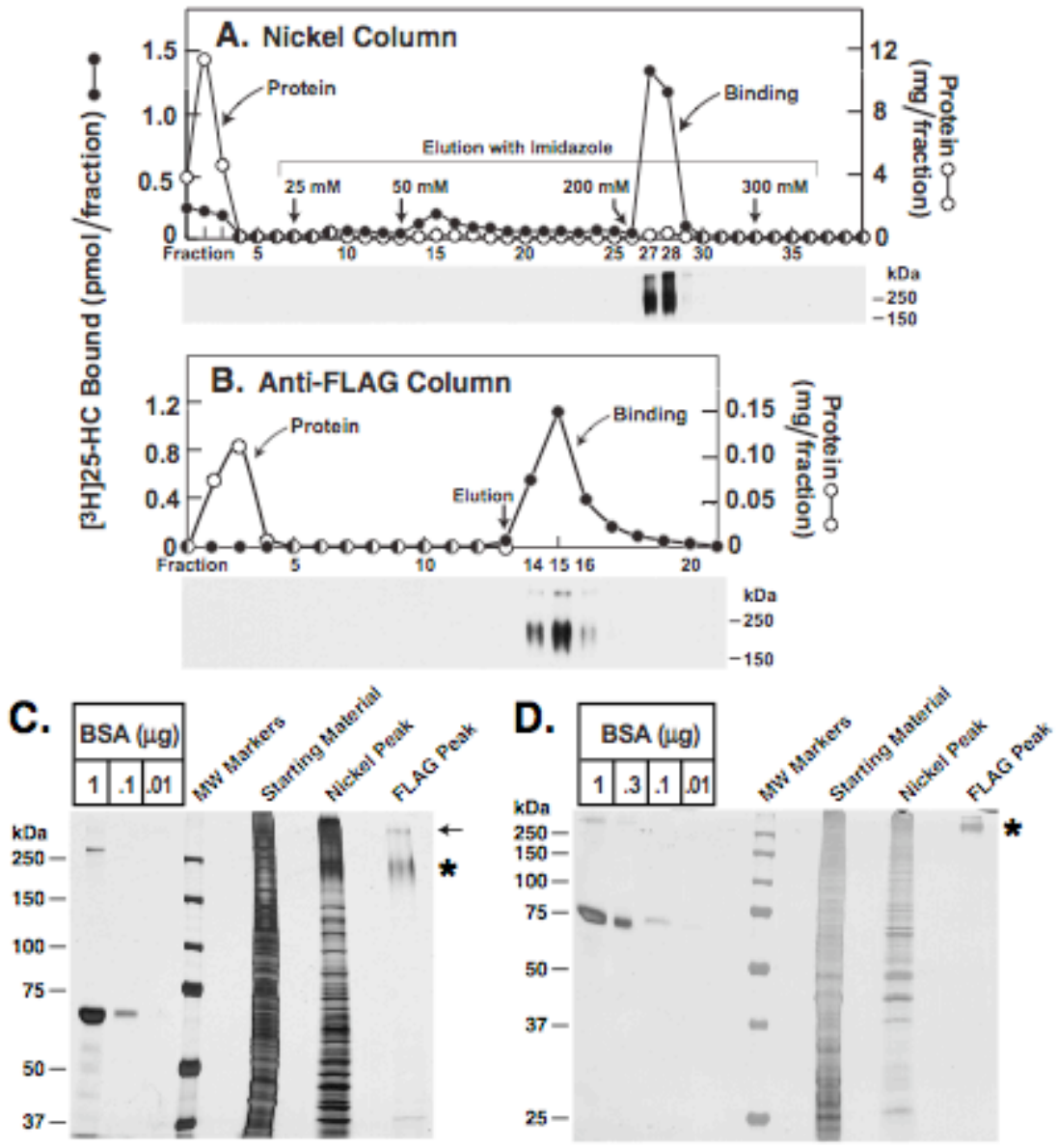
A. Nickel Column
Protein
Binding
Elution with Imidazole
25 mM
50 mM
200 mM
300 mM
Fraction
[³H]25-HC Bound (pmol/fraction)
Protein (mg/fraction)
kDa
250
150
B. Anti-FLAG Column
Protein
Binding
Elution
Fraction
kDa
250
150
C.
BSA (µg)
1
.1
.01
MW Markers
Starting Material
Nickel Peak
FLAG Peak
kDa
250
150
100
75
50
37
D.
BSA (µg)
1
.3
.1
.01
MW Markers
Starting Material
Nickel Peak
FLAG Peak
kDa
250
150
100
75
50
37
25

FIGURE 1-5: Reciprocal [^{3}H]25-HC and [^{3}H]cholesterol binding activities of purified recombinant NPC1 and Scap in presence of 1% NP-40 (*A-C*) or 0.1% Fos-Choline 13 (*D-E*).

A and *B,* saturation curves for NPC1 binding of [^{3}H]25-HC and [^{3}H]cholesterol. Each reaction, in a final volume of 120 μl of buffer G, contained ~250 ng of purified human NPC1-His_8-Flag and 10-400 nM of either [^{3}H]25-HC (*A*) or [^{3}H]cholesterol (*B*) (both solubilized in NP-40) in the absence (●) or presence (○) of 10 μM unlabeled 25-HC (*A*) or cholesterol (*B*) (both solubilized in NP-40). After incubation for 3 h at 4°C, bound [^{3}H]25-HC (*A*) or [^{3}H]cholesterol (*B*) was measured using the Ni-NTA agarose binding assay as described under "Experimental Procedures." Each data point represents total binding without subtraction of blank values. *C*, competitive binding of [^{3}H]25-HC to NPC1 in presence of unlabeled sterols. Each reaction, in a total volume of 140 μl of buffer G, contained ~150 ng of purified NPC1-His_8-Flag, 100 nM of [^{3}H]25-HC, and the indicated concentration of unlabeled 25-HC (●) or cholesterol (■). After incubation for 3 h at 4°C, bound [^{3}H]25-HC was measured as described above. The "100% of control" value with no unlabeled sterol was 26 fmol/tube. A blank value of 1.2 fmol was subtracted from each point. *D* and *E,* comparison of direct sterol binding activities of NPC1 and Scap. Each reaction, in a final volume of 140 μl of buffer H, contained ~400 ng of purified human NPC1-His_8-Flag in 0.1% Fos-Choline 13 (*D*) or 200 ng of purified hamster His_{10}-SCAP(TM1-8) in 0.1% Fos-Choline 13 (*E*) and the indicated concentration of [^{3}H]25-HC (●) or [^{3}H]cholesterol (▲) (both solubilized in 0.1% Fos-Choline 13). After incubation for 3 h at 4°C, binding was measured as described above. Each data point represents total binding without subtraction of blank

values. The experiments in (*A*)-(*E*) were done in two or more independent studies with similar results.

FIGURE 1-5

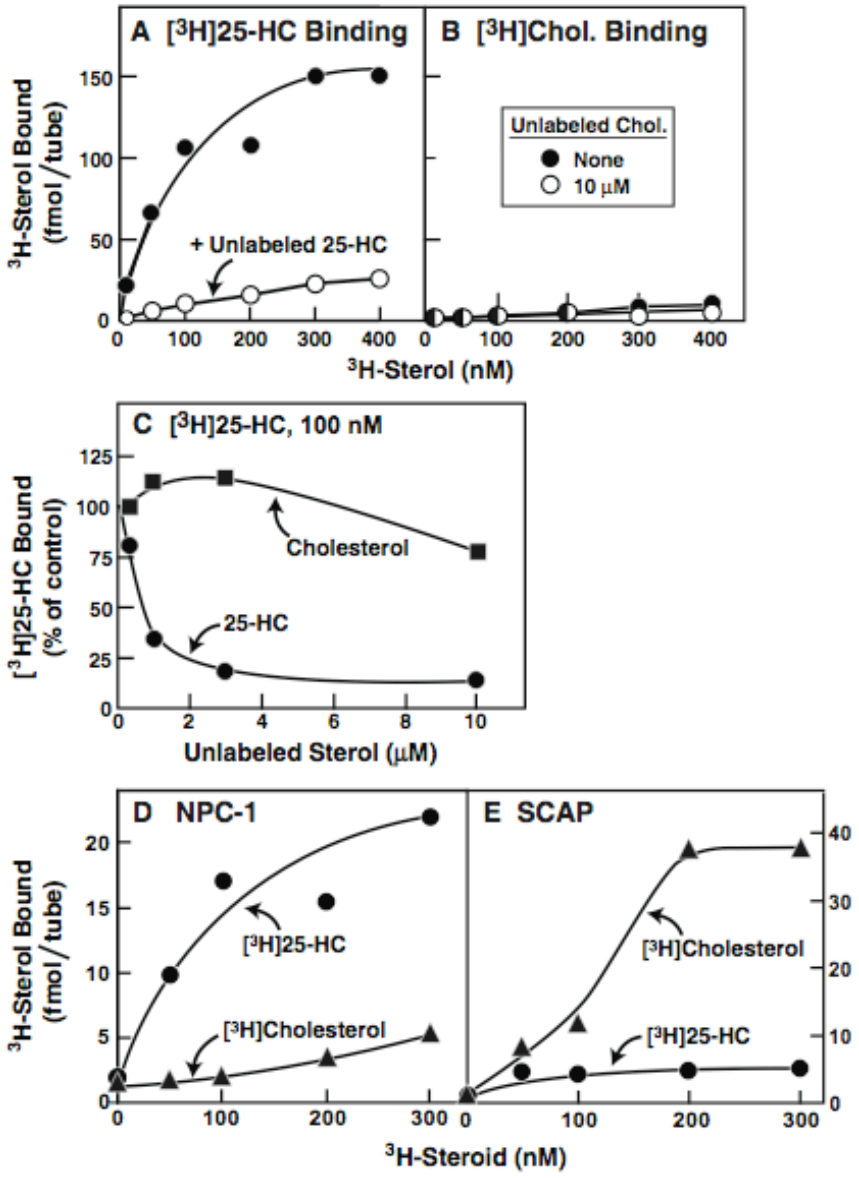

FIGURE 1-6: Ability of unlabeled oxysterols and various sterols to compete for binding of [^{3}H]25-HC to purified recombinant human NPC1 in presence of 1% NP-40.

A, chemical structure of cholesterol. *B*, list of unlabeled sterols tested for their ability to compete with binding of [^{3}H]25-HC to NPC1. Blue and red colored sterols denote those that compete and those that do not compete for [^{3}H]25-HC binding, respectively. *C* and *D*, competitive binding of [^{3}H]25-HC to NPC1. Each reaction, in a total volume of 120 μl of buffer G, contained 250 ng NPC1-His$_8$-Flag, 100 nM [^{3}H]25-HC, and varying concentrations of the indicated unlabeled sterol. After incubation for 3 h at 4°C, bound [^{3}H]25-HC was measured by the Ni-NTA agarose binding assay. Each data point represents the amount of [^{3}H]25-HC bound relative to that in the control tube, which contained no unlabeled sterol. The "100% of control" value was 60 (*C*) and 68 (*D*) fmol/tube, respectively. A blank value of 1 fmol/tube was subtracted from each point. *E*, competitive binding of [^{3}H]25-HC to NPC1 by unlabeled oxysterols, cholesterol precursors and analogues, and other sterols. Competitive assays were performed as in (*C*) and (*D*) except that each reaction contained ~150 ng NPC1-His$_8$-Flag and each unlabeled sterol was tested at one concentration (5 μM). The "100% of control" value in the absence of unlabeled sterol was 37 fmol/tube. A blank value of 1 fmol/tube was subtracted from each point. The experiments in (*C*)-(*E*) were done in two or more independent studies with similar results.

FIGURE 1-6

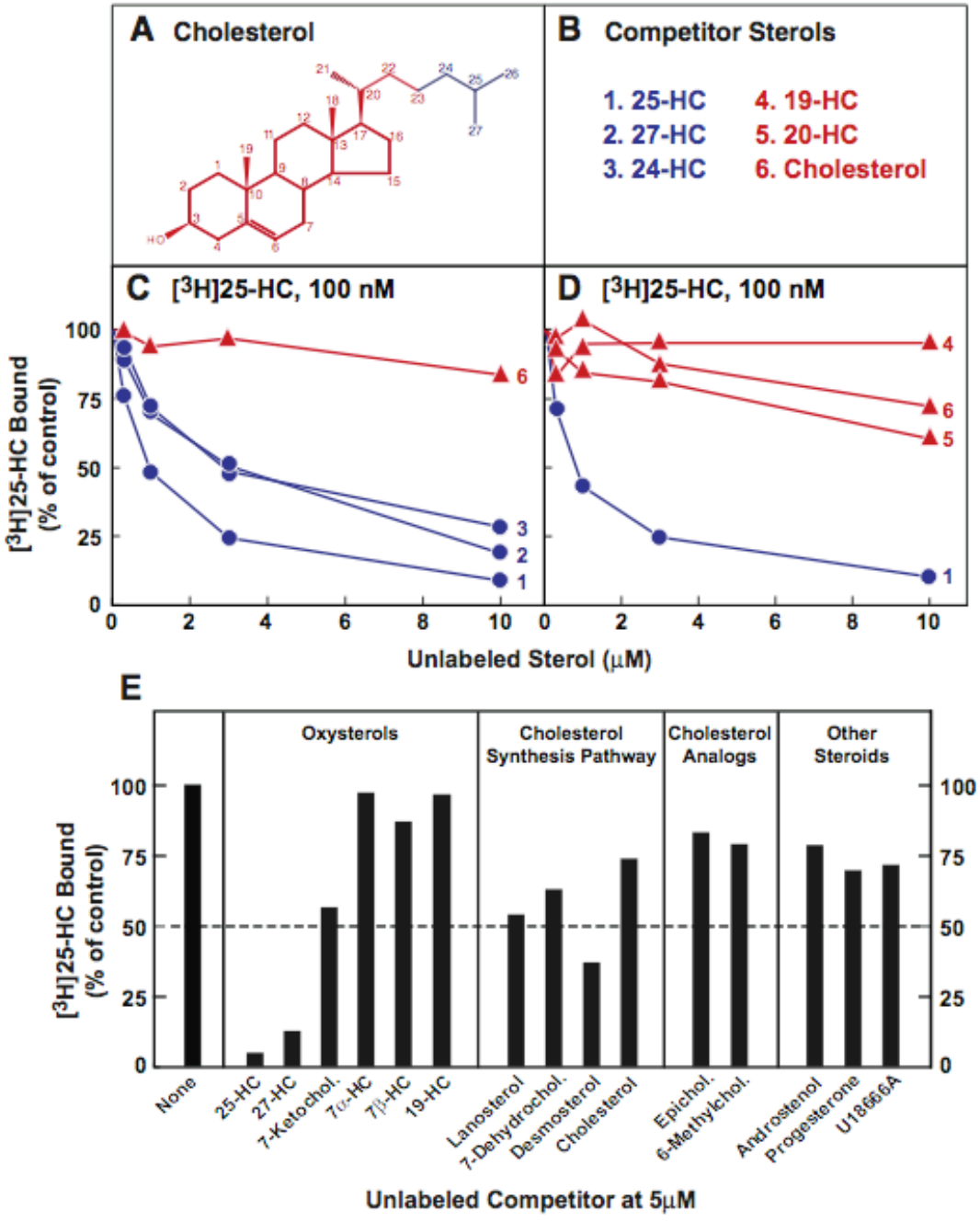
A Cholesterol
B Competitor Sterols
1. 25-HC
2. 27-HC
3. 24-HC
4. 19-HC
5. 20-HC
6. Cholesterol
C [3H]25-HC, 100 nM
D [3H]25-HC, 100 nM
[3H]25-HC Bound (% of control)
Unlabeled Sterol (μM)
E
Oxysterols
Cholesterol Synthesis Pathway
Cholesterol Analogs
Other Steroids
None
25-HC
27-HC
7-Ketochol.
7α-HC
7β-HC
19-HC
Lanosterol
7-Dehydrochol.
Desmosterol
Cholesterol
Epichol.
6-Methylchol.
Androstenol
Progesterone
U18666A
Unlabeled Competitor at 5μM

FIGURE 1-7: [^{3}H]Cholesterol and [^{3}H]25-HC binding activity of purified recombinant human NPC1 in presence of 0.004% NP-40.

A, Gel filtration chromatography of purified NPC1. Recombinant human NPC1-His_8-Flag (1 μg) purified in either 0.004% or 1% NP-40 was loaded onto a 24-ml Superdex 200 column preequilibrated with buffer I (0.004% NP-40) or buffer G (1% NP-40), respectively. Fractions of 1 ml were collected. Aliquots of each fraction (40 μl) were subjected to SDS/PAGE and NPC1 immunoblot analysis using monoclonal anti-Flag antibody. Standard molecular weight markers (thyroglobulin, 670 kDa; γ-globulin, 158; ovalbumin, 44; myoglobulin, 17) were chromatographed on the same column under identical buffer conditions. Filters were exposed for 0.5 to 3 s. *B*, saturation curves for binding of [^{3}H]cholesterol and [^{3}H]25-HC to NPC1 in presence of 0.004% NP-40. Each reaction, in a final volume of 80 μl of buffer I, contained ~100 ng of purified human NPC1-His_8-Flag, 1 μg of bovine serum albumin, and 10-300 nM of either [^{3}H]cholesterol (*left panel*) or [^{3}H]25-HC (*right panel*) delivered in ethanol. After incubation at 4°C for 16 h, bound ^{3}H-sterol was measured using the Ni-NTA agarose binding assay as described under "Experimental Procedures." Each data point represents the average of duplicate assays of total binding without subtraction of blank values. *C*, competitive binding of [^{3}H]cholesterol (*left panel*) and [^{3}H]25-HC (*right panel*) to NPC1 in presence of unlabeled sterols. Each assay tube, in a total volume of 80 μl of buffer I, contained ~100 ng of purified NPC1-His_8-Flag, 1 μg of bovine serum albumin, either 200 nM [^{3}H]cholesterol (*left panel*) or 40 nM [^{3}H]25-HC (*right panel*) delivered in ethanol, and the indicated concentration of unlabeled sterols. After incubation at 4°C for 16 h, bound ^{3}H-sterol was measured as described above. The "100% of

control" values in the absence of unlabeled sterol were 197 and 194 fmol/tube for [^{3}H]cholesterol and [^{3}H]25-HC, respectively. Blank values of 11 and 12 fmol/tube were subtracted from each of the [^{3}H]cholesterol and [^{3}H]25-HC data points, respectively.

FIGURE 1-7

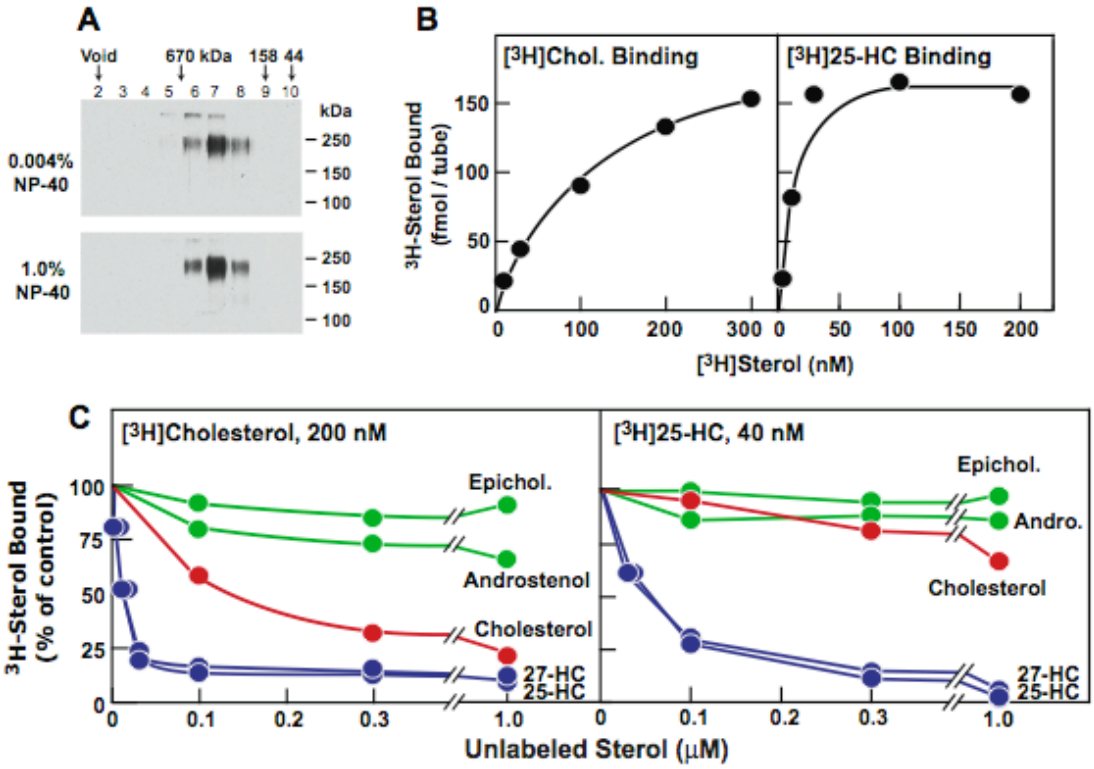

FIGURE 1-8: Effect of detergent concentration on [^{3}H]cholesterol and [^{3}H]25-HC binding to NPC1.

A, [^{3}H]cholesterol binding at NP-40 concentrations from 0.0007 to 0.01%. *Arrow* denotes the measured value for the CMC of NP-40 (0.0015%). *B*, cholesterol and [^{3}H]25-HC binding at NP-40 concentrations from 0.001 to 0.1%. *A* and *B*, each reaction, in a final volume of 80 μl of buffer I, contained ~80 ng of purified NPC1-His$_8$-Flag, 200 nM [^{3}H]cholesterol or 200 nM [^{3}H]25-HC as indicated, and the indicated concentration of NP-40. After incubation at 4°C for 16 h, the total amount of bound ^{3}H-sterol was measured using the Ni-NTA agarose binding assay as described under "Experimental Procedures." The "100% of control" value in the absence of unlabeled sterol were 218 and 108 fmol for [^{3}H]cholesterol and [^{3}H]25-HC, respectively. No blank values were subtracted. Each value is the average of duplicate incubations.

FIGURE 1-8

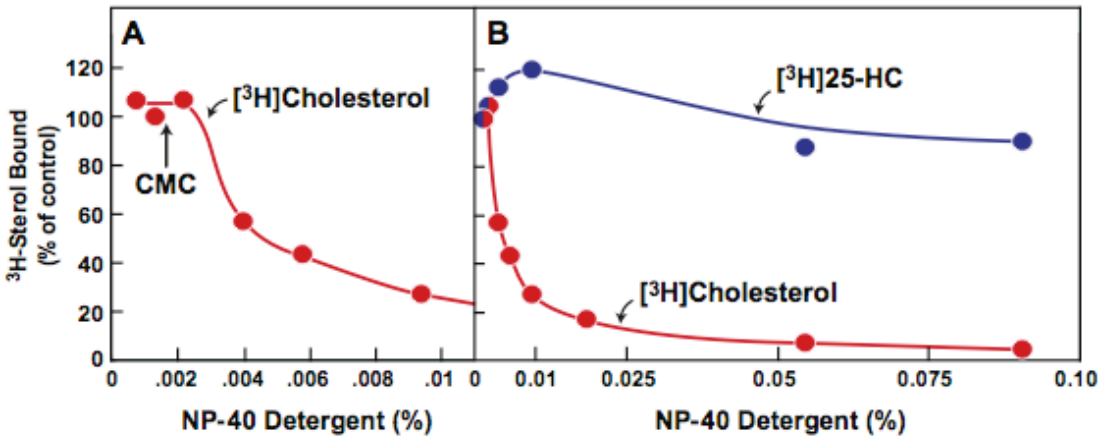

FIGURE 1-9: NPC1 does not regulate oxysterol-mediated inhibition of SREBP-2 processing in cultured cells.

A, cholesterol esterification assay in telomerase-immortalized NPC1 human fibroblasts. On day 0, h-TERT-Control (▲) and h-TERT-NPC-1 (●) fibroblasts were set up at in medium B containing 10% FCS and grown as described under "Experimental Procedures." On day 4, after incubation for 2 days in LPDS, each dish received sterol-depleting medium C supplemented with 10% human LPDS the indicated concentration of β-VLDL (*left*) or 25-HC (*right*). After incubation for 5 h at 37°C, each monolayer was pulse-labeled for 2 h with 0.2 mM [^{14}C]oleate (7681 dpm/pmol). The cells were then harvested for measurement of their cholesteryl [^{14}C]oleate and [^{14}C]triglyceride content as described under "Experimental Procedures." Each value is the average of triplicate incubations. The cellular content of [^{3}H]triglycerides (data not shown in figure) was similar for control and NPC1 cells incubated with 10 μg protein/ml β-VLDL (25 and 21 nmol/h per mg, respectively) or 5 μg/ml 25-HC (39 and 29 nmol/h per mg, respectively). *B*, immunoblot analysis of SREBP-2 cleavage in NPC1 human fibroblasts. hTERT-Control (*left*) and h-TERT-NPC1 (*right*) fibroblasts were set up for experiments as described under "Experimental Procedures." On day 4, after incubation for 2 days in LPDS, the cells were incubated with medium C supplemented with 10% human LPDS the indicated concentration of β-VLDL or 25-HC. After 6 h at 37°C, the cells were harvested. The nuclear extract and 100,000*g* membrane fractions were subjected to immunoblot analysis of SREBP-2. *C*, immunoblot analysis of SREBP-2 cleavage in NPC1 mouse fibroblasts. On day 4, after incubation for 1 day in 5% newborn calf LPDS, the

cells were incubated with medium C supplemented with 5% newborn calf LPDS and the indicated concentration of 25-HC or β-VLDL. After 5 h at 37 C, the cells were harvested, and processed as in *B*. All filters in *B* and *C* were exposed to X-ray film for 1-5 s except for the Scap and NPC1 filters, which were exposed for 20 s.

FIGURE 1-9

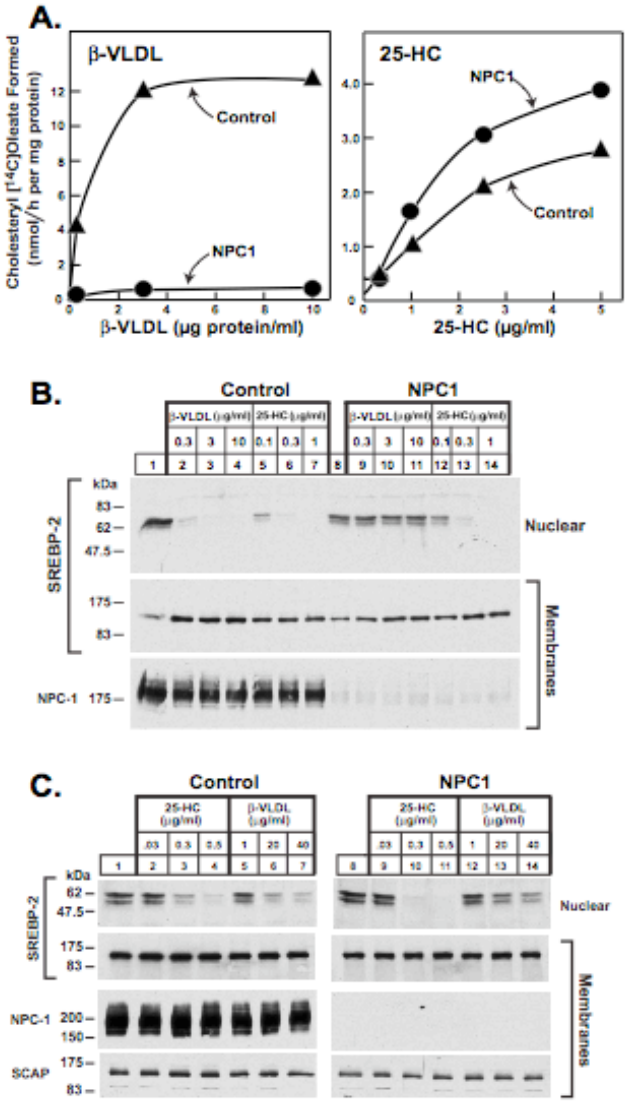

(This data reproduced with permission by Lina Abi-Mosleh)

DISCUSSION

In the present studies we set out to purify a hypothesized membrane-bound oxysterol binding protein (MOBP) that we predicted would differ from the previously described oxysterol-binding proteins of the cytosol (OSBP-1 and ORPs). Our ultimate goal was to find a membrane protein that binds oxysterols and in turn regulates cholesterol synthesis and esterification. We used rabbit liver as a source because of the commercial availability of frozen rabbit livers. We succeeded in identifying and purifying by 14,000-fold a membrane protein that bound [^{3}H]25-HC with high affinity and specificity. When peptides from this protein were sequenced by mass spectrometry, we were surprised to find that the oxysterol-binding protein was NPC1, a previously described protein with a known role in intracellular transport of cholesterol. There was no prior evidence to indicate that NPC1 binds oxysterols.

To confirm the oxysterol binding activity of NPC1, we prepared the human protein through recombinant DNA methodology and purified it through use of affinity tags. The recombinant human NPC1 bound oxysterols with specificity that was similar to that of the rabbit liver protein. Both proteins showed a preference for sterols with a hydroxyl group near the distal end of the 8-carbon side chain, i.e. at positions 24, 25, or 27. Hydroxyl groups elsewhere on the sterol (positions 7, 19, or 20) failed to confer binding.

In the current experiments, recombinant human NPC1 also bound cholesterol. Binding was inhibited when the concentration of NP-40 exceeded the micellar threshold. We hypothesize that detergent micelles block [^{3}H]cholesterol binding not because of an effect on

the protein, but rather because the detergent micelles have a higher affinity and capacity for binding cholesterol than does the NPC1 protein. In this regard, Cheruku et al. (31) performed informative studies with NPC2 protein, a soluble cholesterol binding protein that participates together with NPC1 in intracellular cholesterol transport. NPC2 rapidly transferred cholesterol to phospholipid bilayers. It will be of interest in the future to determine whether phospholipid bilayers also steal cholesterol from NPC1 and whether this relative affinity is important in the ability of NPC1 to transfer cholesterol between membranes and in the ability of sphingolipids or phospholipids to regulate this process.

A remarkable feature of NPC1 sterol binding was the non-reciprocal effect of cholesterol and 25-HC. Whereas 25-HC potently blocked [^{3}H]cholesterol binding, the reverse was not true, i.e., cholesterol failed to block [^{3}H]25-HC binding. This result might be explained by a one-site or two-site model. In the former, NPC1 would have a single sterol binding site, and 25-HC would have a much higher affinity for this site than cholesterol. In the two-site model, 25-HC binding to the oxysterol site would allosterically alter the separate cholesterol binding site, blocking the binding of cholesterol. Distinguishing these possibilities will require purification of larger amounts of recombinant NPC1 than are available presently. These studies may be aided by the identification of the domain of NPC1 that binds cholesterol and 25-HC (see Chapter 2) (33).

As described in the Introduction, we initiated the search for a MOBP in an attempt to explain the ability of oxysterols to inhibit cholesterol synthesis by blocking the proteolytic processing of SREBPs. However, we have been unable to find any evidence that NPC1 is required for this regulatory action. While these studies were in progress, we demonstrated

that the effect of 25-HC on SREBP processing is mediated by 25-HC binding to Insig proteins (54), which in turn prevents SREBPs from exiting from the ER (60). Thus, we have no reason to postulate a direct role for NPC1 in regulating SREBP activity.

CHAPTER TWO

LOCALIZATION OF THE STEROL BINDING DOMAIN OF NIEMANN-PICK C1

SUMMARY

Defects in Niemann-Pick, Type C-1 protein (NPC1) cause cholesterol, sphingolipids, phospholipids, and glycolipids to accumulate in lysosomes of liver, spleen, and brain. In cultured fibroblasts, NPC1 deficiency causes lysosomal retention of lipoprotein-derived cholesterol after uptake by receptor-mediated endocytosis. NPC1 contains 1278 amino acids that form 13 membrane-spanning helices and three large loops that project into the lumen of lysosomes. In Chapter 1, we showed that NPC1 binds cholesterol and oxysterols. Here we localize the binding site to the N-terminus of NPC1, a 240-amino acid luminal domain with 18 cysteines. When produced in cultured cells, the N-terminal domain, NPC1(NTD), was secreted as a soluble dimer. NPC1(NTD) bound [^{3}H]cholesterol (K_d, 130 nM) and [^{3}H]25-hydroxycholesterol (25-HC) (K_d, 10 nM) with one sterol binding site per dimer. Binding of both sterols was competed by oxysterols (24, 25, and 27-HC). Unlabeled cholesterol competed strongly for binding of [^{3}H]cholesterol, but weakly for [^{3}H]25-HC binding. Binding of [^{3}H]cholesterol but not [^{3}H]25-HC was inhibited by detergents. We also studied NPC2, a soluble protein whose deficiency causes a similar disease phenotype. NPC2 bound cholesterol, but not oxysterols. Epicholesterol competed for [^{3}H]cholesterol binding to NPC2, but not NPC1. Glutamine-79 in NPC-1(NTD) is important for sterol binding; a Q79A

mutation abolished binding of [^{3}H]cholesterol and [^{3}H]25-HC to full length NPC1. Nevertheless, the Q79A mutant restored cholesterol transport to NPC1-deficient CHO cells. Thus, oxysterol binding to NPC1(NTD) is not essential for NPC1 function in fibroblasts, but it may function in other cells where NPC1 deficiency produces more complicated lipid abnormalities.

INTRODUCTION

As described in Chapter 1, we encountered NPC1 unexpectedly in a search for a membrane-bound protein that binds oxysterols such as 25-hydroxycholesterol (25-HC). When delivered to cells in ethanol, these oxysterols mimic the ER regulatory actions of cholesterol, i.e., they block SREBP cleavage and they activate ACAT (29, 32). However, oxysterols do not traverse lysosomes, and there is no evidence that they require the actions of NPC1 or NPC2 in order to reach the ER. We were therefore surprised to find that a purified membrane-bound, oxysterol-binding protein turned out to be NPC1. In further studies we showed that recombinant human NPC1 bound cholesterol as well as oxysterols, but cholesterol binding occurred only when the detergent concentration was reduced below micellar levels (32).

In the current studies we localize the sterol binding site in human NPC1 to its N-terminal domain, NPC1(NTD). Using recombinant DNA technology, we prepare NPC1(NTD) as a soluble protein of 240 amino acids that is secreted by cells. Purified NPC1(NTD) binds oxysterols and cholesterol with high affinity. We characterize this binding reaction and provide evidence that NPC1(NTD) contains the majority, if not all, of the cholesterol binding activity of NPC1. Furthermore, the sterol binding specificity of NPC1(NTD) is compared to that of NPC2 depicting a difference in their binding pockets.

EXPERIMENTAL PROCEDURES

Materials – We obtained 1,2-diheptanoyl-*SN*-glycero-3-phosphocholine (DHPC) from Avanti Polar Lipids, Inc.; n-dodecyl-β-D-maltopyranoside (DDM) and CHAPS from Anatrace, Inc.; and bovine serum albumin (BSA) from Pierce (Cat. No. 23210). Radioisotopes, antibodies, sterols, chromatographic supplies, lipoproteins, lipoprotein-deficient serum (LPDS), and all other reagents (unless otherwise specified) were obtained from sources prepared as described in Chapter 1.

Buffers – Buffer A contains 50 mM Tris-chloride at pH 7.4, 150 mM NaCl, and 0.004% (w/v) NP-40. Buffer B contains 50 mM Tris-chloride at pH 7.4, 100 mM KCl, and 1% NP-40. Buffer C contains 50 mM Tris-chloride at pH 7.4 and 150 mM NaCl. Buffer D contains 50 mM Tris-chloride at pH 7.4, 50 mM KCl, 10% (v/v) glycerol, 5 mM dithiothreitol, 1 mM sodium EDTA, and protease inhibitor mixture (1 μg/ml pepstatin A, 2 μg/ml aprotinin, 10 μg/ml leupeptin, 200 μM phenylmethylsulfonyl fluoride, and 25 μg/ml of *N*-acetyl-leucinal-leucinal nonleucinal).

Plasmid Constructions – pCMV-NPC1-His_8-Flag encodes wild-type human NPC1 followed sequentially by eight histidines and a Flag tag under control of the cytomegalovirus (CMV) promoter. This plasmid was constructed as described in Chapter 1. pCMV-NPC1(1-307;1254-1278)-His_8-Flag was constructed from pCMV-NPC1-His_8-Flag by site-directed mutagenesis (QuickChange II XL kit, Stratagene) using the 5'-oligonucleotide, 5'-CTCCGAGTACACTCCCATCGATAGCGTAAATAAAGCCAAAAGTTGTGCC-3' and the 3'oligonucleotide, 5'-GGCACAACTTTTGGCTTTATTTACGCTATC

GATGGGAGTGTAGTCGGA-3'. pCMV-NPC1(1-264)-His_8-Flag was constructed from pCMV-NPC1(1-307;1254-1278)-His_8-Flag by site-directed mutagenesis using the 5'oligonucleotide, 5'-CCTGCTCCCTGGACGATCCTTGGCCATCACCATCACCATCAC CATCACGACTAA-3' and the 3'oligonucleotide, 5'-TTATAGTCGTGATGGTGATGGTG ATGGTGATGGCCAAGGATCGTCCAGGGAGCAGG-3'. When this plasmid is expressed in CHO-K1 cells, the resulting protein (after signal peptide cleavage) consists of the N-terminal domain (NTD) of NPC1 (amino acids 25-264). This protein is hereafter referred to as NPC1(NTD).

The coding region of each plasmid was sequenced to ensure integrity of the construct. Mutations in NPC1 were produced by site-directed mutagenesis of pCMV-NPC1(1-264)-His_8-Flag and pCMV-NPC1-His_8-Flag plasmids.

pCMV-NPC2-His_8 encodes wild-type human NPC2 followed sequentially by eight-histidines under control of the CMV promoter. The plasmid was constructed from pCMV-NPC2 (Origene Technologies) by site-directed mutagenesis (QuickChange II XL kit, Stratagene). The coding region of pCMV-NPC2-His_8 was sequenced to ensure integrity of the construct.

pTK-HSV-BP-2 encodes wild-type *Herpes simplex* virus (HSV)-tagged human SREBP-2 under control of the thymidine kinase promoter (31).

Transfection of NPC1 and NPC2 Constructs in CHO Cells – CHO-K1 cells were grown and transfected in medium A (1:1 mixture of Ham's F12 medium and Dulbecco's modified Eagle's medium, 100 units/ml penicillin and 100 μg/ml streptomycin sulfate) containing 5% (v/v) fetal calf serum (FCS) as described in Chpater 1. Each dish was

transfected with one of the following plasmids: 5 μg of pCMV-NPC1-His_8-Flag, 5 μg of pCMV-NPC1(1-307;1254-1278)-His_8-Flag, 5 μg of pCMV-NPC1(1-264)-His_8-Flag (wild-type or the indicated mutant versions), or 5 μg of pCMV-NPC2-His_8. After 16 h, the transfected cells were used for purification of NPC1 proteins as described below.

Mutant CHO 4-4-19 cells, defective in NPC1 (18), were obtained from Laura Liscum (Tufts University School of Medicine, Boston, MA). The defective NPC1 in 4-4-19 cells results from an amino acid substitution (Gly660Arg).[3] On day 0, 4-4-19 cells were set up in medium A containing 5% FCS at $2x10^5$ cells/60-mm dish. On day 2, each dish was transfected in OPTI-MEM (Gibco) with the indicated plasmid, using Lipofectamine 2000 according to the manufacturer's directions. After 5 h, the medium was switched to medium A containing 5% newborn calf LPDS. After 16 h, the cells were used for assays of ACAT and SREBP-2 processing.

Purification of Full Length NPC1 and Internally Deleted NPC1(1-307;1254-1278) from Transfected CHO Cells – Recombinant NPC1 proteins were overexpressed in CHO-K1 cells as described above and purified in buffer A or B by nickel and M2 anti-Flag agarose chromatography as described in Chapter 1.

Purification of Secreted Forms of NPC1(NTD) and NPC2 from Medium of Transfected CHO Cells – Recombinant NPC1 and NPC2 proteins were overexpressed in CHO-K1 cells as described above. On day 3, the medium was switched to medium A containing 1% (v/v) Cellgro® ITS (Fisher Scientific). After 24 h, the medium was collected and fresh medium A containing 1% Cellgro® ITS was added. This was done for 3 consecutive days for each group of transfected cells. After each collection, the medium was

subjected to centrifugation at 2,500 rpm for 5 min at 4°C and then filtered through an Express PLUS 0.22-μm filter apparatus (Millipore). Medium was stored at 4°C covered in aluminum foil. Gravity columns were each filled with a 20-ml slurry of Ni-NTA agarose beads, after which each column was pre-equilibrated with 4 column volumes of buffer C. Filtered medium (1 L per column) was then passed overnight at 4°C through each Ni-NTA agarose column ~1 ml/min. Each column was washed sequentially with 50 ml of buffer C containing 20 mM and 40 mM imidazole. Bound protein was eluted with 50 ml of buffer C containing 200 mM imidazole. The eluted fraction containing NPC1(25-264)-His_8-Flag or NPC2-His_8 was concentrated to 0.5 ml by using a spin concentrator with an Amicon Ultracel 30K or 10K Filter Device (Millipore), respectively. The concentrated material was then subjected to gel filtration chromatography on a 24-ml Superdex-200 column that was pre-equilibrated with buffer C. The fractions containing the peak A_{280} activity and eluting between 12.5 and 15 ml (for NPC1(25-264)-His_8-Flag) or between 16 and 18 ml (for NPC2-His_8) were pooled, and their protein content was quantified by either the BCA kit (Pierce) or the Lowry method (44). The pooled proteins were subjected to SDS/PAGE followed by Coomassie staining to determine purity.

Ni-NTA Agarose Assay for ^{3}H-Sterol Binding – For the standard assay of wild-type and mutant versions of NPC1 and NPC2, each reaction contained, in a final volume of 80 μl of buffer A, either [^{3}H]25-HC (165-180 dpm/fmol) or [^{3}H]cholesterol (132 dpm/fmol) delivered in ethanol (final ^{3}H-sterol concentration, 10-400 nM), 1 μg of BSA as indicated, and varying amounts of NPC1 or NPC2 protein. After incubation for 4 h or 16 h at 4°C, the mixture was loaded onto a column packed with 0.3 ml of Ni-NTA Agarose beads (Qiagen)

that had been pre-equilibrated with the appropriate assay buffer. Each column was washed for ~ 15 min with 5-6 ml of buffer B, except for the experiments described in Figure 2-8. The protein-bound ^{3}H-sterol was eluted with 250 mM imidazole in buffer B and quantified by scintillation counting as previously described (Radhakrishnan et al., 2004). For competition experiments with unlabeled sterols, the standard assays were carried out in the presence of the indicated unlabeled sterol (0-3 μM) delivered in ethanol (final ethanol concentration, 1-4%). In each experiment, all tubes received the same amount of ethanol.

Glycosidase Treatments – Each reaction, in a final volume of 42 μl, was carried out according to the manufacturer's directions (New England BioLabs) for 16 h at 37°C with the indicated amount of purified protein in the presence or absence of 4000 units of Endo H or 5000 units of peptide N-glycosidase F (PNGase F).

SREBP-2 Processing in Cultured Cells – Mutant CHO 4-4-19 cells (defective in NPC1) were transfected as described above. On day 3, the medium was switched to medium A containing 5% newborn calf LPDS, 5 μM compactin, and 50 μM sodium mevalonate. On day 4, the cells received fresh medium A supplemented with 5% newborn calf LPDS and various concentrations of β-VLDL or 25-HC. After incubation at 37°C for 5 h, cells were treated with 25 μg/ml of *N*-acetyl-leucinal-leucinal-norleucinal for 1 h and then harvested. Duplicate dishes were pooled for preparation of nuclear extract and 100,000*g* membrane fractions, which were then analyzed by immunoblotting for SREBP-2 (described below).

Immunoblot Analysis – The procedure for immunoblot analysis and the concentrations of antibodies used are exactly as described in Chapter 1 except for the use of one additional antibody. Epitope-tagged SREBP-2 was detected with 0.2 μg/ml of IgG-HSV-

Tag™, a monoclonal antibody directed against the glycoprotein D epitope of *Herpes simplex* virus (Novagen, Inc).

ACAT Assay – The rate of incorporation of [^{14}C]oleate into cholesterol [^{14}C]oleate and [^{14}C]triglycerides by intact cell monolayers was measured as previously described (28)

RESULTS

Localization of Oxysterol Binding Site in NPC1 – Figure 2-1*A* shows a diagram of the postulated domain structure of human NPC1, a 1278-amino acid protein. The protein is believed to contain 13 putative transmembrane helices (19) that divide the protein into the following structural domains: 1) a cleaved signal sequence (amino acids 1-24) (11); 2) a soluble, luminal N-terminal domain (amino acids 25-264); 3) large luminal loop-2 (amino acids 371-615); 4) a putative sterol-sensing domain (transmembrane helices 3-7, amino acids 616-791) (45,47); 5) large luminal loop-3 (amino acids 855-1098); and 6) a lysosomal targeting signal (LLNF) at the COOH-terminus (amino acids 1275-1278) (65).

To localize the region in NPC1 that binds 25-HC, we created plasmids encoding the first 307, 644, 809, or 1178 amino acids of the protein fused to a fragment comprising the COOH-terminal 24 amino acids, which contains the lysosomal targeting signal. The epitope-tagged proteins were purified as described for the full length protein in the Chapter 1. All of these internally deleted proteins bound [^{3}H]25-HC with saturation kinetics that were similar to that of the full-length protein (data not shown). The smallest of these deleted proteins contain 332 NPC1-derived amino acids and is designated NPC1-His$_8$-Flag(Δ1-307;1254-1278) (see bottom panel of Figure 2-1*A*). Figure 2-1*B* shows the migration of this internally deleted protein on SDS-PAGE as determined by immunoblotting (*lane 2*). Migration of the full-length protein is also shown (*lane 1*). Both proteins exhibited broad bands, presumably owing to extensive *N*-linked glycosylation. The internally deleted and full-length protein bound similar amounts of [^{3}H]25-HC (Figure 2-1*C*). Unlabeled 25-HC and 27-hydroxycholesterol (27-HC) competed effectively for the binding of [^{3}H]25-HC. Unlabeled

cholesterol and 19-hydroxycholesterol (19-HC) did not compete (Figure 2-1*D*). The binding specificity of the internally deleted NPC1 with respect to oxysterols is thus similar to that of the full-length molecule (see Chapter 1).

Secretion and Purification of NPC1(NTD) - In order to further define the oxysterol-binding site within the membrane-anchored, internally deleted NPC1(1-307;1254-1278), we made a further truncation from the COOH-terminus to remove the single transmembrane domain and the lysosomal targeting sequence. This protein, designated NPC1(25-264)-His_8-Flag, contains the signal sequence and NTD as shown in Figure 2-2*A*. Figure 2-2*B* shows a comparison of the amino acid sequence of human NPC1(NTD) with a consensus sequence that was derived from the sequences of 12 vertebrate species, including 10 mammals. Of the 240 amino acids in this domain, 124 are invariant (Figure 2-2*B*, *black boxes*). Eighteen of the invariant residues are cysteines (Figure 2-2*B, yellow boxes*). The 12 vertebrate sequences are shown in Figure 2-3.

When expressed in CHO cells by transfection, full-length NPC1-His_8-Flag and NPC1(1-307;1254-1278)-His_8-Flag were found exclusively in a 10^5g pellet of cell membranes (Figure 2-2*C*, *lanes 6* and *9*). In contrast, the vast bulk of NPC1(25-264)-His-Flag was secreted into the medium (*lane 10*). Note that the relative amount of the medium fraction applied to the gel was only one-fifth the amount of the cell supernatant and pellet fractions.

To purify NPC1(NTD) from the medium of transfected CHO cells, the medium was subjected to Ni-chromatography followed by gel filtration chromatography in the absence of detergents (see "Experimental Procedures"). When stored at 4°C in buffer C (without

detergent) at concentrations between 0.3-2.0 mg/ml, the protein retained full binding activity and continued to appear monodisperse on gel filtration. The calculated molecular mass for the protein component of the epitope-tagged NPC1(NTD) is 28.7 kDa. However, the secreted protein migrated on SDS-PAGE as a diffuse band slightly above the 50-kDa marker (Figure 2-4*A, lane 1*). Treatment of the secreted protein with the glycosidase PNGaseF under denaturing conditions caused the recombinant protein to migrate as a compact band close to the 30-kDa marker (data not shown). Thus, the diffuse migration is attributable to glycosylation of some or all of the 5 potential *N*-linked glycosylation sites in the loop (Figure 2-2*B*). Upon gel filtration in the absence of detergents, this protein eluted as a single symmetrical peak corresponding to ~100 kDa (Figure 2-4*B*). We believe that the 100-kDa species is a dimer. When the protein was analyzed by circular dichroism (Figure 2-4*C*), it showed a spectrum characteristic of high α-helical content with minima at 207 and 222 nm (61, 15).

Binding Specificity of NPC1(NTD) - To measure the binding of ^{3}H-labeled sterols to purified NPC1(25-264)-His_8-Flag, we used an assay in which the protein was trapped on a nickel agarose column, and bound ^{3}H-sterols were quantified by scintillation counting (32, 54). The binding reactions were conducted in a low concentration of NP-40 (0.004%), which is slightly higher than the critical micellar concentration (CMC), which is 0.0015% (discussed below). Figure 2-5*A* shows binding of [^{3}H]25-HC to NPC1(25-264)-His_8-Flag in the absence and presence of an excess of unlabeled 25-HC. Binding of [^{3}H]25-HC was saturable with an apparent Kd of 10 nM (average of 7 experiments). At saturation, we estimated that 1 molecule of [^{3}H]25-HC bound to 1 dimer of NPC1(25-264)-His_8-Flag.

Binding of [^{3}H]25-HC was inhibited by an excess of unlabeled 25-HC (Figure 2-5*A*) and by similar concentrations of unlabeled 24-HC and 27-HC (data not shown).

We then tested the ability of NPC1(NTD) to bind [^{3}H]cholesterol. As shown in Figure 2-5*B*, this protein fragment bound [^{3}H]cholesterol with an apparent K_d of 130 nM (average of 7 experiments). At saturation, we estimated that 1 molecule of [^{3}H]cholesterol bound to 1 dimer of NPC1(25-264)-His_8-Flag, a similar binding stoichiometry to that of [^{3}H]25-HC. The binding of [^{3}H]cholesterol was inhibited by an excess of unlabeled cholesterol. [^{3}H]Progesterone did not show saturable binding to NPC1(25-264)-His_8-Flag when tested at concentrations from 1-400 nM (data not shown).

In studies not shown, we found that the maximal binding of [^{3}H]cholesterol or [^{3}H]25-HC to NPC1(25-264)-His_8-Flag was similar over a pH range of 4-8. Moreover, binding of [^{3}H]25-HC or [^{3}H]cholesterol was not affected by the presence of EDTA up to 10 mM, but both binding activities were markedly decreased in the presence of 10 mM dithiothreitol, a reducing agent that would be expected to disrupt the multiple disulfide bonds that are postulated based on the cysteine-rich amino acid sequence of NPC1(NTD).

To examine in more detail the binding of [^{3}H]25-HC and [^{3}H]cholesterol to NPC1(NTD), we carried out competitive binding studies, as shown in Figure 2-5*C* and 2-5*D*. When [^{3}H]25-HC was present at a concentration near its K_d (10 nM), unlabeled 25-HC competed with an IC50 value of ~10 nM, whereas unlabeled cholesterol did not effectively compete except at concentrations of 3 μM (Figure 2-5*C*). When [^{3}H]cholesterol was present at a concentration near its K_d (130 nM), unlabeled cholesterol competed with an IC50 of ~100 nM, whereas unlabeled 25-HC inhibited with an IC50 ~5 nM (Figure 2-5*C*) as did

unlabeled 24-HC and 27-HC (data not shown). Thus, by two different assays (direct binding and competition), NPC1(NTD) showed a 13- to 20-fold higher affinity for 25-HC than cholesterol. Epicholesterol showed no ability to compete for binding of either [^{3}H]25-HC or [^{3}H]cholesterol (Figures 2-5*C* and 2-5*D*).

In Chapter 1, we determined that under the buffer and temperature conditions of our assays the CMC for NP-40 is 0.0015%, and we showed that full-length recombinant NPC1 bound [^{3}H]cholesterol most efficiently when the NP-40 detergent concentration was below its CMC. On the other hand, [^{3}H]25-HC bound to the protein at NP-40 concentrations up to 1%, which is greater than 600 times the CMC. Figure 2-6*A* shows an experiment examining the effect of NP-40 on the binding of [^{3}H]cholesterol and [^{3}H]25-HC to NPC1(NTD). Binding of [^{3}H]cholesterol was markedly reduced when the detergent concentration exceeded the CMC, whereas [^{3}H]25-HC binding was intact at detergent concentration that were 1000-fold higher. To determine whether this differential sensitivity applied to other detergents, we measured the binding of [^{3}H]cholesterol and [^{3}H]25-HC in the presence of three other detergents at concentrations that were one-sixth of the CMC or 6-fold above the CMC (Figure 2-6*B*). The CMC for each detergent was determined by a dye encapsulation method (22) under conditions that were identical to those of our binding assay, i.e., in buffer C at 4°C. Binding of [^{3}H]cholesterol was intact at the submicellar concentrations of all four detergents examined (NP-40, DDM, DHPC, and CHAPS). In each case, binding was markedly reduced at supramicellar detergent concentrations. This relationship held even though the CMC values for these four detergents varied over a range of nearly 100-fold (0.0015% for NP-40 to 0.2% for CHAPS). On the other hand, [^{3}H]25-HC was unaffected by

the detergents except for CHAPS, which reduced binding at a concentration that was 6-fold above the CMC (Figure 2-6*B*).

Mutational Analysis of NPC1(NTD) – We subjected NPC1(25-264)-His_8-Flag to mutational analysis in order to pinpoint amino acids crucial for sterol binding. We focused on five residues (Q79, N103, Q117, F120, and Y157) that are conserved in 12 vertebrate NPC1 orthologs and that exhibit >75% identity among homologs of NPC1 found in 76 eukaryotic species (data not shown). These residues were also chosen for their hydrogen-bonding potential (Q79, N103, and Q117) or for their ability to form ring-stacking interactions (F120 and Y157). Each of these residues was mutated to alanine (see Figure 2-2*C, red boxes*). The two hydrophobic residues, F120 and Y157, were also mutated to methionine. In addition to these novel mutations, we reproduced six "clinical" mutations corresponding to substitutions in NPC1(NTD) observed in patients with NPC1 disease (Q92R, T137M, P166S, N222S, D242H, and G248V; see Figure 2-2*C*, *blue boxes*) (58). Plasmids encoding each mutant version of NPC1(NTD) were expressed in CHO cells, and the recombinant proteins were purified from the medium in a similar manner to the wild-type version. All mutant proteins were secreted, and they all showed a normal behavior on gel filtration and SDS-PAGE. The data for the Q79A mutant is shown in Figure 2-4.

Of the 14 mutant proteins, only two of the novel mutants, Q79A and Q117A, showed an abnormality in sterol binding. The most striking abnormality was observed with the Q79A mutant, which showed no detectable binding of [^{3}H]25-HC (Figure 2-7*A*) and a 40% decrease in maximal binding of [^{3}H]cholesterol (Figure 2-7*B*). Similar results were obtained in 4 additional experiments involving 3 different preparations of purified NPC1(NTD).

Circular dichroism (CD) spectra of the Q79A protein was identical to that of the wild-type protein, indicating no major structural changes (Figure 2-4*C*). Mutant Q117A also showed a 40% decrease in binding of [^{3}H]cholesterol (Figure 2-7*B*), but only a slight decrease in [^{3}H]25-HC binding (Figure 2-7A). Figures 2-7*C* and 2-7*D* show the binding data for two of the clinical mutants, Q92R and T137M, both of which showed normal binding for both [^{3}H]25-HC and [^{3}H]cholesterol.

Sterol Binding Properties of Recombinant NPC2 and Luminal Domain-1 of NPC1 – About 5% of patients with Niemann-Pick, Type C disease harbor mutations in NPC2, a soluble 132-amino acid protein that is secreted into plasma and also resides within the cell, primarily in lysosomes (46). Previous studies have shown that NPC2 binds cholesterol with measured K_d values that range from 50 nM to 5 μM in different laboratories (23,36,49). To compare the sterol binding properties of NPC1 and NPC2, we prepared a plasmid encoding pCMV-NPC2-His_8, expressed it in CHO cells, and purified the secreted NPC2 using the same procedure as described for NPC1(NTD). The calculated molecular mass of the secreted protein component of NPC2-His_8 is 15.7 kDa. However, purified NPC2-His_8 migrated on SDS-PAGE as 3 distinct bands (23, 21, and 18 kDa) as visualized by Coomassie staining (Figure 2-8*A*). Previous studies showed that NPC2 contains three *N*-linked carbohydrate chains that contain mannose-6-phosphate (17). Treatment of purified NPC2-His_8 with the glycosidase endo H (which removes only high-mannose chains) reduced the molecular mass of band 2 from 21 to 19 kDa and band 3 from 18 to 16 kDa (Figure 2-8*A*), whereas treatment with PNGase F (which removes all *N*-linked chains) reduced all 3 bands to the predicted protein molecular mass of 16 kDa (Figure 2-8*A*). Gel filtration studies of the recombinant

NPC2 showed that it eluted as a single symmetrical peak corresponding to ~20 kDa (data not shown).

When incubated with [^{3}H]cholesterol, NPC2-His$_8$ showed saturable binding with an apparent K_d of ~150 nM (Figure 2-8*C*). The protein did not bind [^{3}H]25-HC (Figure 2-8*B*). This all-or-none difference in binding of [^{3}H]cholesterol *vs.* [^{3}H]25-HC is in contrast to that of NPC1(NTD), which binds both [^{3}H]cholesterol (Figure 2-8*C*) and [^{3}H]25-HC (Figure 2-8*B*).

Competitive binding studies confirmed that NPC2-His$_8$ binds cholesterol but not 25-HC (Figure 2-8*D*). In contrast, as shown earlier in Figure 2-5, NPC1(25-264)-His$_8$-Flag binds both sterols with different affinities (Figure 2-8*E*). The difference in sterol binding properties of NPC1 and NPC2 was further supported by the competition experiments in which epicholesterol competed efficiently for [^{3}H]cholesterol binding to NPC2 (Figure 2-8*D*), but not to NPC1(NTD) (Figure 2-8*E*). Androstenol, a cholesterol analogue that lacks the iso-octyl side chain, did not compete for [^{3}H]cholesterol binding to either NPC1(NTD) or NPC2.

Sterol Binding Properties of Full-length Mutant NPC1(Q79A) – To determine whether the point mutation Q79A that disrupts 25-HC binding in NPC1(NTD) also affects the binding properties of the full-length NPC1 molecule, we expressed and purified the Q79A mutant version of full-length NPC1-His$_8$-Flag in 0.004% NP-40 as described for the wild-type protein in Chapter 1. As shown in the binding curves in Figure 2-9*A*, [^{3}H]25-HC did not bind to the Q79A mutant protein. The Q79A mutant protein also bound very little [^{3}H]cholesterol as compared with the wild-type version (Figure 2-9*B*).

Full-Length Mutant NPC1(Q79A) Restores NPC1 Function to CHO 4-4-19 Cells – The availability of a point mutation in the full-length NPC1 protein that abolishes its 25-HC binding activity provided the opportunity to determine whether oxysterol binding to wild-type NPC1 influences the transport of lipoprotein-derived cholesterol from endosomes/lysosomes to the ER. To test this hypothesis, we transfected wild-type and mutant versions of NPC1-His_8-Flag into CHO 4-4-19 cells, a mutant line of CHO cells with a deficiency of NPC1 function. In these cells, LDL and β-VLDL have a reduced ability to stimulate ACAT activity as measured by cholesteryl [^{14}C]oleate formation in intact cells (18) On the other hand, 25-HC activates ACAT normally in these cells (18). Figure 2-10*A* shows an immunoblot of membrane extracts from CHO 4-4-19 cells that were transfected with cDNAs encoding wild-type and Q79A mutant versions of NPC1-His_8-Flag. As a result of this transient transfection, these cells expressed high levels of both versions of NPC1 as compared to the mock-transfected cells. When the transfected CHO 4-4-19 cells were incubated with β-VLDL, a cholesterol-rich lipoprotein that binds to LDL receptors with high affinity and delivers cholesterol to lysosomes (62), the cholesterol from β-VLDL reached the ER and markedly stimulated cholesteryl [^{14}C]oleate formation in the cells expressing either the wild-type or the Q79A mutant version of NPC1, but not in the cells transfected with a control mock plasmid (Figure 2-10*B*).

In wild-type cells, when cholesterol derived from β-VLDL reaches the ER, it prevents the exit of SREBP-2, thereby blocking its proteolytic processing (29). In mock-transfected CHO 4-4-19 cells, high concentrations of β-VLDL (30 μg protein/ml) did not block SREBP-2 processing (Figure 2-10C. lane 2). In contrast, when the CHO 4-4-19 cells were transfected

with cDNAs encoding either wild-type NPC1 or its Q79A mutant version, β-VLDL blocked SREBP-2 processing at concentrations as low as 1 μg protein/ml (Figure 2-10*D, lanes 4, 11*). All three transfected CHO 4-4-19 cells (mock, NPC1 wild-type, and NPC1 Q79A mutant) responded to 25-HC (Figure 2-10*C, lane 3*; Figure 2-10*D*, *lanes 8* and *15*).

FIGURE 2-1: **Identification of oxysterol-binding site in recombinant human NPC1.** *A*, predicted topology of full-length (*top panel*) and internally deleted NPC1 (*bottom panel*). The domain structure of NPC1 is discussed in Results. *B*, immunoblot analysis of equimolar amounts of full-length (*lane* 1) and NPC1-His_8-Flag (1-307;1254-1278) (*lane* 2). *C*, saturation curves for [^{3}H]25-HC binding to full-length and NPC1-His_8-Flag (1-307;1254-1278). Binding assays were carried out as described under "Experimental Procedures" except that [^{3}H]25-HC and unlabeled 25-HC were solubilized in 1% NP-40 as described in Chapter 1. Each reaction, in a final volume of 120 μl of buffer B (1% NP-40), contained 200 ng of purified human full-length NPC1 (*circles*) or 60 ng of purified internally deleted NPC1 (*triangles*) and 0-300 nM [^{3}H]25-HC (solubilized in 1% NP-40) in the absence (*closed symbols*) or presence (*open symbols*) of 8 mM unlabeled 25-HC (solubilized in 1% NP-40). After incubation for 3 h at 4C°, bound [^{3}H]25-HC was measured using the Ni-NTA agarose binding assay as described under "Experimental Procedures." Each data point represents total binding without subtraction of blank values. *D*, competitive binding of [^{3}H]25-HC to internally deleted NPC1. Each assay tube, in a total volume of 120 ml of buffer B (1% NP-40), contained 300 ng of NPC1-His_8-Flag (1-307;1254-1278), 100 nM [^{3}H]25-HC (solubilized in 1% NP-40), and varying concentrations of the indicated unlabeled sterol (solubilized in 1% NP-40). After incubation for 3 h at 4°C, bound [^{3}H]25-HC was measured as described in *C*. Each data point represents the amount of [^{3}H]25-HC bound relative to that in the control tube, which contained no unlabeled sterol. The "100% of control" value was 247 fmol/tube. 19-HC, 19-hydroxycholesterol; 27-HC, 27-hydroxycholesterol.

FIGURE 2-1

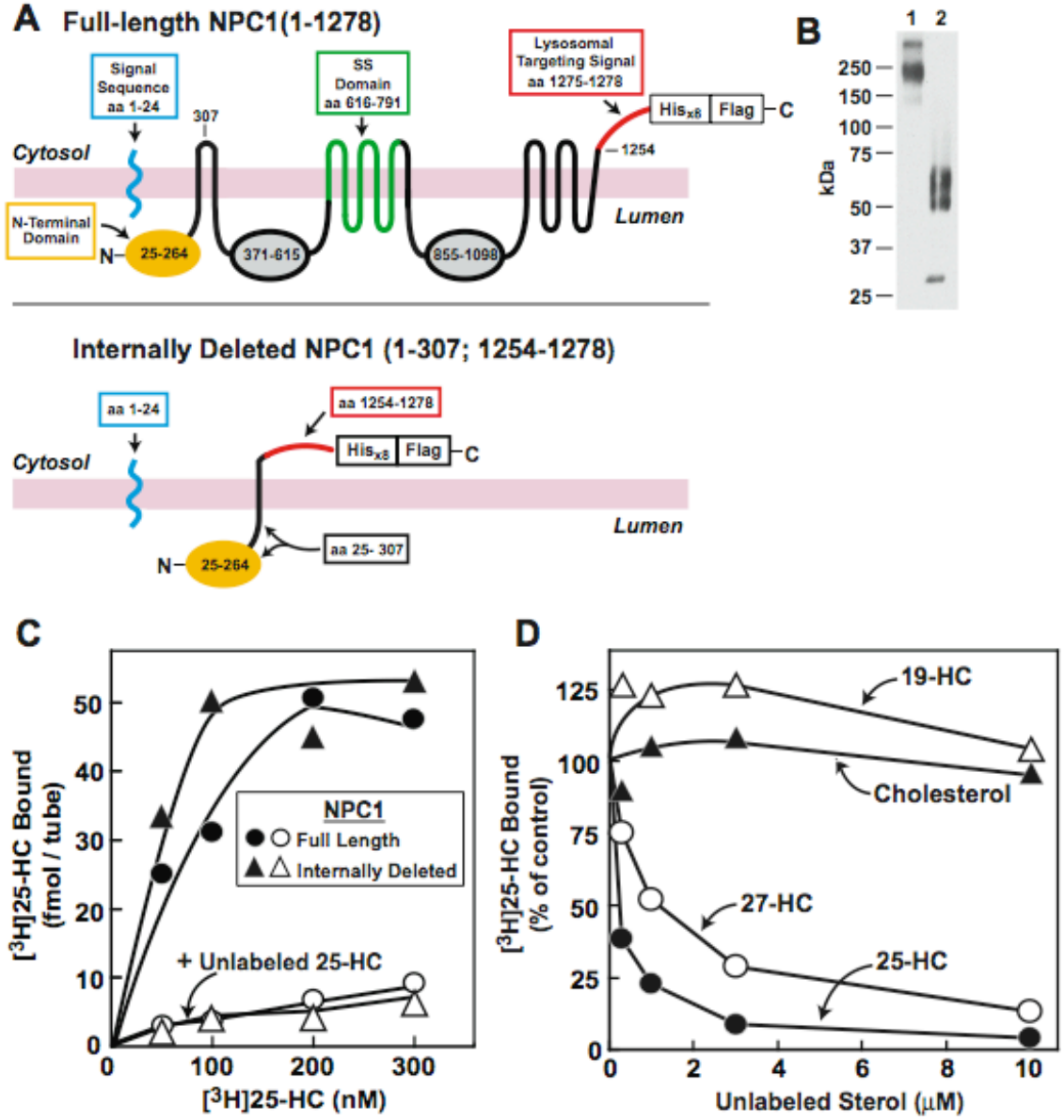
A
Full-length NPC1(1-1278)
Signal Sequence aa 1-24
SS Domain aa 616-791
Lysosomal Targeting Signal aa 1275-1278
307
Cytosol
Lumen
N-Terminal Domain
N
25-264
371-615
855-1098
1254
His x8
Flag
C
B
1 2
250
150
100
75
50
37
25
kDa
Internally Deleted NPC1 (1-307; 1254-1278)
aa 1-24
aa 1254-1278
Cytosol
Lumen
aa 25- 307
C
[3H]25-HC Bound (fmol / tube)
NPC1
Full Length
Internally Deleted
+ Unlabeled 25-HC
[3H]25-HC (nM)
D
[3H]25-HC Bound (% of control)
19-HC
Cholesterol
27-HC
25-HC
Unlabeled Sterol (μM)

FIGURE 2-2: Secretion of NPC1(NTD).

A, diagrammatic illustration of NPC1(25-264)His_8-Flag, showing the cleaved signal sequence (amino acids 1-24) and the secreted soluble domain (amino acids 25-264). *B*, comparison of the amino acid sequence of human NPC1(22-264) with the consensus sequence of NPC1(NTD) from 12 vertebrate species. *Black boxes* denote residues invariant in all 12 vertebrate proteins. *White boxes* denote residues conserved in at least 50% of the aligned vertebrate sequences and are identical to the human sequence. *Yellow boxes* denote cysteine residues. *Red triangles* denote "novel mutations," i.e., alanine or methionine substitutions, created by site-directed mutagenesis. *Blue triangles* denote "clinical mutations," i.e., substitutions corresponding to naturally occurring mutations in patients with NPC1 disease. *Asterisks* (*) denote location of 5 potential *N*-linked glycosylation sites in the human sequence. *C*, immunoblot analysis of secreted NPC1(25-264). On day 0, CHO-K1 cells were set up and transfected with 5 μg pcDNA3.1 (mock), 5 μg pCMV-NPC1-His_8-Flag, 5 μg pCMV-NPC1(1-307;1254-1278)-His_8-Flag, or 5 μg pCMV-NPC1(1-264)-His_8-FLAG as described in "Experimental Procedures." After incubation for 48 h at 37°C, the medium was collected, and the cells were washed and homogenized through a 1-ml syringe with a 22-gauge needle in 0.6 ml of buffer D. The homogenate was centrifuged at 10^5g, after which the supernatant was collected and the pellet was solubilized in 10 mM Tris-chloride at pH 7.4, 100 mM NaCl, and 1% SDS and shaken at 37°C overnight. Fractions of medium (m), supernatant (s), and 10^5g pellet (p) were applied to the gel in a 1:5:5 ratio, respectively, and then subjected to 8% SDS/PAGE and immunoblot analysis using monoclonal anti-Flag antibody. The filter was exposed to X-ray film for 30 s.

FIGURE 2-2

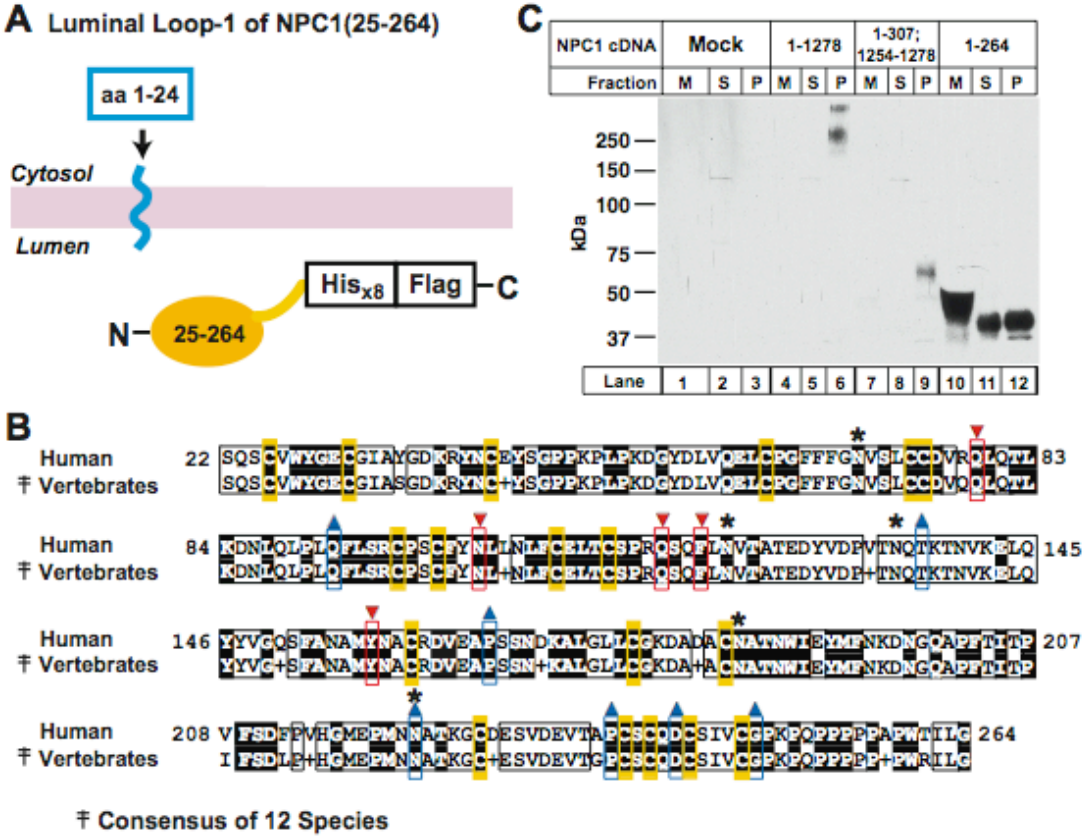
A Luminal Loop-1 of NPC1(25-264)
aa 1-24
Cytosol
Lumen
His x8
Flag
C
N
25-264
C
NPC1 cDNA
Mock
1-1278
1-307; 1254-1278
1-264
Fraction
M S P M S P M S P M S P
kDa
250
150
100
75
50
37
Lane
1 2 3 4 5 6 7 8 9 10 11 12
B
Human
Vertebrates
22
83
84
145
146
207
208
264
Consensus of 12 Species

FIGURE 2-3: Sequence alignment of NPC1(NTD) from 12 vertebrate species.

Sequence homologs of the NTD of NPC1 were identified by using blastp or PSI BLAST on the non-redundant protein database or by using tblastn on various eukaryotic genomic databases (2,3). Translated sequences from tblastn searches of nucleotide databases were assembled manually, based on the amino acid composition and spacing of the query protein sequence. The resulting amino acid sequences of all NPC1 homologs were aligned using MAFFT E-ins-i strategy (34).

FIGURE 2-3

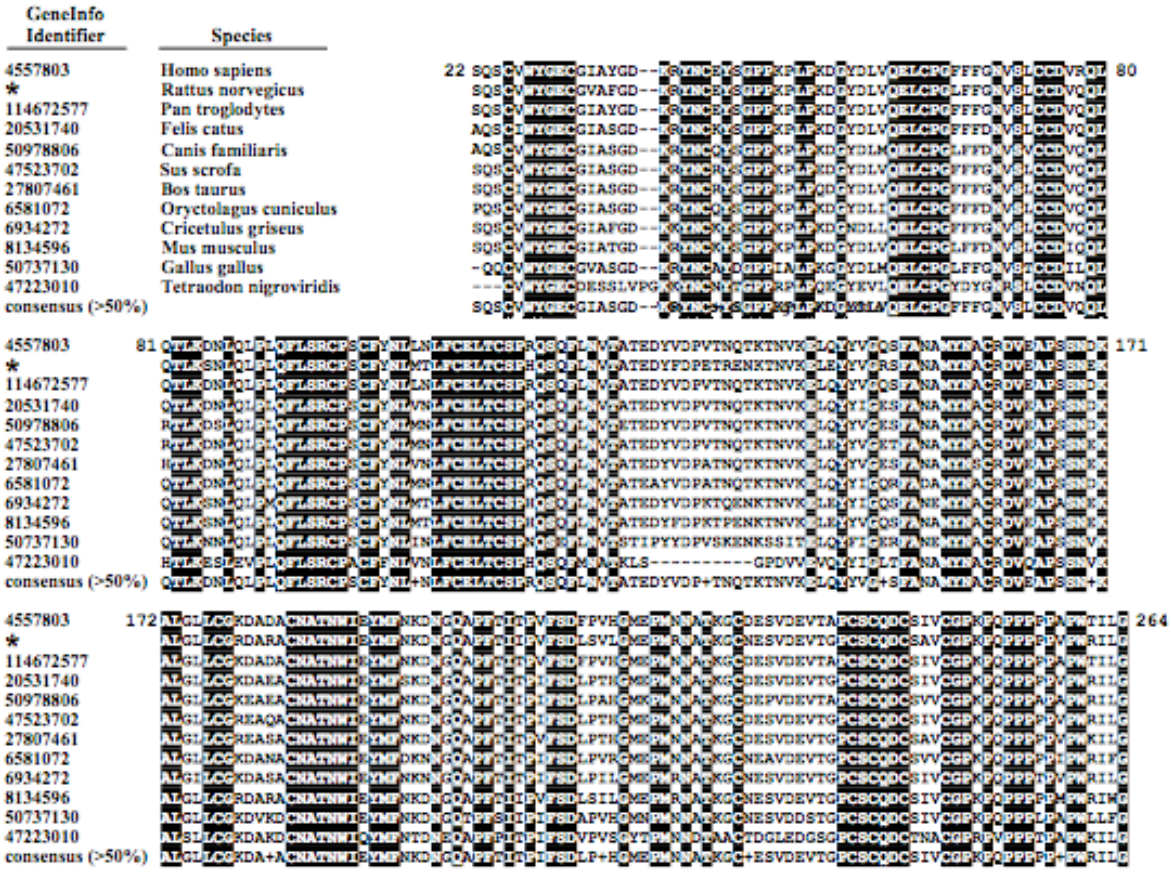

* Rattus norvegicus was translated from its genome sequence based on similarity to the Mus musculus sequence using "tblastn", and the translated pieces were assembled manually.

(This data reproduced with permission by Lisa Kinch and Nick Grishin)

FIGURE 2-4: Characterization of secreted NPC1(NTD).

A, Coomassie staining. Recombinant NPC1(NTD) proteins were purified in two steps as described in "Experimental Procedures." Aliquots (5 μg) of wild-type and the Q79A mutant version of NPC1(25-264)-His_8-Flag were subjected to 8% SDS/PAGE, and the proteins were visualized with Coomassie brilliant blue R-250 stain (Bio-Rad). Molecular masses of protein standards are indicated. *B*, gel filtration chromatography of purified proteins. Buffer C (0.5 ml) containing 6 mg of either wild-type or Q79A mutant version of NPC1(25-264)-His_8-Flag was loaded onto a 10/300 Superdex 200 column and chromatographed at a flow rate of 0.5 ml/min. Absorbance at 280 nm was monitored continuously to identify the indicated NPC1 protein. Standard molecular mass markers (thyroglobulin, 670 kDa; γ-globulin, 158; ovalbumin, 44; myoglobin, 17; and vitamin B12, 1.35) were chromatographed on the same column (arrows). The apparent molecular mass of NPC1(25-264)-His_8-Flag is ~100 kDa. *C*, circular dichroism of 200 mg of wild-type or Q79A mutant version of NPC1(25-264)-His_8-Flag in buffer C was measured on an Aviv 62DS spectrometer using a 2-mm path length cuvette. The data shown represent the averaged values from 9 spectra.

FIGURE 2-4

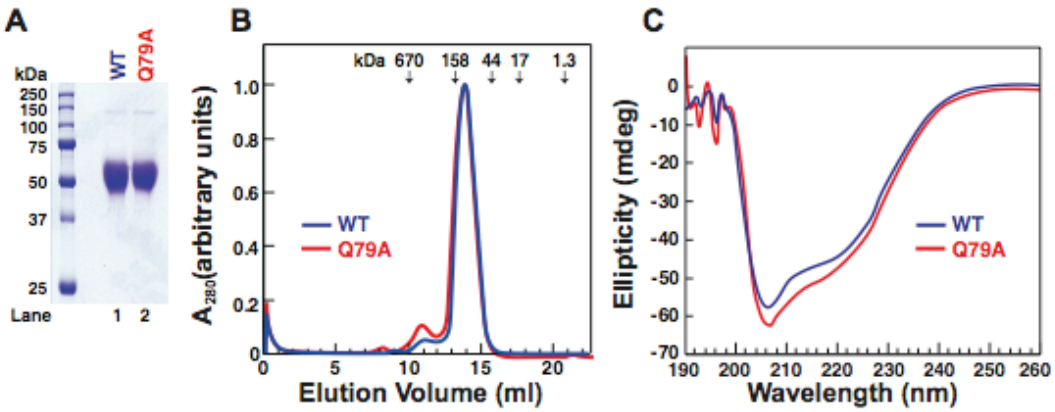
A
kDa
WT
Q79A
250
150
100
75
50
37
25
Lane
1 2
B
kDa 670 158 44 17 1.3
A_{280}(arbitrary units)
1.0
0.8
0.6
0.4
0.2
0
WT
Q79A
0 5 10 15 20
Elution Volume (ml)
C
Ellipticity (mdeg)
0
-10
-20
-30
-40
-50
-60
-70
WT
Q79A
190 200 210 220 230 240 250 260
Wavelength (nm)

FIGURE 2-5: [^{3}H]25-HC and [^{3}H]cholesterol binding activities of purified NPC1(NTD).

A and *B*, saturation curves for NPC1(NTD) binding of [^{3}H]25-HC and [^{3}H]cholesterol. Each reaction, in a final volume of 80 ml of buffer A (0.004% NP-40), contained 100 ng of purified human NPC1(25-264)-His_8-Flag, 1 μg of BSA, and 10-300 nM of either [^{3}H]25-HC (*A*) or [^{3}H]cholesterol (*B*) both delivered in ethanol, in the absence (black) or presence of 3 mM unlabeled 25-HC (blue) or cholesterol (red) as indicated. After incubation for 4 h at 4°C, bound [^{3}H]25-HC (*A*) or [^{3}H]cholesterol (*B*) was measured using the Ni-NTA agarose binding assay as described under "Experimental Procedures." Each data point is the average of duplicate assays and represents total binding without subtraction of blank values. *C* and *D*, competitive binding of [^{3}H]25-HC (*C*) and [^{3}H]cholesterol (*D*) to NPC1(25-264). Each assay tube, in a total volume of 80 ml of buffer A (0.004% NP-40), contained 100 ng NPC1(25-264)-His_8-Flag, 1 μg of BSA, either 10 nM [^{3}H]25-HC (*C*) or 130 nM [^{3}H]cholesterol (*D*), and varying concentrations of the indicated unlabeled sterol. After incubation at 4°C for 16 h, bound [^{3}H]25-HC (*C*) or [^{3}H]cholesterol (*D*) was measured using the Ni-NTA agarose binding assay. Each data point is the average of duplicate assays and represents the amount of ^{3}H-sterol bound relative to that in the control tube, which contained no unlabeled sterol. The "100% of control" values were 340 fmol/tube (*C*) and 580 fmol/tube (*D*). Blank values of 3 fmol/tube (*C*) and 68 fmol/tube (*D*) were subtracted from these values.

FIGURE 2-5

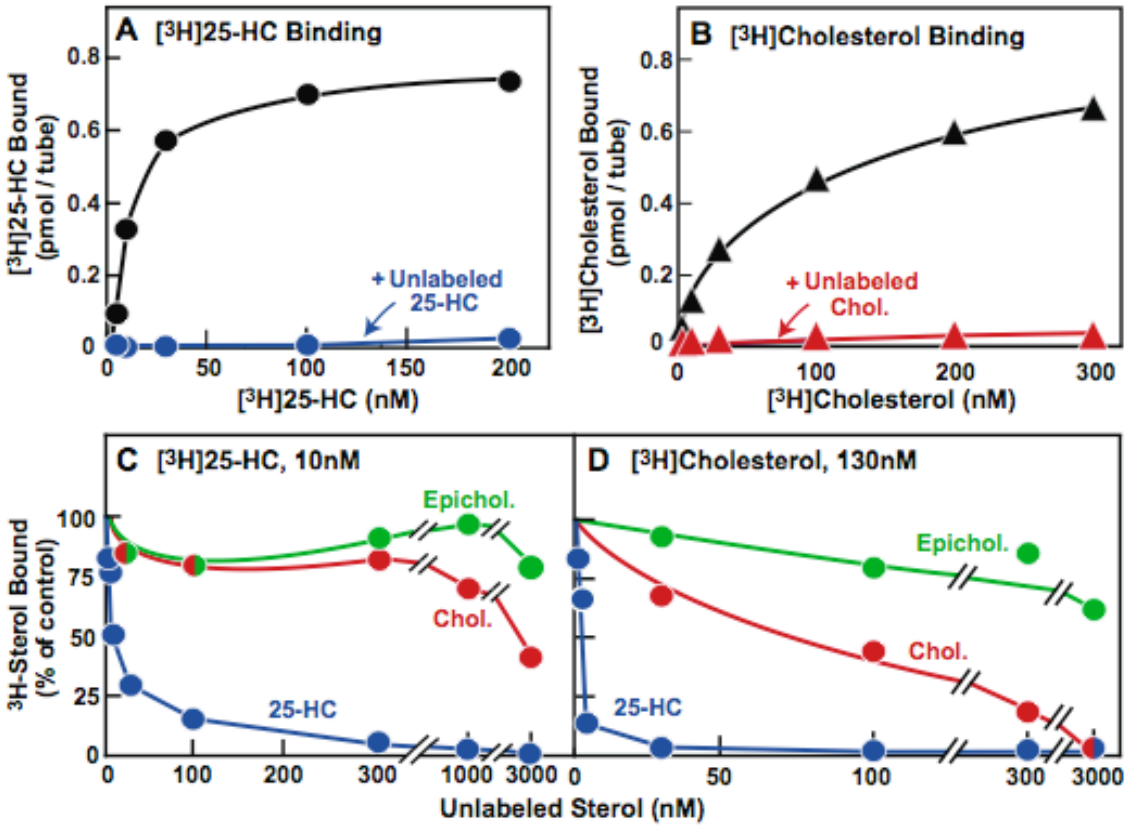
A [3H]25-HC Binding
[3H]25-HC Bound (pmol / tube)
0.8
0.6
0.4
0.2
0
+ Unlabeled 25-HC
0
50
100
150
200
[3H]25-HC (nM)
B [3H]Cholesterol Binding
[3H]Cholesterol Bound (pmol / tube)
0.8
0.6
0.4
0.2
0
+ Unlabeled Chol.
0
100
200
300
[3H]Cholesterol (nM)
C [3H]25-HC, 10nM
3H-Sterol Bound (% of control)
100
75
50
25
0
Epichol.
Chol.
25-HC
0
100
200
300
1000
3000
D [3H]Cholesterol, 130nM
Epichol.
Chol.
25-HC
0
50
100
300
3000
Unlabeled Sterol (nM)

FIGURE 2-6: Detergent effects on ^{3}H-sterol binding activity of NPC1(NTD).

A and *B,* each assay tube, in a total volume of 80 ml of buffer C supplemented with the indicated detergent (see below), contained 100 ng NPC1(25-264)-His_8-Flag, 1 μg of BSA, and 200 nM [^{3}H]25-HC (▲) or [^{3}H]cholesterol (●). After incubation at 4°C for 4 h, bound [^{3}H]25-HC or [^{3}H]cholesterol was measured using the Ni-NTA agarose binding assay. Each data point is the average of duplicate values and represents the amount of ^{3}H-sterol bound relative to that in the control tube, which contained no detergent. *A*, buffer C was supplemented with the indicated concentration of NP-40. The "100% of control" values were 391 and 236 fmol/tube for [^{3}H]cholesterol and [^{3}H]25-HC, respectively. *B*, buffer C was supplemented with the indicated detergent concentrations relative to its CMC. The CMC's, determined in buffer C at 4°C, were as follows: NP-40, 0.0015%; DDM, 0.002%; DHPC, 0.06%; and CHAPS, 0.2%. The "100% of control" values for [^{3}H]cholesterol and [^{3}H]25-HC were 237 fmol/tube and 511 fmol/tube, respectively.

FIGURE 2-6

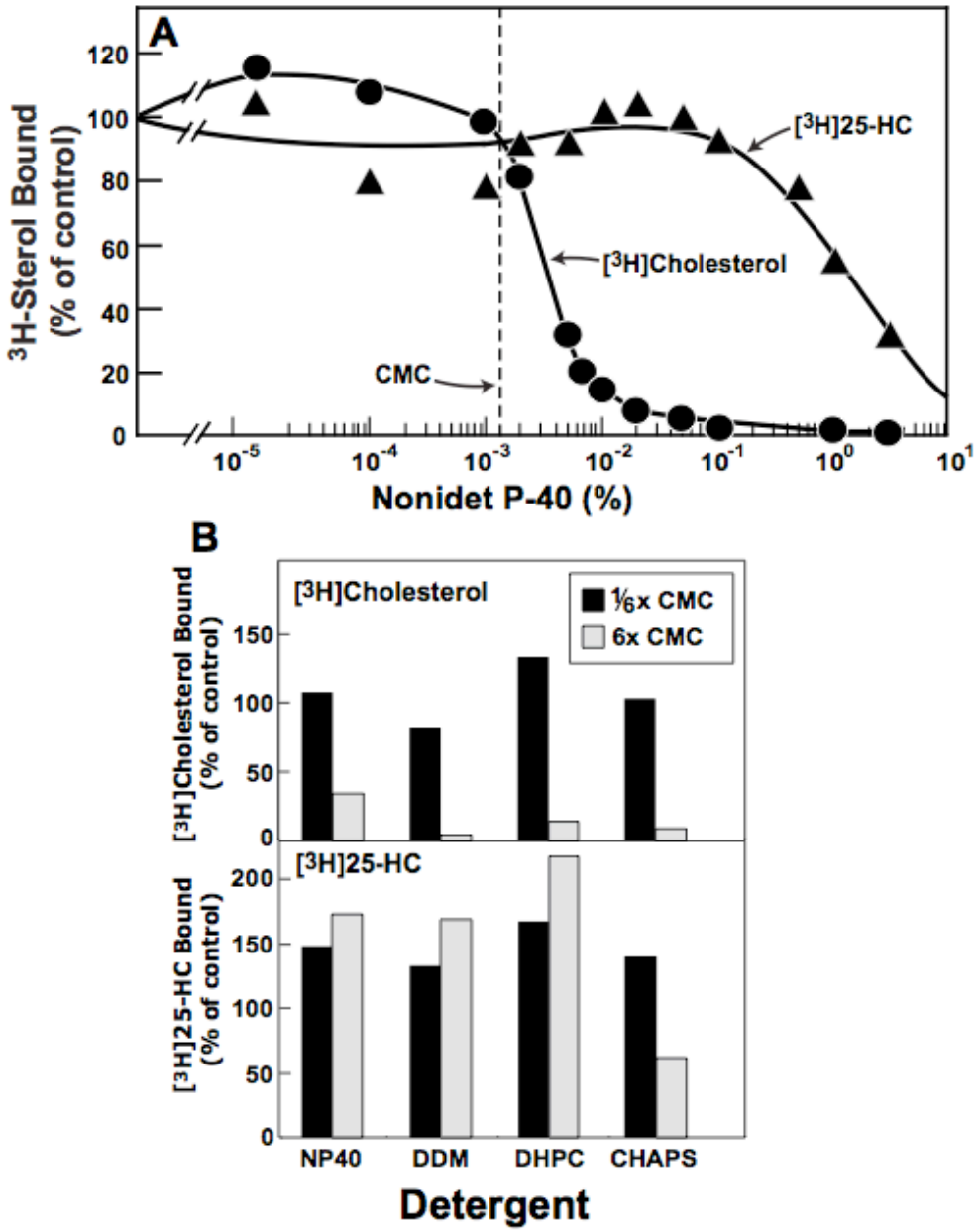
A
120
100
80
60
40
20
0
^{3}H-Sterol Bound
(% of control)
[^{3}H]25-HC
[^{3}H]Cholesterol
CMC
10^{-5}
10^{-4}
10^{-3}
10^{-2}
10^{-1}
10^{0}
10^{1}
Nonidet P-40 (%)
B
[^{3}H]Cholesterol
1/6x CMC
6x CMC
[^{3}H]Cholesterol Bound
(% of control)
150
100
50
0
[^{3}H]25-HC
[^{3}H]25-HC Bound
(% of control)
200
150
100
50
0
NP40
DDM
DHPC
CHAPS
Detergent

FIGURE 2-7: [^{3}H]25-HC and [^{3}H]cholesterol binding to versions of NPC1 corresponding to novel mutations in conserved residues and clinical mutations in patients with NPC1.

A-D, saturation curves for ^{3}H-sterol binding to wild-type and mutant NPC1 proteins. Each reaction, in a final volume of 80 ml of buffer A (0.004% NP-40), contained 100 ng of purified wild-type or the indicated mutant version of NPC1(25-264)-His_8-Flag, 1 μg of BSA, and 10-300 nM of either [^{3}H]25-HC (*A* and *C*) or [^{3}H]cholesterol (*B* and *D*), both delivered in ethanol. After incubation for 4 h at 4°C, bound [^{3}H]25-HC (*A*) or [^{3}H]cholesterol (*B*) was measured using the Ni-NTA agarose binding assay as described under "Experimental Procedures." Each data point is the average of duplicate assays and represents total binding without subtraction of blank values.

FIGURE 2-7

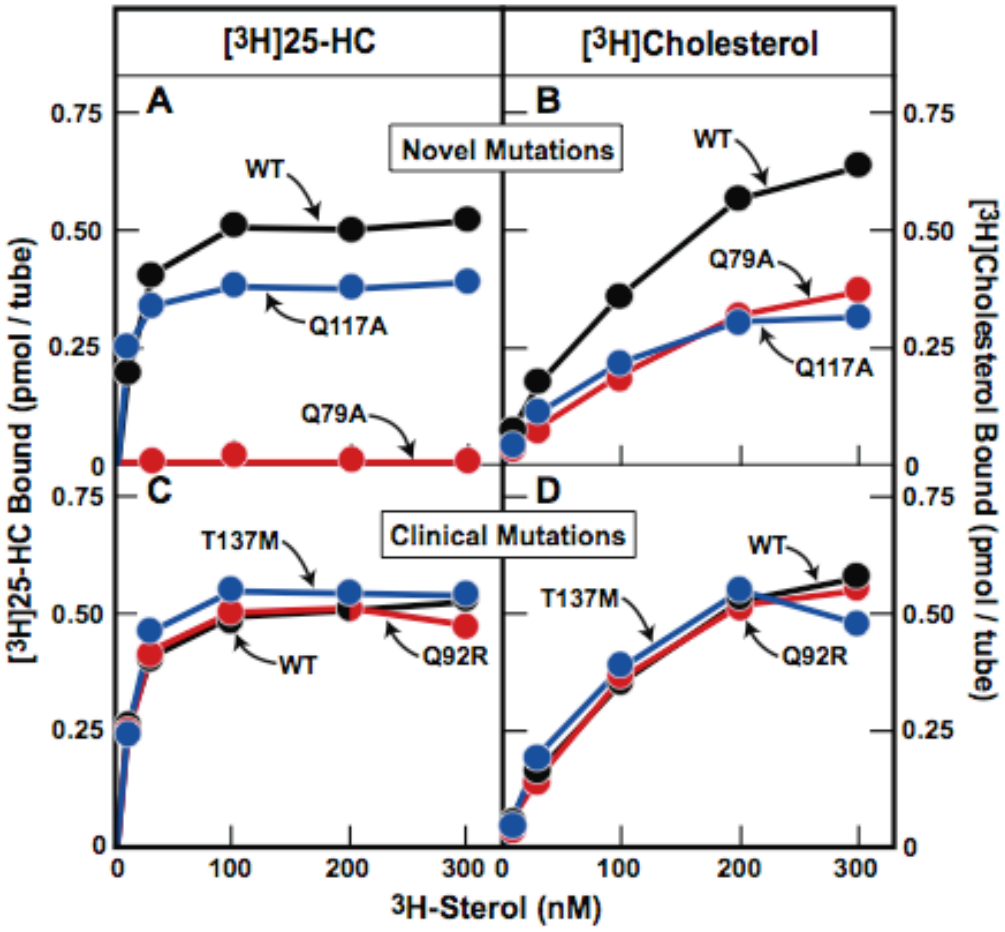
[3H]25-HC
[3H]Cholesterol
A
B
C
D
Novel Mutations
Clinical Mutations
WT
Q117A
Q79A
T137M
Q92R
0.75
0.50
0.25
0
100
200
300
[3H]25-HC Bound (pmol / tube)
[3H]Cholesterol Bound (pmol / tube)
3H-Sterol (nM)

FIGURE 2-8: Comparison of the ^{3}H-sterol binding activities of purified NPC1(NTD) and purified NPC2.

A, Coomassie staining of purified NPC2 before and after glycosidase treatment. Purified NPC2-His_8 (7.6 μg) was treated with or without Endo H or PNGase F as described under "Experimental Procedures" and then subjected to 15% SDS-PAGE, and the proteins were visualized with Coomassie brilliant blue R-250. Molecular masses of protein standards are indicated. *Asterisks* (*) denote the migration of Endo H (*lane 2*) and PNGase *F* (*lane 3*). *Bands 1-3* denote different glycosylated forms of purified NPC2-His_8. *B* and *C*, saturation curves for binding of ^{3}H-sterols to NPC1(NTD) and NPC2. Each reaction, in a final volume of 80 ml of buffer A (0.004% NP-40), contained either 290 ng of purified human NPC2 (▲) or 200 ng of purified human NPC1(25-264)-His_8-Flag (●), 1 μg of BSA, and 0-400 nM of [^{3}H]25-HC (*B*) or [^{3}H]cholesterol (*C*), both delivered in ethanol. After incubation at 4°C for 16 h, bound ^{3}H-sterols were measured using the Ni-NTA agarose binding assay as described under "Experimental Procedures" except that the column washes were done with buffer A. Each data point is the average of duplicate values and represents total binding without subtraction of blank values. *D* and *E*, competitive binding of [^{3}H]cholesterol to NPC2 and NPC1(25-264). Each assay tube, in a total volume of 80 μl of buffer A (0.004% NP-40), contained either 200 ng of NPC2-His_8 (*D*) or 150 ng of NPC1(25-264)-His8-Flag (*E*), 1 μg of BSA, 200 nM [^{3}H]cholesterol, and varying concentrations of the indicated unlabeled sterol. After incubation for 4 h at 4°C, bound [^{3}H]cholesterol was measured as described above. Each data point is the average of duplicate assays and represents the amount of [^{3}H]cholesterol bound relative to that in the control tube, which contained no unlabeled

sterol. The "100% of control" values were 1221 fmol/tube (*D*) and 1279 fmol/tube (*E*). Blank values of 73 fmol/tube (*D*) and 109 fmol/tube (*E*) was subtracted from this value.

FIGURE 2-8

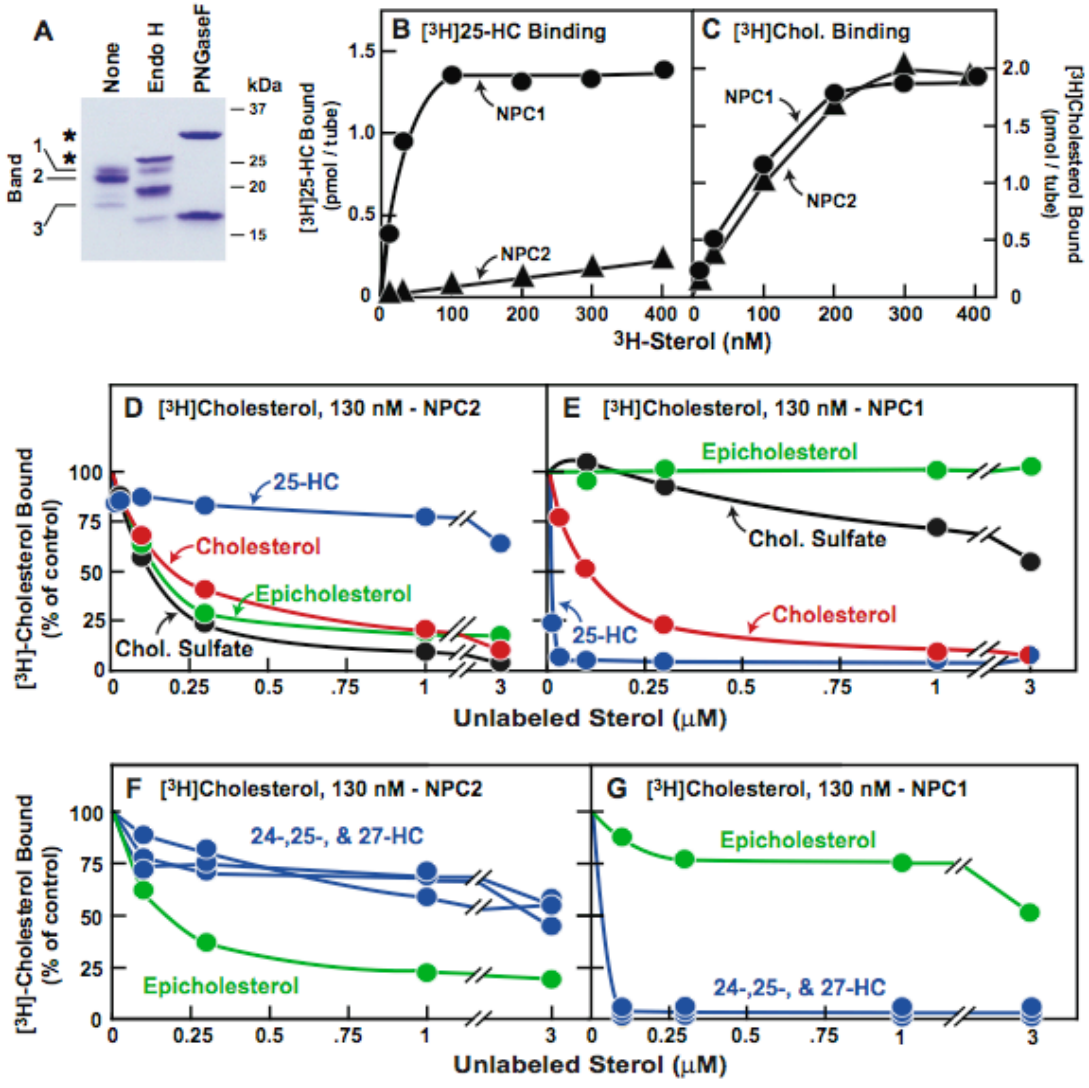

FIGURE 2-9: [^{3}H]25-HC and [^{3}H]cholesterol binding activities of wild-type and mutant Q79A versions of full-length NPC1.

Each reaction, in a final volume of 80 ml of buffer C (no NP-40), contained ~50 ng of human NPC1-His$_8$-Flag (●) or NPC1-His$_8$-Flag(Q79A) (▲) purified in 0.004% NP-40, 1 μg of BSA, and 10-300 nM of either [^{3}H]25-HC (*A*) or [^{3}H]cholesterol (*B*), both delivered in ethanol. The final combination of NP-40 was ~0.0008%. After incubation for 16 h at 4°C, bound [^{3}H]25-HC (*A*) or [^{3}H]cholesterol (*B*) was measured using the Ni-NTA agarose binding assay as described under "Experimental Procedures." Each data point is the average of duplicate assays and represents total binding without subtraction of blank values.

FIGURE 2-9

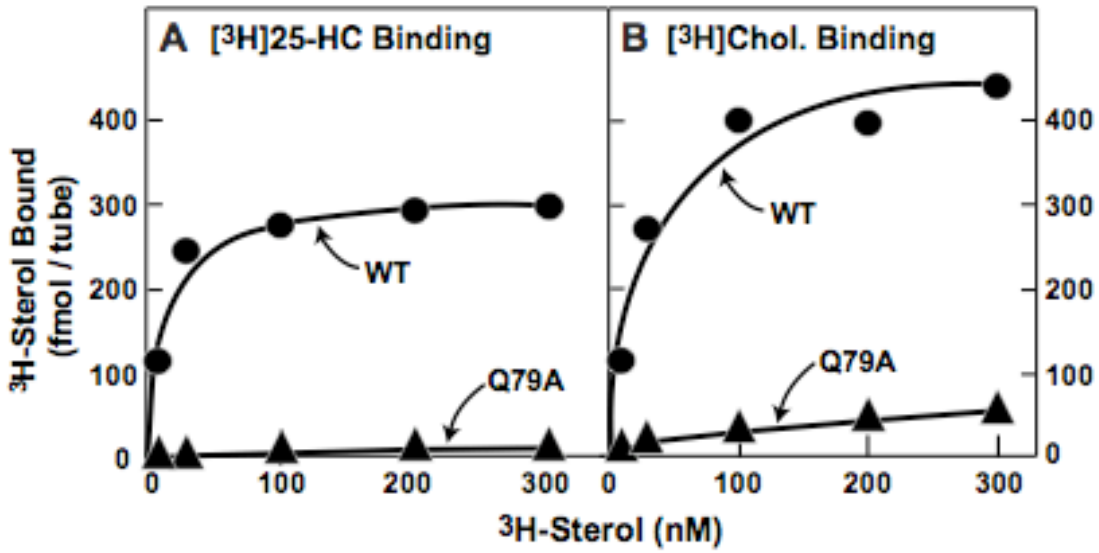

FIGURE 2-10: Regulatory actions of transfected wild-type and mutant Q79A versions of full-length NPC1 in mutant CHO 4-4-19 cells defective in NPC1.

On day 0, mutant CHO 4-4-19 cells were set up in medium A containing 5% FCS as described in "Experimental Procedures." *A*, immunoblot analysis of NPC1 proteins. On day 2, the cells were transfected with 2 μg pcDNA3.1 (mock, M) or 2 μg of wild-type or mutant Q79A version of pCMV-NPC1-His_8-Flag as described in "Experimental Procedures." On day 3, the cells were harvested, and whole cell extracts were prepared (1) and processed for immunoblot analysis of the indicated proteins. *B*, cholesterol esterification assay in mutant CHO cells. On day 2, the cells were transfected as described in *A*. On day 3, the medium was switched to medium A containing 5% newborn calf LPDS, 5 μM compactin, and 50 μM sodium mevalonate. On day 4, the medium was switched to medium A supplemented with 5% newborn calf LPDS and the indicated concentration of β-VLDL. After incubation for 5 h at 37°C, each monolayer was pulse-labeled for 2 h with 0.2 mM sodium [^{14}C]oleate (6446 dpm/pmol). The cells were then harvested for measurement of their content of cholesteryl [^{14}C]oleate and [^{14}C]triglycerides as described under "Experimental Procedures." Each value is the average of duplicate incubations. The cellular content of [^{14}C]triglycerides (data not shown in Figure) for mock, NPC1 wild-type, or NPC1(Q79A) transfected cells incubated with 10 μg protein/ml of β-VLDL were 209, 184, and 194 nmol/h per mg, respectively. *C*, immunoblot analysis of SREBP-2 in mutant CHO cells overexpressing SREBP-2. On day 2, the cells were transfected with 3 μg of pTK-HSV-BP2. *D,* immunoblot analysis of SREBP-2 cleavage in mutant CHO cells overexpressing full-length NPC1 (wild-type or Q79A). On day 2, the cells were either mock transfected with pcDNA3.1 (M) or co-transfected with 3 μg

pTK-HSV-BP-2 together with 2 μg of either wild-type or mutant Q79A version of pCMV-NPC1-Flag. *C* and *D*, on day 3, the medium was switched to medium A supplemented with 5% newborn calf LPDS, 5 μM compactin, and 50 μM sodium mevalonate. On day 4, the medium was switched to medium A supplemented with 5% newborn calf LPDS with the indicated concentration of β-VLDL or 1 μg/ml of 25-HC. After incubation for 6 h, the cells were harvested and processed for immunoblot analysis of the indicated proteins. *A* and *C*, all filters were exposed on X-ray film for 5-10 s except for the nuclear SREBP-2 filter, which was exposed for 20 s.

FIGURE 2-10

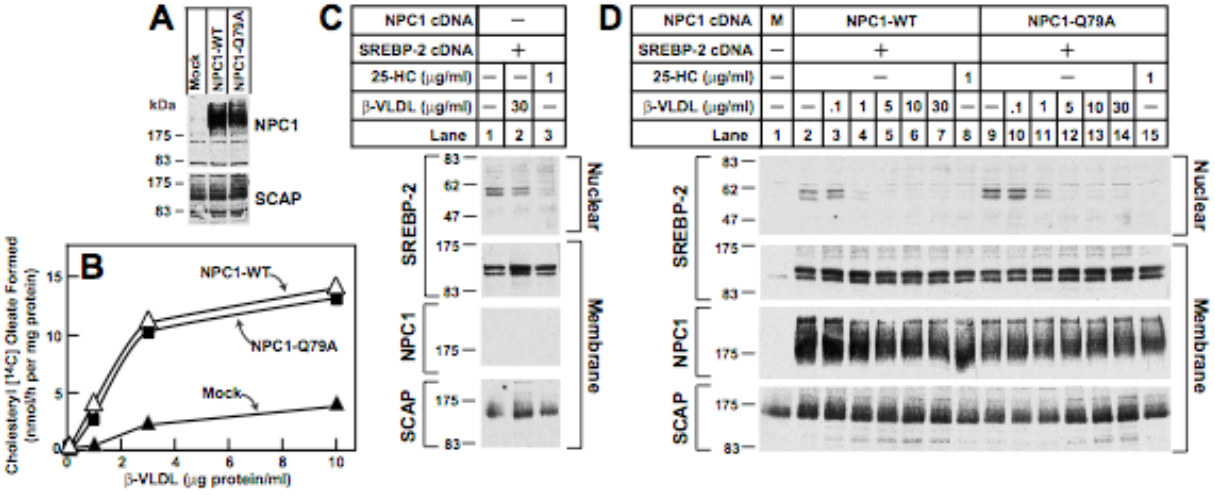

(This data reproduced with permission by Lina Abi-Mosleh)

DISCUSSION

The current data reveal a saturable sterol binding site on the N-terminus of human NPC1. The importance of this 240-amino acid luminal, soluble protein is revealed by its strong sequence conservation in all vertebrate orthologs of NPC1 and in related proteins from eukaryotes as remote as yeast. When isolated as a soluble, secreted protein, this domain appears to form a homodimer as indicated by gel filtration. At saturation, one molecule of cholesterol or 25-HC is bound to each dimer of NPC1(NTD). Under the conditions of our *in vitro* assay, the affinity for 25-HC (K_d, 10 nM) was 13-fold higher than the affinity for [^{3}H]cholesterol (K_d, 130 nM). Consistent with this difference, 25-HC was an effective competitor of cholesterol binding, whereas cholesterol was a poor competitor for 25-HC binding.

As we observed with full-length NPC1, binding of cholesterol, but not 25-HC to NPC1(NTD) was sensitive to the concentration of detergent in the assay. Cholesterol binding was abolished by supramicellar concentrations of a variety of detergents, including uncharged detergents (NP-40 and DDM) and zwitterionic detergents (DHPC and CHAPS) (Figure 2-6*B*). Of these detergents, CHAPS was the only one that partially reduced binding of 25-HC. We interpret this finding to indicate that cholesterol has a tendency to partition into micelles rather than to bind to NPC1(NTD). If manifest within cells, this tendency might be important in regulating the ability of NPC1 to move cholesterol from one membrane compartment to another.

In this regard, it is interesting that NPC2 has been shown to transfer its bound cholesterol to phospholipid liposomes in a reaction that is accelerated by a phospholipid, bis(monooleoylglycerol)phosphate (16). This observation was possible because Cheruku, et al. (16) observed that cholesterol binding quenches the tryptophan fluorescence of NPC2. In preliminary studies, we found that 25-HC binding to NPC1(NTD) does not alter its tryptophan fluorescence. Other methods will have to be employed to test the ability of NPC1(NTD) to transfer its bound sterols to membranes.

In the current studies, we found evidence that NPC1(NTD) is the sole oxysterol-binding site on NPC1, at least under the conditions of our *in vitro* assays. Thus, a point mutation in NPC1(NTD) (Q79A) abolished binding of 25-HC to the soluble NPC1(NTD) (Figure 2-7*A*), and it also abolished binding to full-length recombinant NPC1 (Figure 2-9*A*). The situation with regard to cholesterol binding is less clear. When produced in soluble NPC1(NTD), the Q79A mutation reduced binding of [^{3}H]cholesterol by about 40% (Figure 2-7*B*), yet this mutation in full-length NPC1 abolished binding of [^{3}H]cholesterol completely (Figure 2-9*B*). This difference could be attributable to the sensitivity of the cholesterol binding reaction to the presence of detergents. It is possible that the Q79A mutation impairs cholesterol binding to the extent that it becomes more sensitive to the presence of even small amounts of detergent, and that the full-length protein has more detergent bound to it than does the soluble protein. The important question of whether NPC1(NTD) is the sole cholesterol binding site on NPC1 will not be resolved until *in vitro* assays can be performed with NPC1 in a more normal environment, either *in situ* in isolated membranes or after reconstitution in liposomes.

The difference in the specificity of sterol binding between NPC1 and NPC2 suggests major differences in the sterol binding pocket of the two proteins. Whereas NPC1(NTD) of NPC1 and NPC2 both bound [^{3}H]cholesterol with similar affinities, only NPC1 bound [^{3}H]25-HC (Figure 2-8*B*). Moreover, binding of [^{3}H]cholesterol to NPC2 was inhibited by epicholesterol, whereas binding to NPC1(NTD) was not inhibited. The crystal structure of cholesterol sulfate bound to NPC2 provides an explanation for the specificity of NPC2's binding reaction (70). The cholesterol moiety binds with its hydrophobic side chain deeply embedded in a hydrophobic pocket that molds itself to accommodate the side chain and would not be expected to tolerate the presence of a polar hydroxyl. On the other hand, the 3-hydroxyl of cholesterol is fully exposed to solvent, and therefore the binding would not be disrupted by the α-orientation of this hydroxyl in epicholesterol. The sterol binding site on NPC1(NTD) must be quite different. This site must be able to accommodate polar groups on the side chain since the addition of a 25-hydroxyl group increases the affinity of binding by 13-fold. The site must also recognize the 3-hydroxyl on the other end of the cholesterol molecule since binding strongly prefers the β-orientation. It should be possible to define the sterol binding site crystallographically since it is possible to produce large amounts of soluble, secreted NPC1(NTD).

CHAPTER THREE

NPC2 FACILITATES BIDIRECTIONAL TRANSFER OF CHOLESTEROL BETWEEN NPC1 AND LIPID BILAYERS

SUMMARY

Egress of lipoprotein-derived cholesterol from lysosomes requires two lysosomal proteins, polytopic membrane-bound Niemann-Pick C1 (NPC1) and soluble Niemann-Pick C2 (NPC2). The reason for this dual requirement is unknown. Previously, we showed that the soluble luminal N-terminal domain of NPC1 (amino acids 25-264) binds cholesterol. This N-terminal domain (NTD) is designated NPC1(NTD). We and others showed that soluble NPC2 also binds cholesterol. Here, we establish an *in vitro* assay to measure transfer of [^{3}H]cholesterol between these two proteins and phosphatidylcholine liposomes. Whereas NPC2 rapidly donates or accepts cholesterol from liposomes, NPC1(NTD) acts much more slowly. Bidirectional transfer of cholesterol between NPC1(NTD) and liposomes is accelerated more than 100-fold by NPC2. A naturally-occurring human mutant of NPC2 (Pro120Ser) fails to bind cholesterol and fails to stimulate cholesterol transfer from NPC1(NTD) to liposomes. NPC2 may be essential to deliver or remove cholesterol from NPC1, an interaction that links both proteins to the cholesterol egress process from lysosomes. These findings may explain how mutations in either protein can produce a similar clinical phenotype.

INTRODUCTION

NPC disease has been traced to mutations in either one of two genes, both of whose products are required for cholesterol export from lysosomes. These genes, *NPC1* and *NPC2*, encode a lysosomal membrane protein and a lysosomal soluble protein, respectively (11,46). It appears that both gene products function in a coordinated pathway of cholesterol egress from the lysosome, because homozygous loss-of-function mutations in either gene cause a similar NPC phenotype (51).

Of the two NPC proteins, NPC2 is the more well-studied. NPC2 has been shown to bind cholesterol and derivatives such as cholesterol sulfate (8-10). X-ray crystallography reveals that cholesterol sulfate binds in such a manner that the iso-octyl side chain of the sterol is deeply buried in a hydrophobic pocket and the sulfate on the 3 position of the A ring is exposed to solvent (70). As shown in Chapter 2, introduction of a hydrophilic moiety, such as a hydroxyl group, on the cholesterol side chain prevents binding (33). On the other hand, changing the configuration of the 3-hydroxyl group, as with cholesterol sulfate or epicholesterol, does not reduce binding (33). Because of its ability to bind cholesterol, NPC2 can transfer cholesterol from one liposome to another (4). This transfer is accelerated in the presence of anionic phospholipids such as bis(monooleoylglycero)phosphate and phosphatidyl inositol, which are found in lysosomes (4, 16).

Recently, the NPC1 protein has come under study as a result of its purification from rabbit liver membrane as described in Chapter 1. The 1254 amino acids of the mature

protein (after removal of its signal peptide) are organized into 13 putative membrane-spanning helices separated by 12 cytosolic or luminal loops (19). A noteworthy feature is the presence of three large luminal domains. The first luminal domain consists of the N-terminal 240 amino acids (residues 25-264) whose N-terminus lies free in the lumen after cleavage by signal peptidase. We designate this sequence as the N-terminal domain, i.e., NPC1(NTD), which is the most highly conserved sequence in the full length protein (11). The second and third luminal domains are loops that connect transmembrane helices 2/3 and 8/9, respectively. Full-length NPC1 was shown to bind cholesterol with saturation kinetics in Chapter 1(32), and the binding site was localized to the NPC1(NTD) in Chapter 2 (33). NPC1(NTD) was prepared as a soluble secreted protein by transfecting cells with a cDNA encoding the signal sequence (amino acids 1-24), followed by amino acids 25-264, followed by a an epitope tag (33). In direct contrast to the findings with NPC2, sterol binding to NPC1(NTD) was not blocked by addition of hydroxyl groups to the 24, 25, or 27 positions on the iso-octyl side chain (33). Indeed, these modifications increased the apparent affinity for the protein. On the other hand, binding was abolished when the 3-hydroxyl was switched from the ß to the α orientation. These findings led to the suggestion that NPC1(NTD) binds primarily to the A ring, whereas NPC2 binds to the opposite end of the sterol, namely the iso-octyl side chain (33).

The current study addresses the question of how NPC1(NTD) and NPC2 interact in the transfer of cholesterol. In agreement with previous findings (4, 16), we show that the on-rate and off-rate of cholesterol from NPC2 is rapid. In sharp contrast, the on- and off-rates of cholesterol from NPC1(NTD) are slow, even in the presence of liposomal membranes.

NPC2 accelerates both the binding and release of cholesterol by NPC1(NTD). These findings suggest that NPC2 functions to transfer cholesterol to and/or from NPC1, thereby explaining the requirement for both proteins in the exit of LDL-cholesterol from lysosomes.

EXPERIMENTAL PROCEDURES

Materials - We obtained [1,2,6,7-^{3}H]cholesterol (60 Ci/mmol) from American Radiolabeled Chemicals; anti-FLAG M2-agarose affinity beads and monoclonal anti-FLAG M2 antibody from Sigma; QuikChange II XL Site-Directed Mutagenesis kit from Stratagene; Texas Red 1,2-dihexadecanoyl-*sn*-glycero-3-phosphoethanolamine from Invitrogen; egg yolk L-α-phosphatidylcholine (chicken) from Avanti Polar Lipids, Inc.; FuGENE 6 and Nonidet P-40 (NP-40) from Roche Applied Sciences; and Hybond-C Extra nitrocellulose filters and all chromatography products (unless otherwise stated) from GE Healthcare Biosciences.

Buffers - Buffer A contained 50 mM Tris-chloride (pH 7.4) and 150 mM NaCl. Buffer B contained 50 mM MES-chloride (pH 5.5 or pH 6.5) and 150 mM NaCl. Buffer C contained 25 mM Tris-chloride (pH 7.5), 150 mM NaCl, and 0.01% (w/v) sodium azide. Buffer D contained 25 mM Tris-chloride (pH 7.5), 50 mM NaCl, and 0.01% sodium azide. Buffer E contained 50 mM sodium citrate (pH 4.5) and 150 mM NaCl.

Plasmid Construction - pCMV-NPC2-His10 encodes human NPC2 followed sequentially by 10 histidines under control of the cytomegalovirus (CMV) promoter. pCMV-NPC2-FLAG encodes human NPC2 followed sequentially by the FLAG sequence DYKDDDDK. Both plasmids were constructed from pCMV-NPC2 (Origene Technologies) by site-directed mutagenesis (QuikChange II XL kit). The P120S mutant version of NPC2 was produced by site-directed mutagenesis of pCMV-NPC2-His10. pCMV-NPC1(1-264)-LVPRGS-His8-

FLAG encodes human NPC1(1-264), followed by sequentially a 6-amino acid thrombin cleavage site, eight histidines, and a FLAG tag under control of the CMV promoter. This plasmid was constructed from pCMV-NPC1(1-264)-His8-FLAG (33) by site-directed mutagenesis using the 5′-oligonucleotide, 5′-CCT GCT CCC TGG ACG ATC CTT GGC TTA GTC CCC CGA GGC AGC CAT CAC CAT CAC CAT CAC CAT CAC GAC TAT AAA-3′; and the 3′-oligonucleotide 5'-TTT ATA GTC GTG ATG GTG ATG GTG ATG GTG ATG GCT GCC TCG GGG GAC TAA GCC AAG GAT CGT CCA GGG AGC AGG-3′. The coding region of each plasmid was sequenced to ensure integrity of the construct.

When this plasmid is expressed in CHO-KI cells, the resulting protein (after signal peptide cleavage) consists of the N-terminal domain (NTD) of NPC1 (amino acids 25-264) (33). This protein is hereafter referred to as NPC1(NTD).

Purification of Epitope-Tagged NPC2 from Medium of Transiently Transfected CHO Cells - CHO-K1 cells were set up on day 0 at 6×10^5 cells/100-mm dish in medium A (1:1 mixture of Ham's F-12 medium and Dulbecco's modified Eagle's medium, 100 units/ml penicillin, and 100 μg/ml streptomycin sulfate) containing 5% (v/v) fetal calf serum (FCS), grown in monolayer at 37°C in 8-9% CO_2, and transfected on day 2 with 5 μg of wild-type or mutant pCMV-NPC2-His10 or 5 μg pCMV-NPC2-FLAG as described (32). On day 3, the medium (7 ml/dish) was switched to medium A containing 1% (v/v) Cellgro® ITS (Fisher Scientific). After 24 h, the medium was collected, and fresh medium A containing 1% ITS was added. This cycle of collection/replenishment of medium was repeated for 3 consecutive days. All

subsequent operations were carried out at 4°C. The medium from each daily collection was centrifuged at 2500 rpm for 5 min, filtered through an Express Plus 0.22-μM filter apparatus (Millipore), stored at 4°C for up to 7 days, and then loaded onto a 30-ml column (BioRad) filled with either a 20-ml slurry of Ni-NTA-agarose beads (Qiagen) for purification of wild-type or mutant versions of NPC2-His10 or a 5-ml slurry of anti-FLAG M2-Agarose affinity beads for purification of NPC2-FLAG. Each column was pre-equilibrated with 4 column volumes of buffer A. A total of 1 liter of medium was applied to each column (flow rate of ~1 ml/min over ~16 h). Each column was then washed sequentially with 5 column volumes of buffer A with 20 mM imidazole and then with 40 mM. Bound protein was eluted with buffer A supplemented either with 250 mM imidazole for Ni-NTA-agarose beads or with 0.1 mg/ml FLAG peptide for anti-FLAG beads. Eluted fractions containing wild-type or mutant versions of NPC2-His10 or NPC2-FLAG were each concentrated to 0.5 ml in a spin concentrator using an Amicon Ultracel 10K Filter device (Millipore). The concentrated material was then subjected to gel-filtration chromatography on a 24-ml Superdex-200 column pre-equilibrated with buffer A. Fractions containing the peak A^{280} activity, which eluted between 15.5 and 17.5 ml, were pooled, and their protein content was quantified with the BCA kit (Pierce). Pooled proteins were subjected to 13% SDS-PAGE followed by Coomassie staining to determine purity.

Stably Transfected CHO Cells Expressing NPC1(NTD) - CHO-K1 cells were grown in monolayer at 37ºC in 8-9% CO_2. On day 0, cells were plated at a density of 6×10^6 cells/100-

mm dish in medium A containing 5% FCS. On day 3, the cells were co-transfected with 0.3 μg pcDNA3.1 and 2.0 μg pCMV-NPC1(1-264)-LVPRGS-His8-FLAG using FuGENE 6 as described (56). Twenty-four h after transfection, the medium was switched to medium A containing 5% FCS and 700 μg/ml G418 to select for cells expressing the *neo*-containing plasmid. Fresh medium was added every 2 to 3 days until colonies formed at ~14 days. Individual colonies were isolated with cloning cylinders and subcloned by dilution plating. Expression of NPC1(NTD)-LVPRGS-His8-FLAG was assessed by immunoblot analysis. Once a stably transfected cell line was established, it was grown in roller bottles as described below.

Purification of NPC1(NTD) from Medium of Stably Transfected CHO Cells - The above stably transfected CHO cell line expressing NPC1(NTD)-LVPRGS-His8-FLAG was set up for experiments on day 0 in 850 cm^2 roller bottles (Falcon) containing 100 ml medium A supplemented with 5% FCS and 500 μg/ml G418. The cells were cultured at 37°C at a CO_2 concentration of 8%. On day 4, the medium was switched to 100 ml medium A containing 5% FCS and 1% ITS. After 3-4 days, the medium was collected, and fresh medium A containing 5% FCS and 1% ITS was added. This 3 to 4-day cycle of collecting/replenishing the medium was done over a 3-week period. After each collection, the medium was centrifuged at 2500 rpm for 5 min at 4°C, filtered through an Express Plus 0.22-μM filter apparatus, and stored at 4°C for up to 2 weeks.

All subsequent operations were carried out at 4°C. One liter of filtered medium was concentrated, exchanged into buffer C to a final volume of 150 ml using a 10-kDa Pellicon 2 Ultrafiltration Module (Millipore), loaded onto a 10 ml Ni-NTA-agarose column, and washed sequentially with 100 ml buffer C and 100 ml buffer C containing 25 mM imidazole. Bound protein was eluted with buffer C containing 250 mM imidazole and buffer-exchanged into buffer D by successive concentration/dilution using a 10K Amicon Ultracel Centrifugal Filter device (Millipore). The concentrated protein was loaded onto a 7-ml MonoQ column, washed with 70 ml buffer D, and eluted using a linear gradient from 50-500 mM NaC1. Fractions containing NPC1(NTD)-LVPRGS-His8-FLAG were concentrated and subjected to size exclusion chromatography using a 24-ml Superdex 200 column equlibrated with buffer C. Fractions containing NPC1(NTD)-LVPRGS-His8-Flag were pooled and concentrated.

In some cases the His8 and FLAG epitope tags of the NPC1(NTD) protein were removed by incubation with 5 units of thrombin (Cat. No. T6634, Sigma) for 1 h at 25°C followed by 11 h at 4°C. The digest was passed through a Ni-NTA column equilibrated with buffer C to separate cleaved and uncleaved forms of NPC1(NTD). The flow-through was diluted to 50 mM NaC1 and purified by MonoQ and Superdex 200 chromatography as described above. The resulting purified protein is referred to as NPC1(NTD)-LVPR.

[^{3}H]Cholesterol Binding Assay - This assay was previously described (33). In brief, each reaction contained, in a final volume of 80 μl, the indicated buffer, varying concentrations of [^{3}H]cholesterol ($132x10^3$ dpm/pmol; delivered in ethanol at final concentration of 2%), 1 μg bovine serum albumin, and varying amounts of purified human NPC1 or NPC2. After

incubation for the indicated time at 4°C or 37°C, the mixture in buffer A was loaded onto a column packed with 0.3 ml Ni-NTA-agarose beads (Qiagen) that had been pre-equilibrated with buffer A with 0.004% (w/v) NP-40, and then washed with 6 ml of the same buffer. (Prior to Ni chromatography, mixtures in buffer B were diluted 5-fold with buffer A containing 0.004% NP-40). Protein-bound [^{3}H]cholesterol was eluted with 1 ml buffer A containing 250 mM imidazole and 0.004% NP-40 and quantified by scintillation counting.

Isolation of Complexes of [^{3}H]Cholesterol-NPC1(NTD) and [^{3}H]Cholesterol-NPC2 - Each reaction contained, in a final volume of 300 μl buffer B (pH 5.5), 500 nM [^{3}H]cholesterol (132x10^3 dpm/pmol; delivered in ethanol at final concentration of 3%) and one of the following NPC proteins: 30 μg NPC2-His10, 30 μg NPC2-FLAG, 60 μg NPC1(NTD)-LVPRGS-His8-FLAG, or 60 μg NPC1-NTD)-LVPR, each delivered in 3-30 μl buffer A. The final pH of the reaction was 5.5. After incubation for 24-48 h at 4°C, the mixture was passed through a 24-ml Superdex-200 column pre-equilibrated with buffer B (pH 5.5). Protein-bound [^{3}H]cholesterol emerged between 15.5-17.5 ml for NPC2 and 13.5-15.5 ml for NPC1(NTD). The respective pooled fractions were used for the [^{3}H]cholesterol transfer assays described below.

Preparation of Liposomes - Liposomes were generated using a standard sonication procedure (39). Briefly, a chloroform solution (1 ml) containing 9.8-10 mg egg yolk L-α-phosphatidylcholine (PC) and 10 μg Texas Red dye in the absence or presence 0.2 mg [^{3}H]cholesterol (930 dpm/pmol; ~4 mole %)) was added to a round bottom flask. The

solvent was evaporated under a stream of nitrogen, leaving behind a thin uniform film of lipid. The flask was placed under vacuum for at least 24 h to remove any trace of organic solvent, sealed, and stored at -20°C until use. The dry lipid film was hydrated by addition of 2 ml of buffer A. After incubation at room temperature for 30 min, the large multilamellar vesicle suspension was disrupted with a Branson tip-sonicator until the suspension cleared. Metal particles from the sonicator tip and undisrupted lipid aggregates were removed by centrifugation at 100,000*g* for 30 min at 4°C. The resulting hazy supernatant, comprised primarily of small unilamellar vesicles, was stored at 4°C for a maximum of 5 days before use.

The concentration of liposome solutions was determined by a malachite green colorimetric assay of inorganic phosphate released from phospholipids after acidic digestion (12). The location of liposomes in column fractions during nickel agarose chromatography was tracked by measuring the fluorescence of Texas Red dye (excitation/emission wavelengths: 595/615 nm).

[^{3}H]Cholesterol Transfer Assays - Three types of transfer assays were performed: 1) movement of [^{3}H]cholesterol from a donor protein (NPC1(NTD) or NPC2) to an acceptor protein (NPC1(NTD) or NPC2); 2) movement of [^{3}H]cholesterol from NPC proteins to liposomes; and 3) movement of [^{3}H]cholesterol from liposomes to NPC proteins. In the NPC protein-to-NPC protein transfer assays, each reaction contained, in a final volume of 100 μl buffer B (pH 5.5) supplemented with 0.004% NP-40, 0.4-2 pmol [^{3}H]cholesterol complexed

to ~40 pmol of a donor protein, either NPC1(NTD)-LVPR or NPC2-FLAG. The donor proteins did not contain a His tag. The assay mixture contained varying amounts of an acceptor protein (either NPC1(NTD)-LVPRGS-His8-FLAG or NPC2-His10), both of which contained His tags. After incubation for 30 min at 4°C or 37°C, each reaction mixture was diluted with 500 μl buffer A supplemented with 0.004% NP-40 and loaded onto a 2-ml column (BioRad) packed with 0.3 ml Ni-NTA-agarose beads (Qiagen) that had been pre-equilibrated with buffer A with 0.004% NP-40. Each column was washed at 4°C with 3 ml buffer A with 0.004% NP-40, after which the His-tagged acceptor proteins were eluted with 1 ml buffer A containing 0.004% NP-40 and 250 mM imidazole. The amount of [^{3}H]cholesterol transferred to each His-tagged acceptor protein was quantified by scintillation counting of the eluate as described (55).

In the NPC protein-to-liposome transfer assays, each reaction contained, in a final volume of 200 μl buffer B, 0.4-2 pmol [^{3}H]cholesterol complexed to 40 pmol of either NPC1(NTD)-LVPRGS-His8-Flag or NPC2-His10, and varying amounts of acceptor PC liposomes in the absence or presence of the other His-tagged NPC protein. After incubation for 30 min at 4°C or 37°C, each mixture was processed as described above except that reactions were diluted with 750 μl buffer A and none of the buffers contained NP-40. The amount of [^{3}H]cholesterol transferred to liposomes was quantified by scintillation counting of the flow-through.

In the [^{3}H]cholesterol:liposome-to-NPC protein transfer assays, each reaction contained, in a final volume of 200 μl buffer B, 20 μg PC:[^{3}H]cholesterol liposomes (930 dpm/pmol), and increasing amounts of an acceptor protein, either NPC1(NTD)-LVPRGS-

His8-FLAG or NPC2-His10, in the absence or presence of the other non-His tagged NPC protein. After incubation for 30 min at 4°C, each mixture was processed as described above except that reactions were diluted with 750 μl buffer A and none of the buffers contained NP-40. The amount of [^{3}H]cholesterol transferred to the respective His-tagged NPC protein was quantified by scintillation counting of the eluate.

Immunoblot Analysis - After SDS-PAGE on 13% gels, proteins were transferred to Hybond-C Extra nitrocellulose filters. The filters were incubated at room temperature with one of the following primary antibodies: 1.0 μg/ml monoclonal anti-FLAG M2 antibody and 1/1000 dilution of polyclonal antibodies against human NPC1(NTD)-His8-FLAG and NPC2-His10 (see below). Bound antibodies were visualized by chemiluminescence (Super Signal Substrate; Pierce) using a 1:5000 dilution of donkey anti-mouse IgG (Jackson ImmunoResearch) or a 1:2000 dilution of anti-rabbit IgG (Amersham) conjugated to horseradish peroxidase. Filters were exposed to Phoenix Blue X-Ray Film (F-BX810, Phoenix Research Products) at room temperature for 1-60 s.

Polyclonal antibodies directed against recombinant human NPC1(NTD)-His8-FLAG (purified as previously described (33)) and NPC2-His10 (purified as described above) were produced by immunizing each rabbit subcutaneously with 500 μg of the recombinant protein in incomplete Freud's adjuvant, followed by alternating subcutaneous booster injections every 2 weeks of 250 μg of the protein.

RESULTS

Kinetics of [^{3}H]cholesterol binding to purified NPC proteins - The current studies take advantage of the fact that NPC1(NTD) as well as NPC2 are water soluble proteins, and therefore transfer assays can be carried out in the absence or presence of very low concentrations of detergents, i.e., 0.004% Nonidet P-40 (NP-40). For this purpose, we isolated recombinant NPC1(NTD) and NPC2 from the culture medium of CHO cells that were transfected with plasmids encoding the proteins with or without C-terminal His or FLAG tags. After purification as described in Methods, NPC1(NTD) gave a single diffuse Coomassie stained band on SDS-PAGE (Figure 3-1). NPC2 gave multiple bands, owing to differing degrees of N-linked glycosylation (33, 17).

To measure cholesterol binding, we incubated the His-tagged proteins with [^{3}H]cholesterol at either 4°C or 37°C in the presence of 0.004% NP-40. Protein-bound [^{3}H]cholesterol was isolated by nickel chromatography and quantitated by scintillation counting (Figure 3- 2). To measure dissociation rates, we first incubated the proteins with [^{3}H]cholesterol at 4°C and then isolated the cholesterol-protein complexes by gel filtration as described in Methods. The proteins were then bound to nickel agarose beads and dissociation was measured by release of [^{3}H]cholesterol into the supernatant. The rates of association and dissociation of [^{3}H]cholesterol to and from NPC1(NTD) were strongly influenced by temperature (Figure 3-2*A* and 3-2*C*). At 4°C binding was extremely slow (Figure 3-2*A*), and dissociation was so slow as to be unmeasurable, even after 2 h (Figure 3-2*C*). Both processes were accelerated dramatically at 37°C. In comparison to NPC1(NTD),

NPC2 bound and released [^{3}H]cholesterol relatively rapidly at 4°C as well as 37°C (Figure 3-2*B* and 3-2*D*). To measure saturation binding at equilibrium for NPC1(NTD), we carried out incubations for 45 min at 37°C and for 20 h at 4°C (Figure 3-2*E*). The calculated K_d for [^{3}H]cholesterol binding was 50 nM at 4°C and 90 nM at 37°C; maximal binding was slightly higher at 37°C. For NPC2, saturation binding at equribibrium was done for 45 min at both 4°C and 37°C (Figure 3-2*F*). The calculated K_d was 90 nM at 4°C and 130 nM at 37°C. The binding of [^{3}H]cholesterol to both proteins was unaffected when the pH was varied from 5.5 to 7.5 at either 4°C or 37°C (data not shown).

Tranfer of [^{3}H]cholesterol between NPC proteins - We conducted protein-to-protein cholesterol transfer assays in which [^{3}H]cholesterol was transferred from a donor NPC protein that lacks a His tag to an acceptor NPC protein that possesses a His tag. To prepare the donors, we incubated NPC1(NTD) or NPC2 with [^{3}H]cholesterol at 4°C and isolated each sterol-protein complex by gel filtration (Figure 3-3). The transfer reactions were conducted either at 4°C or at 37°C (Figure 3-4). After incubation, the reaction mixture was subjected to nickel agarose chromatography, and the amount of [^{3}H]cholesterol transferred to the indicated His-tagged NPC protein was measured by scintillation counting of the imidazole-eluted fraction. No donor protein was detected in the eluted fraction as determined by immunoblot analysis (data not shown). At 4°C untagged NPC1(NTD) rapidly transferred [^{3}H]cholesterol to His-tagged NPC2 (Figure 3-4*A, closed circles*). The measured values are probably an underestimate of true transfer, owing to the relatively long time required to process the sample, i.e. ~8-10 min. Remarkably, at 4°C untagged NPC1(NTD) did not

transfer [^{3}H]cholesterol to His-tagged NPC1(NTD) (*open circles*). On the other hand, even at 4°C, untagged NPC2 rapidly transferred [^{3}H]cholesterol to tagged versions of both NPC1(NTD) and NPC2 (Figure 3-4*B*). The differences between NPC1(NTD) and NPC2 persisted when the concentrations of the acceptor protein were varied (Figures 3-4*E* and 3-4*F*). At 4°C transfer of [^{3}H]cholesterol from NPC1(NTD) to NPC2 showed a maximum at pH 5.5, which reflects the pH of endosomes/lysosomes (Figure 3-4*G, closed circles*). NPC1(NTD) did not transfer to itself at any pH (Figure 3-4*G*, *open circles*). When NPC2 was the donor, the transfer rates were relatively constant over the pH range of 5.5 to 8.5 (Figure 3-4*H*).

At 37°C NPC1(NTD) was able to transfer [^{3}H]cholesterol to the His-tagged version of itself (Figure 3-4*C*, *open circles*), but even at this temperature the transfer to NPC2 was much faster (*closed circles*). Again, NPC2 transferred its [^{3}H]cholesterol rapidly either to NPC1(NTD) or NPC2 at 37°C (Figure 3-4*D*).

Transfer of [^{3}H]cholesterol from NPC proteins to lipid bilayers - To measure protein-to-liposome transfer, we prepared unilamellar phosphatidylcholine (PC) liposomes by sonication as described in Methods. The donors were His-tagged NPC1(NTD) or NPC2 that had been complexed with [^{3}H]cholesterol and isolated by gel filtration. After incubation with liposomes, the reaction mixture was applied to a nickel agarose column. The liposomes (labeled with Texas Red dye) appeared in the flow-through fractions, whereas the His-tagged NPC proteins appeared in the imidazole-eluted fractions (Figure 3-5). We measured the amount of [^{3}H]cholesterol transferred from donor NPC proteins to liposomes by scintillation counting of the flow-through fraction. To assure that transfer of [^{3}H]cholesterol was

liposome-dependent, we conducted parallel incubations in the absence of liposomes, and the amount of [^{3}H]cholesterol in the flow-through was measured. These values were subtracted from those in the liposome-containing incubations to measure liposome-dependent transfer. At 4°C NPC1(NTD) failed to transfer [^{3}H]cholesterol to liposomes (Figure 3-6*A*, *open circles*). Transfer to liposomes was enhanced dramatically (>100-fold) when NPC2 was included in the incubation (*closed circles*). As the temperature was increased from 4°C to 22°C to 37°C, there was a progressive increase in the ability of NPC1(NTD) to transfer [^{3}H]cholesterol to liposomes (Figure 3-7). This rate was enhanced dramatically when NPC2 was present (Figures 3-6*A* and 3-6*C*; Figure 3-7*A*). When NPC2 was the donor, [^{3}H]cholesterol was transferred rapidly to liposomes at all temperatures, and the addition of NPC1(NTD) had no significant effect (Figures 3-6*B* and 3-6*D*; Figure 3-7). To confirm that the [^{3}H]cholesterol in the nickel agarose flow-through had indeed been transferred to liposomes, we isolated the liposomes by flotation through a discontinuous sucrose gradient in an ultracentrifuge. All of the [^{3}H]cholesterol co-migrated with the Texas Red dye-labeled liposomes (data not shown).

Figure 3-6*E* shows the transfer of [^{3}H]cholesterol from NPC1(NTD) to liposomes as a function of the concentration of liposomes. Transfer required the presence of NPC2 at all liposome concentrations, whereas transfer from NPC2 to liposomes did not require NPC1(NTD) (Figure 3-6*F*). The transfer reactions showed only minor effects of pH in the range of 4.5 to 8.5 (Figures 3-6*G* and *3-6H*).

To confirm that the transfer activity of NPC2 required cholesterol binding, we exploited a naturally occurring missense mutation in NPC2(P120S). Homozygosity for this

mutation was observed in a patient with NPC2 disease (64). Immunofluorescence of the patient's fibroblasts showed that the mutant protein reaches lysosomes, suggesting that the protein folds sufficiently to escape the quality control system of the ER. However, the mutant protein is unable to carry out its function in facilitating cholesterol egress from lysosomes (64). To study NPC2(P120S), we prepared a cDNA encoding the mutant protein and introduced it into CHO cells by transfection. The protein was purified from the culture medium like native NPC2. SDS-PAGE, gel filtration, and circular dichroism spectroscopy (wavelength scan at 4°C) showed that the mutant protein behaved similarly to the wild-type (Figure 3-8*A*, *inset* and data not shown). The human P120S mutation replaces a residue that lies at the edge of the hydrophobic cholesterol-binding pocket as indicated by the crystal structure of the bovine NPC2 (70). Indeed, as shown in Figure 3-8*A*, the P120S mutant failed to bind [^{3}H]cholesterol under our assay conditions. The mutant NPC2 was also severely defective in facilitating the transfer of [^{3}H]cholesterol from NPC1(NTD) to liposomes (Figure 3-8*B*). These data confirm that NPC2 must bind cholesterol in order to facilitate transfer of cholesterol from NPC1(NTD) to liposomes.

Transfer of [^{3}H]choleterol from lipid bilayers to NPC proteins - Figure 3-9 shows the results of the reciprocal assay, namely, the transfer of [^{3}H]cholesterol from PC liposomes to NPC1(NTD) or NPC2. At 4°C there was little transfer to NPC1(NTD), and transfer was stimulated markedly by NPC2 (Figure 3-9*A*). As the temperature was increased from 4°C to 22°C to 37°C, there was a progressive increase in the ability of NPC1(NTD) to accept [^{3}H]cholesterol from liposomes (data not shown). This rate was enhanced markedly at 4°C and 37°C when NPC2 was added (Figure 3-9*A* and 3-9*C*). Here again, NPC2 showed no

requirement for NPC1(NTD). NPC2 rapidly accepted [^{3}H]cholesterol from liposomes at all temperatures, and there was no effect of adding NPC1(NTD) (Figure 3-9*B* and 3-9*D*).

Figure 3-9*E* shows the transfer of [^{3}H]cholesterol from PC liposomes to NPC1(NTD) as a function of increasing concentrations of NPC1(NTD) in the absence or presence of NPC2. As seen with the protein-to-liposome transfer, little transfer occurred unless NPC2 was present. Similarily, when the acceptor was NPC2, it alone effected transfer of [^{3}H]cholesterol from liposomes to itself, and this transfer was not influenced by NPC1(NTD) (Figure 3-9*F*). Interestingly, the liposome-to-protein assay was pH dependent at 4°C. In the presence of NPC2, NPC1(NTD) accepted cholesterol optimally at pH 5.5 (Figure 3-9*G*). NPC2 accepted cholesterol optimally at pH 4.5 (Figure 3-9*H*).

FIGURE 3-1: Coomassie staining of purified NPC proteins.

Recombinant human NPC1(NTD) and human NPC2 proteins were purified as described in Methods. Aliquots (5 μg) of NPC1(NTD)-LVPRGS-His8-FLAG (*A*), NPC1(NTD)-LVPR (*B*), NPC2-FLAG (*C*), and NPC2-His10 (*D*) were subjected to 13% SDS-PAGE, and the proteins were visualized with Coomassie Brillant Blue R-250 stain (Bio-Rad). Molecular masses of protein standards are indicated.

FIGURE 3-1

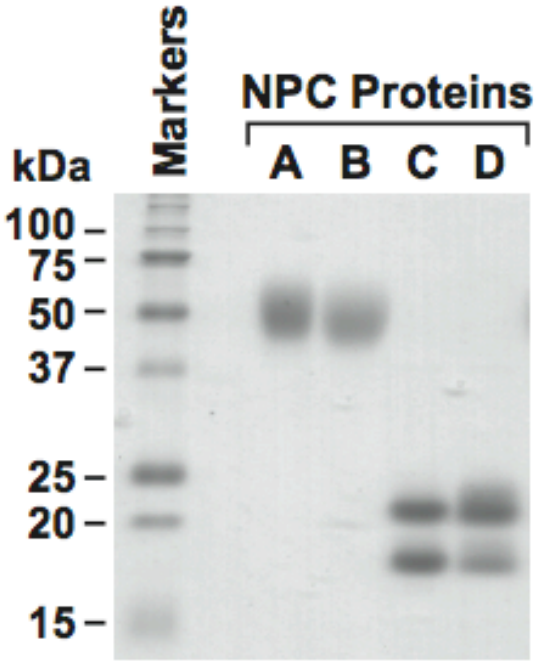

FIGURE 3-2: Kinetics of [^{3}H]cholesterol binding to purified NPC proteins.

(*A, B*) Time course at different temperatures. Each reaction, in a final volume of 80 μl buffer B (pH 6.5) with 0.004% NP-40, contained 4 pmol NPC1(NTD)-LVPRGS-His8-FLAG (*A*) or 8 pmol NPC2-His10 (*B*) and 100 nM [^{3}H]cholesterol (132x10^3 dpm/pmol). After incubation for indicated time at 4°C (○) or 37°C (●), the amount of bound [^{3}H]cholesterol was measured with the Ni-NTA-agarose binding assay. Each value is the average of duplicate assays and represents total binding after subtraction of a blank value (0.01-0.02 pmol/tube). (*C, D*) Dissociation of previously bound [^{3}H]cholesterol from NPC proteins at different temperatures. [^{3}H]Cholesterol complexed to NPC1(NTD)-LVPRGS-His8-FLAG (*C*) or NPC2-His10 (*D*) at 4°C was isolated by gel filtration. Fractions containing NPC1 or NPC2 complexed to [^{3}H]cholesterol were pooled (3 ml), diluted 7-fold with buffer B (pH 6.5) containing 0.004% NP-40 and 10 μM unlabeled cholesterol, and incubated at 4°C (○) or 37°C (●). At the indicated time, a 1 ml-aliquot of the pooled 21-ml sample was transferred to a tube containing 600 μl of Ni-NTA-agarose beads. After incubation for 3 min at 4°C, the beads were centrifuged at 600*g* for 1 min, after which the supernatant was assayed for radioactivity. Each value is the average of duplicate assays and represents % [^{3}H]cholesterol remaining bound to the beads relative to zero-time value. The "100% initial binding" values at zero time for NPC1(NTD) and NPC2 were 1.6 and 0.24 pmol/tube, respectively. (*E, F*) Saturation curves for equilibrium binding at different temperatures. This experiment was carried out as in (*A, B*) except that [^{3}H]cholesterol concentration varied as indicated and incubation time at 4°C was 20 h for NPC1(NTD) and 45 min for NPC2 and at 37°C, 45 min for both proteins.

FIGURE 3-2

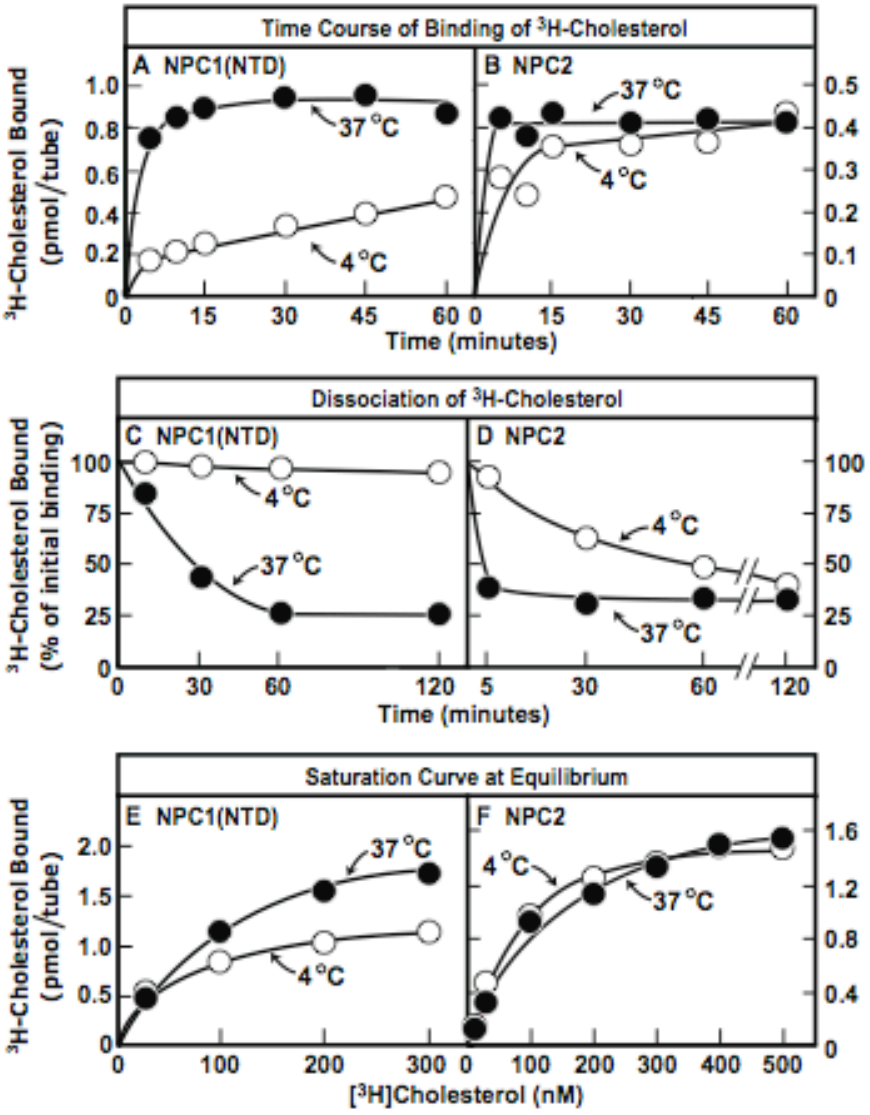
Time Course of Binding of ³H-Cholesterol
A NPC1(NTD)
B NPC2
37 °C
4 °C
³H-Cholesterol Bound (pmol/tube)
Time (minutes)
Dissociation of ³H-Cholesterol
C NPC1(NTD)
D NPC2
³H-Cholesterol Bound (% of initial binding)
Saturation Curve at Equilibrium
E NPC1(NTD)
F NPC2
[³H]Cholesterol (nM)

FIGURE 3-3: Isolation of NPC proteins complexed to [^{3}H]cholesterol.

Each reaction, in a final volume of 300 µl buffer B (pH 5.5), contained either 60 µg of NPC1(NTD)-LVPR (*A*) or 30 µg NPC2-FLAG (*B*) and 500 nM [^{3}H]cholesterol (132x10^3 dpm/pmol). After incubation for 24 h at 4°C, bound [^{3}H]cholesterol was separated from unbound by applying the reaction to a 24-ml Superdex-200 column pre-equilibrated with buffer B (pH 5.5). Fractions (1 ml) were collected starting at 7.5 ml (Fraction 1). The content of [^{3}H]cholesterol in each fraction was determined by scintillation counting of a 0.1 ml aliquot. Each value represents the total binding in each fraction. The column was calibrated with the following molecular mass markers: thyroglobulin, 670 kDa; γ-globulin, 158; ovalbumin, 44; and myoglobin, 17. Each fraction was also subjected to immunoblot analysis (*inset*) with polyclonal NPC1(NTD) antibody (*A*) or polyclonal NPC2 antibody (*B*). Filters were exposed to film for 5 s.

FIGURE 3-3

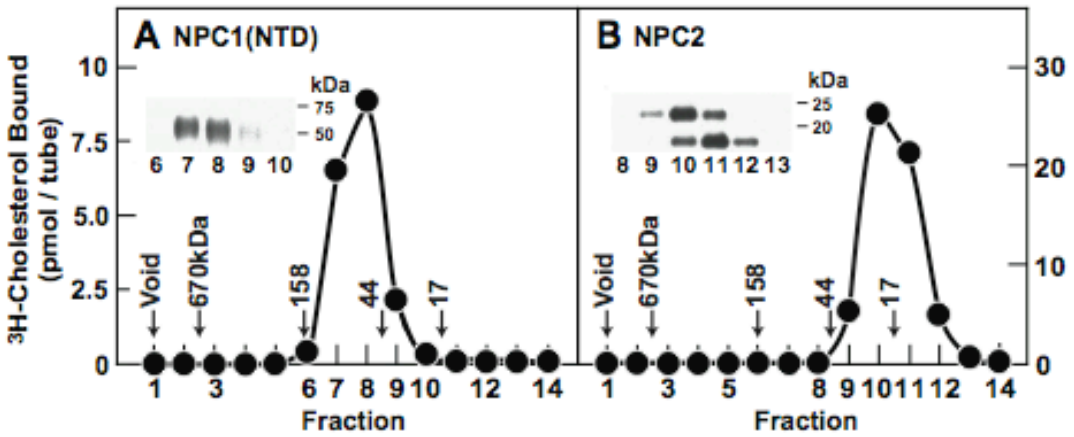

FIGURE 3-4: Transfer of [^{3}H]cholesterol from donor NPC protein to acceptor NPC protein.

Transfer of [^{3}H]cholesterol from donor NPC protein to acceptor NPC protein. Schematic diagrams of the two transfer assays are shown at the top of each column. (*A-D*) Time course at different temperatures. Each reaction, in a final volume of 100 μl buffer B (pH 5.5) with 0.004% NP-40, contained ~40 pmol of NPC1(NTD)-LVPR (*A*, *C*) or NPC2-FLAG (*B*, *D*) each complexed to [^{3}H]cholesterol (1.3-1.9 pmol; 132x10^3 dpm/pmol) and 200 pmol of NPC1(NTD)-LVPRGS-His8-FLAG (○) or NPC2-His10 (●). After incubation for indicated time at 4°C (*A*, *B*) or 37°C (*C, D*), the amount of [^{3}H]cholesterol transferred to the indicated acceptor His-tagged NPC protein was measured with the Ni-NTA-agarose cholesterol transfer assay. Each value represents % [^{3}H]cholesterol transferred. The "100% values" for transfer from donor were 1.9 pmol (*A*), 1.5 (*B, C*), and 1.3 (*D*). (*E, F*) Transfer at 4°C as function of the amount of acceptor NPC protein. This experiment was carried out as in *A-D* except that the amount of acceptor NPC protein varied as indicated and time of incubation at 4°C was 30 min. The "100% values" for transfer of [^{3}H]cholesterol from NPC1(NTD) and NPC2 were 2.0 and 1.2 pmol, respectively. (*G, H*) Transfer at 4°C as function of pH. Each reaction in a final volume of 300 μl buffer A, B, or E with 0.004% NP-40 at the indicated pH, contained ~30 pmol of NPC1(NTD)-LVPR (*G*) or NPC2-FLAG (*H*) each complexed to [^{3}H]cholesterol (1.6 and 1.0 pmol, respectively) and 200 pmol of either NPC1(NTD)-LVPRGS-His8-FLAG (○) or NPC2-His10 (●). After incubation for 30 min at 4°C, the amount of [^{3}H]cholesterol transferred to the indicated acceptor His-tagged NPC was measured as described above except samples were diluted with 1.1 ml of buffer A with

0.004% NP-40. Each value is average of duplicate assays and represents % [^{3}H]cholesterol transferred. The "100% values" for transfer from NPC1(NTD) and NPC2 were 1.6 and 1.0 pmol, respectively.

FIGURE 3-4

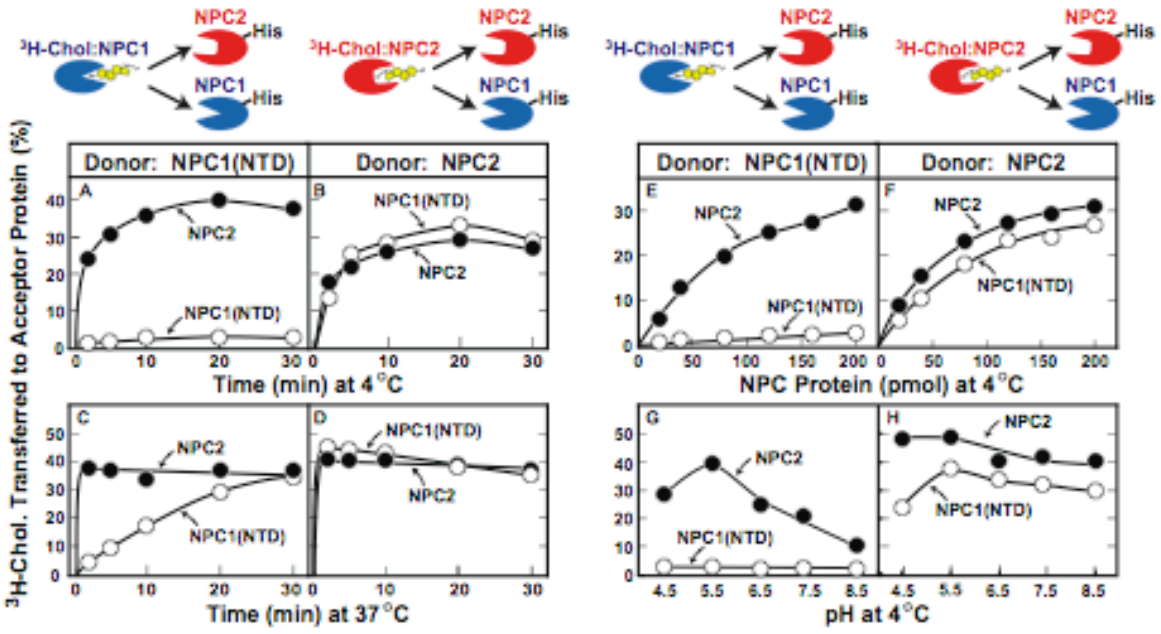

FIGURE 3-5: Separation of liposomes from His-tagged versions of NPC proteins.

The reaction, in a final volume of 200 µl buffer B (pH 5.5), contained 120 µg phosphatidylcholine liposomes labeled with Texas Red dye, 40 pmol NPC1(NTD)-LVPRGS-His8-FLAG, and 200 pmol NPC2-His10. After incubation for 30 min at 4°C, the reaction mixture was diluted with 750 µl buffer A and loaded onto a Ni-NTA agarose column as described for the cholesterol transfer assay, washed with 6 ml buffer A, and eluted with 1 ml buffer A containing 250 mM imidazole. Fractions (1 ml) were collected, assayed for their liposome content by fluorescence, and subjected to immunoblot analysis (*inset*) with a monoclonal antibody against the FLAG epitope and a polyclonal antibody against NPC2. Filters were exposed to film for 5 s.

FIGURE 3-5

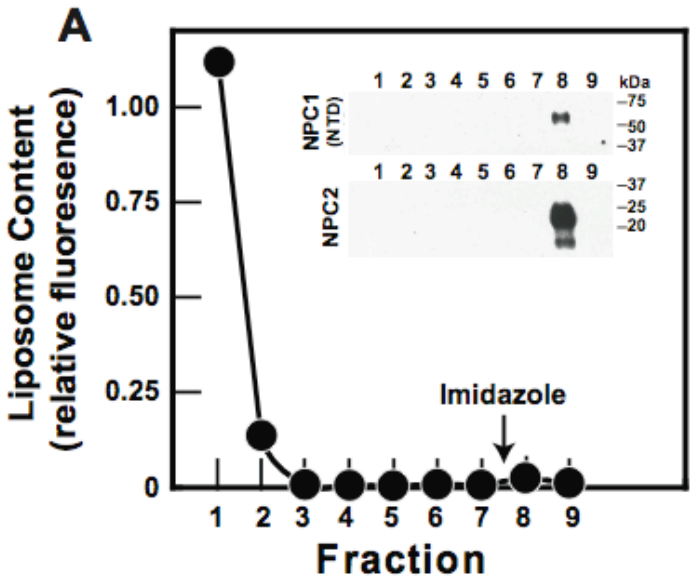

FIGURE 3-6: Transfer of [^{3}H]cholesterol from donor NPC protein to acceptor PC liposomes.

Transfer of [^{3}H]cholesterol from donor NPC protein to acceptor PC liposomes. Schematic diagrams of the two transfer assays are shown at the top of each column. (*A-D*) Time course at different temperatures. Each reaction, in a final volume of 200 μl buffer B (pH 5.5), contained ~30 pmol of NPC1(NTD)-LVPRGS-His8-FLAG (*A, C*) or NPC2-His10 (*B, D*) each complexed to [^{3}H]cholesterol (1.0 and 0.3 pmol, respectively; 132x10^3 dpm/pmol) and 60 μg PC liposomes labeled with Texas Red dye in the absence (○) or presence (●) of 100 pmol NPC2-His10 (*A, C*) or NPC1(NTD)-LVPRGS-His8-FLAG (*B, D*). After incubation for indicated time at 4°C (*A, B*) or 37°C (*C, D*), the amount of [^{3}H]cholesterol transferred to liposomes was measured in the Ni-NTA-agarose cholesterol transfer assay. Each value is average of duplicate assays and represents % [^{3}H]cholesterol transferred to liposomes. The "100% values" for transfer from NPC1(NTD) and NPC2 were 1.0 and 0.3 pmol, respectively. Blank values in absence of liposomes (1-4%) were subtracted. (*E-F*) Transfer at 4°C as function of the amount of liposomes. This experiment was carried out as in *A-D* except that the amount of liposomes varied as indicated and time of incubation at 4°C was 30 min. The "100% values" for transfer of [^{3}H]cholesterol from NPC1(NTD) and NPC2 were 0.4 and 1.7 pmol, respectively. Blank values in absence of liposomes (2-5%) were subtracted. (*G, H*) Transfer at 4°C as function of pH. The conditions for this experiment are the same as those in *E* and *F* except that the final volume of the reaction was 300 μl in buffer *A,* B, or E at the indicated pH, and the acceptor was 60 μg PC liposomes in absence (○) or

presence (●) of 100 pmol NPC2-His10 (*G*) or 100 pmol NPC1(NTD)-LVPRGS-His8-FLAG (*H*). The "100% values" for transfer of [^{3}H]cholesterol from NPC1(NTD) and NPC2 were 0.8 and 0.5 pmol, respectively. Blank values in absence of liposomes (1-5%) were subtracted.

FIGURE 3-6

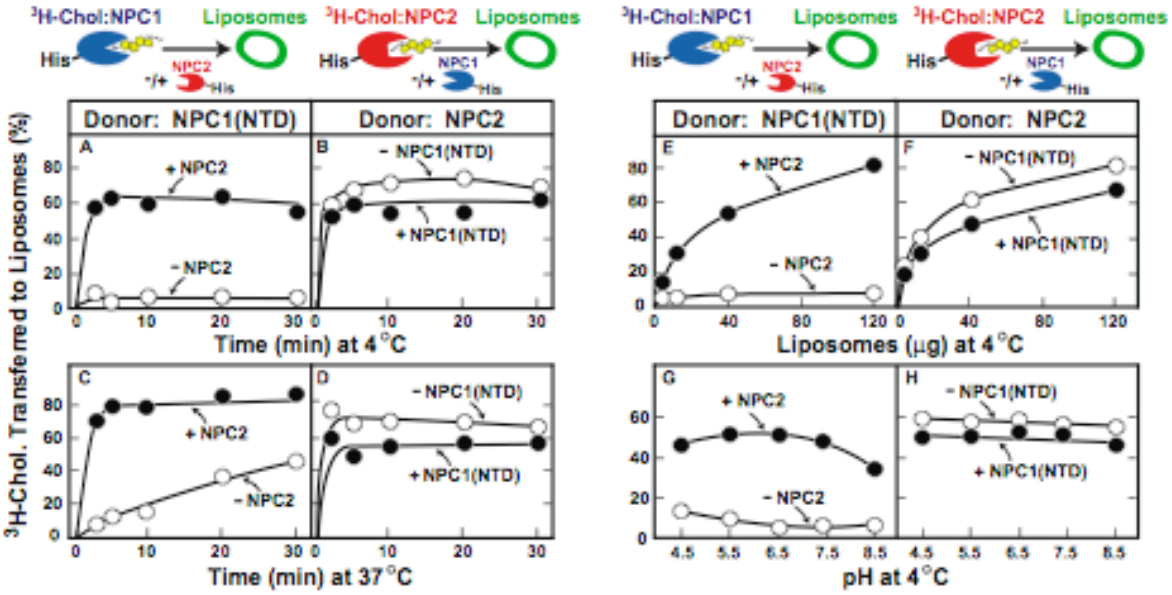

FIGURE 3-7: Transfer of [^{3}H]cholesterol to PC liposomes as a function of temperature. Each reaction, in a final volume of 200 μl buffer B (pH 5.5), contained ~50 pmol of either NPC1(NTD)-LVPRGS-His8-FLAG (*A*) or NPC2-His10 (*B*) each complexed to [^{3}H]cholesterol (0.8 and 1.1 pmol, respectively; 132x10^3 dpm/pmol) and 40 μg PC liposomes labeled with Texas Red dye in the absence (*open circles*) or presence (*closed circles*) of 100 pmol of either NPC2-His (*A*) or NPC1(NTD)-LVPRGS-His8-FLAG (*B*). After incubation for 30 min at the indicated temperature, the amount of [^{3}H]cholesterol transferred to liposomes was measured in the Ni-NTA-agarose cholesterol transfer assay. Each value is the average of duplicate assays and represents the amount of [^{3}H]cholesterol transferred to liposomes. Blank values in the absence of liposomes (0.07 pmol) were subtracted.

FIGURE 3-7

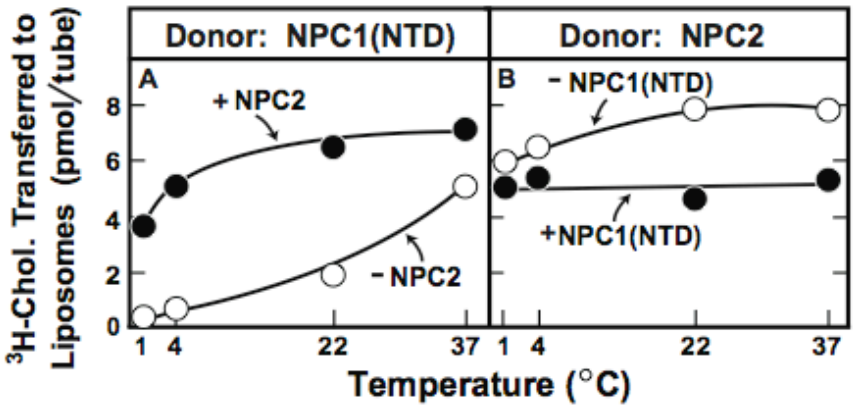

FIGURE 3-8: Mutant NPC2 fails to transfer [^{3}H]cholesterol from NPC1(NTD) to acceptor PC liposomes.

(*A*) Saturation curves for equilibrium binding of [^{3}H]cholesterol for wild-type and mutant NPC2. Binding reactions were carried out as described in Figure 1-2F except that each reaction was incubated for 2 h at 4°C and contained 8 pmol of wild-type (●) or P120S mutant (○) version of NPC2-His10. Each value is average of duplicate assays and represents binding after subtraction of blank values (0.01-0.11 pmol). *Inset* shows a Coomassie Brilliant Blue R-250 stain of wild-type and mutant NPC2 proteins after electrophoresis on 13% SDS-PAGE (3 μg of each protein loaded on gel). (*B*) Transfer of [^{3}H]cholesterol from donor NPC1(NTD) to acceptor liposomes as function of varying concentrations of wild-type or mutant NPC2. Assays were carried out as in Figures 3-6 except that each reaction was carried out for 10 min at 4°C and contained ~50 pmol NPC1(NTD)-LVPRGS-His8-FLAG complexed to [^{3}H]cholesterol (1.2 pmol; 132x10^3 dpm/pmol), 60 μg PC liposomes, and the indicated concentration of wild-type (●) or P120S mutant (○) version of NPC2-His10. Each value is average of duplicate assays and represents % [^{3}H]cholesterol transferred to liposomes. The "100% value" for transfer from NPC1(NTD) was 1.2 pmol. Blank values in absence of NPC2 protein (8%) were subtracted.

FIGURE 3-8

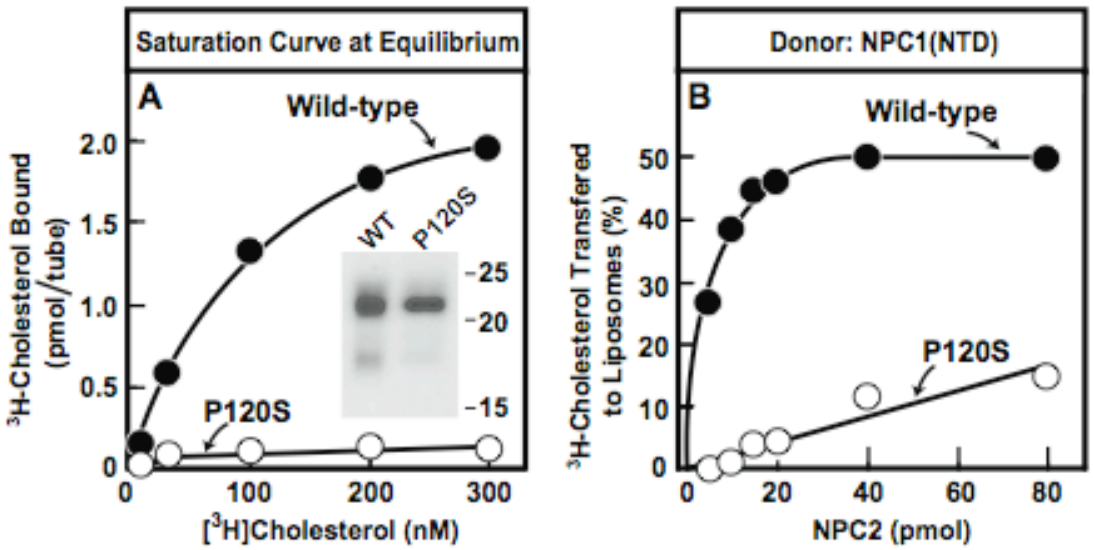
Saturation Curve at Equilibrium
A
Wild-type
P120S
WT
P120S
-25
-20
-15
^{3}H-Cholesterol Bound (pmol/tube)
2.0
1.5
1.0
0.5
0
0
100
200
300
[^{3}H]Cholesterol (nM)
Donor: NPC1(NTD)
B
Wild-type
P120S
^{3}H-Cholesterol Transfered to Liposomes (%)
50
40
30
20
10
0
0
20
40
60
80
NPC2 (pmol)

FIGURE 3-9: Transfer of [^{3}H]cholesterol from donor PC liposomes to acceptor NPC protein.

Schematic diagrams of the two transfer assays are shown at the top of each column. (*A-D*) Time course at different temperatures. Each reaction, in a final volume of 200 μl buffer B (pH 5.5), contained 17 μg PC liposomes containing 540 pmol [^{3}H]cholesterol (930 dpm/pmol) labeled with Texas Red dye and 100 pmol of NPC1(NTD)-LVPRGS-His8-FLAG (*A, C*) or NPC2-His10 (*B, D*) in presence (●) or absence (○) of 100 pmol of either NPC2-FLAG (*A, C*) or NPC1(NTD)-LVPR (*B, D*). After incubation for the indicated time at 4°C (*A, B*) or 37°C (*C, D*), the amount of [^{3}H]cholesterol transferred to acceptor His-tagged NPC protein was measured in the Ni-NTA-agarose cholesterol transfer assay. Each value is average of duplicate assays and represents amount of [^{3}H]cholesterol transferred from liposomes to the indicated acceptor His-tagged NPC protein. Blank values in absence of His-tagged NPC protein (0.2-0.3 pmol) were subtracted. (*E, F*) Transfer at 4°C as a function of the concentration of NPC protein. This experiment was carried out as in (*A-D*) except that the amount of acceptor NPC1(NTD)-LVPRGS-His8-FLAG (*E*) or acceptor NPC2-FLAG (*F*) varied as indicated and time of incubation at 4°C was 30 min. Each value is average of duplicate assays and represents amount of [^{3}H]cholesterol transferred from liposomes to the indicated acceptor NPC protein. Blank values in absence of His-tagged NPC protein (0.2-0.4 pmol) were subtracted. (*G, H*) Transfer at 4°C as function of pH. The conditions for this experiment are the same as those in Figures 3-6*G* and 3-6*H* except that the donor was 17 μg PC:[^{3}H]cholesterol liposomes (930 dpm/fmol), and acceptor was 100 pmol of NPC1(NTD)-LVPRGS-His8-FLAG (*G*) or NPC2-His10 (*H*) in the absence (○) or presence (●) of 100

pmol of either NPC2-FLAG (*G*) or NPC1(NTD)-LVPR(*H*). Each value is average of duplicate assays and represents amount of [^{3}H]cholesterol transferred from liposomes to the indicated His-tagged NPC protein. Blank values in absence of His-tagged NPC protein (0.2 to 0.3 pmol) were subtracted.

FIGURE 3-9

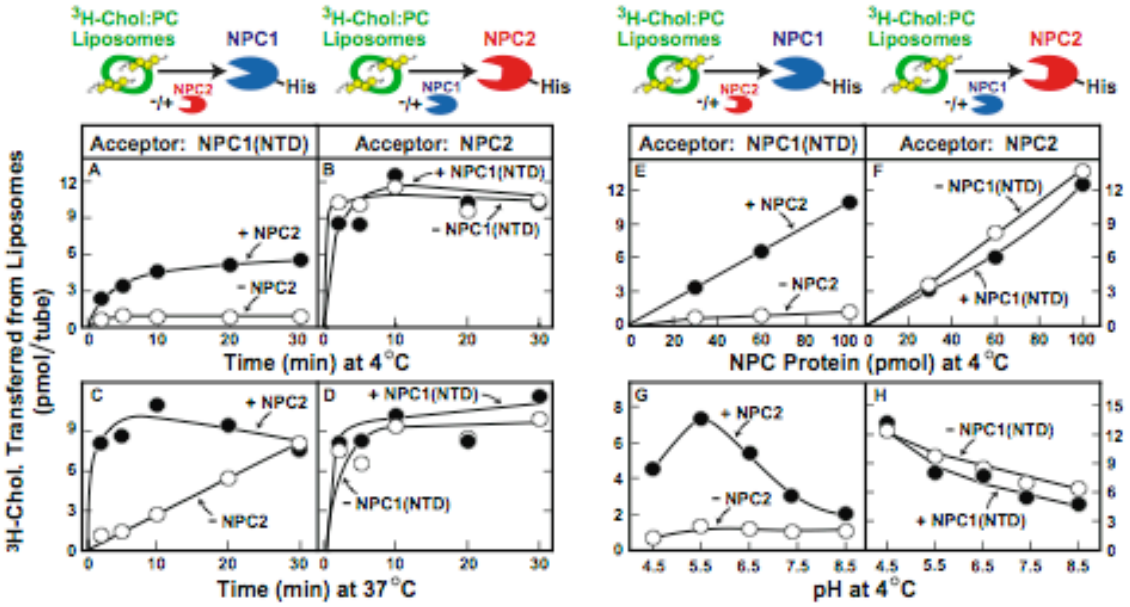

DISCUSSION

The present studies establish conditions for study of the transfer of cholesterol between the water-soluble N-terminal domain of NPC1 and water-soluble NPC2 and between both proteins and liposomes. NPC1 and NPC2 are both required in order for lipoprotein-derived cholesterol to leave late endosomes and lysosomes. Consistent with this common function, NPC2 and NPC1 can both bind cholesterol, the latter in the luminal N-terminal domain (32, 33). Despite these similarities, the cholesterol binding reactions exhibit major differences, as shown in Figure 3-2. NPC2 behaves like a typical receptor. Binding is rapid and reversible at both 4°C and 37°C. NPC1(NTD) behaves quite differently. The protein binds cholesterol extremely slowly at 4°C. The rate of binding is accelerated at least 140-fold at 37°C. Once bound to NPC1(NTD), cholesterol does not dissociate from NPC1(NTD) at 4°C over at least 2 h. At 37°C the dissociation is much faster. Because of these reciprocal changes, the equilibrium dissociation constant for NPC1(NTD) is similar at the two temperatures (50 nM and 90 nM at 4°C and 37°C, respectively).

The above data suggest that the binding site on NPC1(NTD) exists in a relatively closed conformation, although less so at 37°C then at 4°C. Remarkably, this site on NPC1(NTD) can be opened by NPC2. When NPC2 is used as a donor to transfer cholesterol to NPC1(NTD), the transfer is rapid both at 4°C and 37°C (Figure 3-4*B*). Indeed, NPC2 transfers cholesterol to NPC1(NTD) as rapidly as it transfers cholesterol to unoccupied NPC2 molecules. NPC2 can also rapidly remove cholesterol from NPC1(NTD) (Figure 3-4*A* and

C) even under conditions where cholesterol has not dissociated from NPC1(NTD) (Figure 3-2*C*).

Although, the physical basis for the temperature effect on NPC1(NTD) is not yet known, the ability to slow the reaction at 4°C experimentally permits detailed study of the kinetics using the relatively slow bead-trapping assay. In the cell, NPC1 operates at 37°C where it has an intrinsic ability to bind and release cholesterol. However, even at 37°C the binding and release reactions are markedly accelerated by NPC2, suggesting that NPC2 performs this function in the living cell.

Because of its ability to open the binding site on NPC1(NTD), NPC2 facilitates the transfer of cholesterol from NPC1(NTD) to PC liposomes (Figure 3-6) and from liposomes to NPC1(NTD) (Figure 3-9). Genetic evidence for this function of NPC2 was provided by the studies in Figure 3-8 in which a naturally occurring NPC2 mutant (P120S) failed both to bind [^{3}H]cholesterol and to facilitate its transfer from NPC1(NTD) to lysosomes. The precise mechanism for the facilitated transfer reaction cannot be ascertained with the relatively slow bead-trapping assay, which requires several minutes of adherence and washing before the bound [^{3}H]cholesterol can be quantified. It seems likely that the process is catalytic, i.e., NPC2 accepts or donates a cholesterol molecule in a hit-and-run fashion. Consistent with this hypothesis, we were unable to isolate a stable complex between untagged versions of NPC1(NTD) and NPC2 and His-tagged versions of these proteins as determined by nickel agarose chromatography (data not shown).

CONCLUSION AND PERSEPECTIVE

After receptor endocytosis of LDL particles, the cholesterol esters within the particles are hydrolyzed to unesterified cholesterol by acid lipase in the lysosome (7,26). Genetic evidence suggests this cholesterol is transported out of the lysosomes in a NPC1 and NPC2 dependent pathway to serve its structural and regulatory roles in the plasma and ER membranes, respectively (51). Although much has been learned about NPC disease through genetic and cell biology studies, biochemical studies were limited to the soluble protein component, NPC2. This was due to the difficulty of characterizing a membrane protein, such as NPC1. This thesis provides the first biochemical characterization of the membrane protein component of NPC disease, NPC1. These studies also further the biochemical understanding of the other protein component of this disease, NPC2. For the first time, these two proteins are shown to be in a direct interaction involving the movement of cholesterol between NPC1 and membranes.

In Chapter 1, an integral membrane protein that binds [^{3}H]25-HC from rabbit liver was isolated. Mass spectrometry sequenced peptides from this protein and identified NPC1, one of two proteins defective in NPC disease. Through recombinant DNA technology, we purified full-length human NPC1 to confirm that it was indeed a high affinity receptor for oxysterols. It was also demonstrated full-length NPC1 also bound directly to [^{3}H]cholesterol when detergent concentrations were lowered slightly above their CMC. Presumably, this

detergent affect is due to the capacity of the micelles as a second cholesterol receptor in the reaction.

Initially, the focus was the identification of a membrane protein that could bind oxysterols and block the proteolytic activation of SREBPs. During these studies, Radhakrishnan, et al. (2007) demonstrated that the ER membrane protein Insig was the high affinity receptor responsible for the oxysterol effect on SREBP activation. This coupled with the fact oxysterols continue to block SREBP cleavage in NPC deficient cells (Figure 1-9) suggested that NPC1's oxysterol binding does not directly affect SREBP activation.

In Chapter 2, the sterol binding domain was localized to the N-terminus of human NPC1. Recombinant human NPC1(NTD) expressed as a secreted soluble protein, purified as a homodimer on size-exclusion chromatography, and binds one ^{3}H-sterol per dimer. The difference in affinity for cholesterol (Kd, 130nM) and 25-HC (Kd, 10nM) could be attributed to solubility differences of these two ligands. Similar to the full-length version of NPC1, cholesterol binding to NPC1(NTD) was only observed when detergent concentrations were lowered slightly above their CMC. The point mutation Q79A in NPC1(NTD) abolished binding of 25-HC and reduced binding of [^{3}H]cholesterol by 40%. Although the Q79A mutation in full-length NPC1 abolished binding to both ^{3}H-sterols, this difference could be attributed to more detergent associated with the full-length protein.

A major challenge for the future is to define the functional role, if any, of oxysterol binding to NPC1(NTD). Does 25-HC or other oxysterols regulate the activity of NPC1? In cultured fibroblasts, NPC1 is required primarily for transport of LDL-derived cholesterol from its site of liberation in endosomes and lysosomes to its sites of function in the ER and

plasma membrane (51, 42). In humans and animals, NPC1 deficiency leads to accumulation of gangliosides and other lipids in brain (53). The brain converts cholesterol to 24-HC, which is then transported to the liver (5, 69). It is possible that oxysterols such as 24-HC or 25-HC play some role in regulating the transport function of NPC1 in neurons and glial cells.

As yet, oxysterol binding to this NPC1(NTD) site does not seem to be important for the known function of NPC1 in fibroblasts. Thus, in NPC1-deficient cells 25-HC blocks SREBP cleavage (see Chapter 1), accelerates the degradation of 3-hydroxy-3-methlglutyl CoA reductase (data not shown), and activates ACAT in a normal manner (32, 41). Moreover, the Q79A mutant of NPC1, which does not bind ^{3}H-oxysterols *in vitro*, nevertheless restored the ability of cholesterol-carrying β-VLDL to activate ACAT and block SREBP-2 processing in mutant CHO cells that lack NPC1 function (Figure 2-10). It should be noted that these latter studies all involved marked overexpression of the Q79A mutant using a strong CMV promoter and thus could be obscuring a sterol-dependent regulatory role for the NPC1(NTD). Future studies will need to be done in stably transfected cells expressing wild type and mutant NPC1 under control of a weak promoter. Furthermore, the Q79A version of NPC1(NTD) binds [^{3}H]-cholesterol with only a 40% reduction relative to wild-type. If this is physiological, it is understandable that the overexpressed Q79A mutant NPC1 protein restores the ability of β-VLDL to activate ACAT and block SREBP-2 processing in NPC1 deficient cells.

Surprisingly, NPC1(NTD) and NPC2 bind to cholesterol with similar affinity (Kd, 130nM) but only NPC1 bound 25-HC (Figure 2-8). Cross-competition studies suggested that NPC1(NTD) binds the cholesterol molecule on its steroid nucleus side, whereas NPC2 binds

towards the iso-octyl side chain of cholesterol. This explains why a hydroxyl group addition to the iso-octyl side chain, such as 25-HC, disrupts the ability of this molecule to bind to NPC2 but not NPC1.

In Chapter 3, kinetics studies suggest [^{3}H]cholesterol binding to NPC1(NTD) and NPC2 are quite different, although overall affinity is similar. NPC2 behaved like a typical receptor with fast [^{3}H]cholesterol association and dissociation rates, whereas NPC1(NTD) demonstrated relatively slow association and dissociation rates. At 4°C, most of NPC2's bound [^{3}H]cholesterol dissociated within 1 hour, whereas it took over 48 hours for NPC1(NTD) to dissociate a similar percentage (data not shown). The binding pocket on NPC1(NTD) must exist in a relatively closed confirmation relative to NPC2.

Interestingly, NPC2 is able to transfer its [^{3}H]cholesterol to the NPC1(NTD) binding site as quickly as it transfers [^{3}H]cholesterol to itself. Remarkably, NPC2 also facilitates the rapid release of bound [^{3}H]cholesterol from NPC1(NTD) under conditions where cholesterol has not dissociated from NPC1(NTD). NPC2 also facilitated the bidirectional transfer of [^{3}H]cholesterol between lipid bilayers (PC liposomes) and NPC1(NTD). A naturally occurring mutation in NPC2 (P120S) abolished cholesterol binding to NPC2 and diminished its ability to facilitate transfer of [^{3}H]cholesterol between NPC1(NTD) and lipid bilayers. The exact mechanism NPC2 uses to make NPC1(NTD) more permissive in releasing or receiving [^{3}H]cholesterol to and from lipid bilayers remains unclear. Future studies will need to determine the requirement of NPC2's sterol binding domain in this transfer. NPC2 could act as a middleman where it's sterol binding domain is used during the transfer of cholesterol

between NPC1(NTD) and lipid bilayers. It is also conceivable NPC2 interaction with NPC1(NTD) changes its confirmation releasing its cholesterol directly to lipid bilayers.

Within cells, cholesterol egress from lysosomes is unidirectional, i.e., from LDL to lysosomal membranes to ER. To establish this unidirectional flux, NPC1 and NPC2 could act in one of two possible orders, as illustrated in Figure 2. In both models, NPC2 performs a shuttling function with respect to NPC1. In Model A, acid lipase liberates cholesterol which is then bound by NPC2 and delivered to the NTD of NPC1. NPC1 then inserts the cholesterol into lysosomal membranes, from which it is transferred to the ER. In this case membrane insertion is likely mediated by the complex membranous domain of NPC1. In Model B, acid lipase interacts with the membranous domain of NPC1 and releases cholesterol directly to the NTD of NPC1, which then transfers it to NPC2. Given the relative simplicity of NPC2's structure, insertion of cholesterol into the lysosomal membrane, from which it travels to the ER, would likely require NPC2 to interact with a lysosomal cholesterol transporter (a putative NPC3), as yet unidentified. The current *in vitro* data do not permit an experimental distinction between these two models.

FIGURE 2

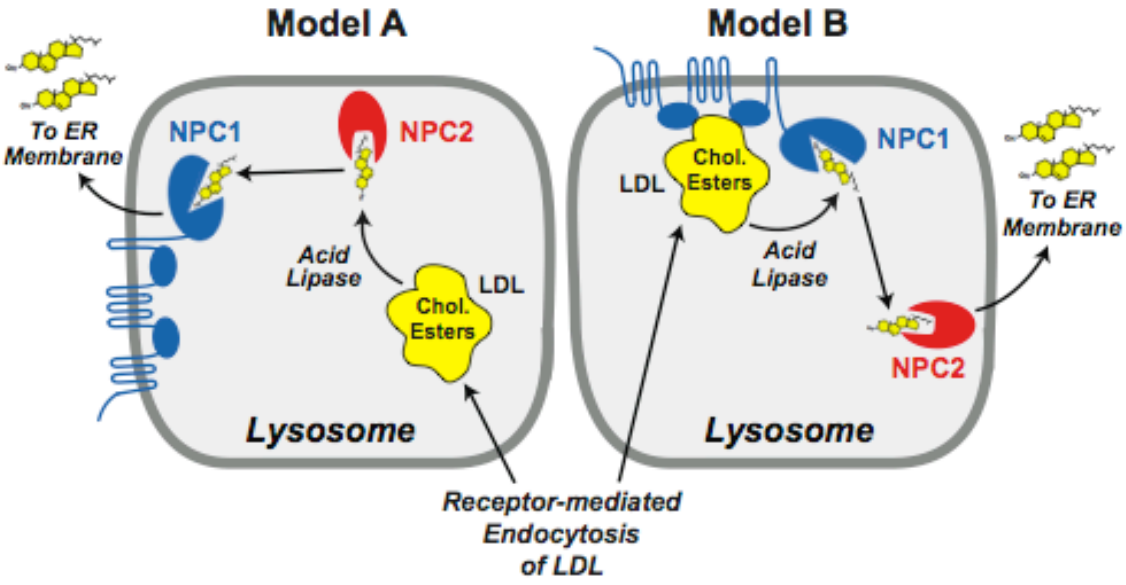

FIGURE 2: Alternative models for the transfer of cholesterol from LDL to lysosomal membranes.

The interpretations of Model A and Model B are explained in Conclusions and Perspective

Another important unanswered question concerns the role of the lysosomal anionic phospholipids such as bis(monooleoylglycerol)phosphate and phosphatidyl inositol that have been reported to accelerate the transfer of cholesterol from NPC2 to liposomes (4, 16). Do either or both of these two lipids influence the rate and/or direction of transfer between the two NPC proteins? Furthermore, once cholesterol is inserted into the limiting membrane of

the lysosome, what proteins or lipids are instrumental for the movement to the plasma membrane or ER. The answers to these questions may be forthcoming now that it is possible to study the cholesterol transfer reactions with soluble forms of both NPC proteins in a test tube.

BIBLIOGRAPHY

1. Adams, C. M., Reitz, J., DeBrabander, J. K., Feramisco, J. D., Brown, M. S., and Goldstein, J. L. (2004) *J. Biol. Chem.* **279,** 52772-52780.

2. Altschul, S. F., Gish, W., Miller, W., Myers, E. W., and Lipman, D. J. (1990) *J. Mol. Biol.* **215**, 403-410.

3. Altschul, S. F., Madden, T. L., Schaffer, A. A., Zhang, J., Zhang, Z., Miller, W., and Lipman, D. J. (1997) *Nucleic Acids Res.* **25**, 3389-3402.

4. Babalola, J.O., Wendeler, M., Breiden, B., Arenz, C., Schwarzmann, G., *et al.* (2007) *Biol Chem* **388**, 617-626.

5. Bjorkhem, I. and Meaney, S. (2004) *Arterioscler. Thromb. Vasc. Biol.* **24,** 806-815.

6. Brady, R. O. (1978) *Annu. Rev. Biochem.* **47,** 687-713.

7. Brown, M. S. and Goldstein, J. L. (1986) *Science* **232,** 34-47.

8. Brown, M. S., Dana, S. E., and Goldstein, J. L. (1975) *J. Biol. Chem.* **250,** 4025-4027.

9. Brown, M. S., Faust, J. R., Goldstein, J. L., Kaneko, I., and Endo, A. (1978) *J. Biol. Chem.* **253,** 1121-1128.

10. Cadigan, K. M., Heider, J. G., and Chang, T.-Y. (1988) *J. Biol. Chem.* **263,** 274-282.

11. Carstea, E. D., Morris, J. A., Coleman, K. G., Loftus, S. K., Zhang, D., Cummings, C., Gu, J., Rosenfeld, M. A., Pavan, W. J., Krizman, D. B., Nagle, J., Polymeropoulos, M. H.,

Sturley, S. L., Ioannou, Y. A., Higgins, M. E., Comly, M., Cooney, A., Brown, A., Kaneski, C. R., Blanchette-Mackie, J., Dwyer, N. K., Neufeld, E. B., Chang, T.-Y., Liscum, L., Strauss, J. F., III, Ohno, K., Zeigler, M., Carmi, R., Sokol, J., Markie, D., O'Neill, R. R., van Diggelen, O. P., Elleder, M., Patterson, M. C., Brady, R. O., Vanier, M. T., Pentchev, P. G., and Tagle, D. A. (1997) *Science* **277,** 228-231.

12. Chalvardjian A, Rudnicki E (1970) *Anal Biochem* **36,** 225-226.

13. Chang, C. C. Y., Huh, H. Y., Cadigan, K. M., and Chang, T. Y. (1993) *J. Biol. Chem.* **268,** 20747-20755.

14. Chen, Y., Kwon, S. W., Kim, S. C., and Zhao, Y. (2005) *J. Proteome Res.* **4,** 998-1005.

15. Chen, Y.-H., Yang, J. T., and Chau, K. H. (1974) *Biochem.* **13,** 3350-3359.

16. Cheruku, S. R., Xu, Z., Dutia, R., Lobel, P., and Storch, J. (2006) *J. Biol. Chem.* **281,** 31594-31604.

17. Chikh, K., Vey, S., Simonot, C., Vanier, M. T., and Millat, G. (2004) *Mol. Gen. Metabol.* **83,** 220-230.

18. Dahl, N. K., Reed, K. L., Daunais, M. S., Faust, J. R., and Liscum, L. (1992) *J. Biol. Chem.* **267,** 4889-4896.

19. Davies, J. P. and Ioannou, Y. A. (2000) *J. Biol. Chem.* **275,** 24367-24374.

20. Dawson, P. A., Ridgway, N. D., Slaughter, C. A., Brown, M. S., and Goldstein, J. L. (1989) *J. Biol. Chem.* **264,** 16798-16803.

21. Dawson, P. A., van der Westhuyzen, D. R., Goldstein, J. L., and Brown, M. S. (1989) *J. Biol. Chem.* **264,** 9046-9052.

22. Fisher, L. E., Engelman, D. M., and Sturgis, J. N. (2003) *Biophys. J.* **85,** 3097-3105.

23. Friedland, N., Liou, H.-L., Lobel, P., and Stock, A. M. (2003) *Proc. Natl. Acad. Sci. USA* **100,** 2512-2517.

24. Frolov, A., Zielinski, S. E., Crowley, J. R., Dudley-Rucker, N., Schaffer, J. E., and Ory, D. S. (2003) *J. Biol. Chem.* **278,** 25517-25525.

25. Gil, G., Faust, J. R., Chin, D. J., Goldstein, J. L., and Brown, M. S. (1985) *Cell* **41,** 249-258.

26. Goldstein JL, Dana SE, Faust JR, Beaudet AL, Brown MS (1975) *J Biol Chem* **250**, 8487-8495.

27. Goldstein, J. L. and Brown, M. S. (2001) *Science* **292,** 1310-1312.

28. Goldstein, J. L., Basu, S. K., and Brown, M. S. (1983) *Meth. Enzymol.* **98,** 241-260.

29. Goldstein, J. L., DeBose-Boyd, R. A., and Brown, M. S. (2006) *Cell* **124,** 35-46.

30. Hua, X., Nohturfft, A., Goldstein, J. L., and Brown, M. S. (1996) *Cell* **87,** 415-426.

31. Hua, X., Sakai, J., Brown, M. S., and Goldstein, J. L. (1996) *J. Biol. Chem.* **271,** 10379-10384.

32. Infante, R.E., Abi-Mosleh, L., Radhakrishnan, A., Dale, J.D., Brown, M.S., *et al.* (2008) *J Biol Chem* **283**, 1052-1063.

33. Infante, R.E., Radhakrishnan, A., Abi-Mosleh, L., Kinch, L.N., Wang, M.L., *et al.* (2008) *J Biol Chem* **283**, 1064-1075.

34. Katoh, K., Kuma, K., Toh, H., and Miyata, T. (2005) *Nucleic Acids Res*. **33**, 511-518.

35. Kita, T., Brown, M. S., and Goldstein, J. L. (1980) *J. Clin. Invest.* **66,** l094-ll00.

36. Ko, D. C., Binkley, J., Sidow, A., and Scott, M. P. (2003) *Proc. Natl. Acad. Sci. USA* **100,** 2518-2525.

37. Kolter, T. and Sandhoff, K. (2006) *Biochim. Biophys. Acta* **1758,** 2057-2079.

38. Kovanen, P. T., Brown, M. S., Basu, S. K., Bilheimer, D. W., and Goldstein, J. L. (1981) *Proc. Natl. Acad. Sci. USA* **78,** l396-l400.

39. Lasch, J., Weissig, V., & Brandl, M. (2003) in *Liposomes: A Practical Approach*, eds. Torchilin, V. & Weissig, V. (Oxford Univ. Press, New York), pp. 3-29.

40. Li AC, Tanaka RD, Callaway K, Fogelman AM, Edwards PA (1988) *J Lipid Res* **29**, 781-796.

41. Liscum, L. and Faust, J. R. (1987) *J. Biol. Chem.* **262,** 17002-17008.

42. Liscum, L. and Sturley, S. L. (2004) *Biochim. Biophys. Acta* **1685,** 22-27.

43. Loftus, S. K., Morris, J. A., Carstea, E. D., Gu, J. Z., Cummings, C., Brown, A., Ellison, J., Ohno, K., Rosenfeld, M. A., Tagle, D. A., Pentchev, P. G., and Pavan, W. J. (1997) *Science* **277,** 232-235.

44. Lowry, O. H., Rosebrough, N. J., Farr, A. L., and Randall, R. J. (1951) *J. Biol. Chem.* **193,** 265-275.

45. Millard, E. E., Gale, S. E., Dudley, N., Zhang, J., Schaffer, J. E., and Ory, D. S. (2005) *J. Biol. Chem.* **280,** 28581-28590.

46. Naureckiene, S., Sleat, D. E., Lackland, H., Fensom, A., Vanier, M. T., Wattiaux, R., Jadot, M., and Lobel, P. (2000) *Science* **290,** 2298-2301.

47. Nohturfft, A., Brown, M. S., and Goldstein, J. L. (1998) *Proc. Natl. Acad. Sci. USA* **95,** 12848-12853.

48. Ohgami, N., Ko, D. C., Thomas, M., Scott, M. P., Chang, C. C. Y., and Chang, T.-Y. (2004) *Proc. Natl. Acad. Sci. USA* **101,** 12473-12478.

49. Okamura, N., Kiuchi, S., Tamba, M., Kashima, T., Hiramoto, S., Baba, T., Dacheux, F., Dacheux, J.-L., Sugita, Y., and Jin, Y.-Z. (1999) *Biochim. Biophys. Acta* **1438,** 377-387.

50. Ouellette, M. M., Aisner, D. L., Savre-Train, I., Wright, W. E., and Shay, J. W. (1999) *Biochem. Biophys. Res. Commun.* **254,** 795-803.

51. Pentchev, P. G. (2004) *Biochim. Biophys. Acta* **1685,** 3-7.

52. Pentchev, P. G., Comly, M. E., Kruth, H. S., Vanier, M. T., Wenger, D. A., Patel, S., and Brady, R. O. (1985) *Proc. Natl. Acad. Sci. USA* **82,** 8247-8251.

53. Pentchev, P. G., Vanier, M. T., Suzuki, K., and Patterson, M. C. (1995) Niemann-Pick disease type C: A cellular cholesterol lipidosis. In Scriver, C. R., Beaudet, A. L., Sly, W.

S., and Valle, D., editors. *The Metabolic and Molecular Basis of Inherited Disease*, McGraw-Hill Inc., New York

54. Radhakrishnan, A., Ikeda, Y., Kwon, H. J., Brown, M. S., and Goldstein, J. L. (2007) *Proc. Natl. Acad. Sci. USA* **104,** 6511-6518.

55. Radhakrishnan, A., Sun, L.-P., Kwon, H. J., Brown, M. S., and Goldstein, J. L. (2004) *Mol. Cell* **15,** 259-268

56. Rawson, R. B., DeBose-Boyd, R. A., Goldstein, J. L., and Brown, M. S. (1999) *J. Biol. Chem.* **274,** 28549-28556.

57. Sakai, J., Nohturfft, A., Cheng, D., Ho, Y. K., Brown, M. S., and Goldstein, J. L. (1997) *J. Biol. Chem.* **272,** 20213-20221.

58. Scott, C. and Ioannou, Y. A. (2004) *Biochim. Biophys. Acta* **1685,** 8-13.

59. Sleat, D. E., Wiseman, J. A., El-Banna, M., Price, S. M., Verot, L., Shen, M. M., Tint, G. S., Vanier, M. T., Walkley, S. U., and Lobel, P. (2004) *Proc. Natl. Acad. Sci. USA* **101,** 5886-5891.

60. Sun, L.-P., Seemann, J., Brown, M. S., and Goldstein, J. L. (2007) *Proc. Natl. Acad. Sci. USA* **104,** 6519-6526.

61. Tinoco, I. and Woody, R. W. (1963) *J. Chem. Phys.* **38,** 1117-1125.

62. van Driel, I. R., Goldstein, J. L., Sudhof, T. C., and Brown, M. S. (1987) *J. Biol. Chem.* **262,** 17443-17449.

63. Vanier, M. T. and Millat, G. (2003) *Clin. Genet.* **64,** 269-281.

64. Verot, L., Chikh, K., Freydiere, E., Honore, R., Vanier, M.T., *et al.* (2007) *Clin Genet* **71**,320-330.

65. Watari, H., Blanchette-Mackie, E. J., Dwyer, N. K., Watari, M., Neufeld, E. B., Patel, S., Pentchev, P. G., and Strauss III, J. F. (1999) *J. Biol. Chem.* **274,** 21861-21866.

66. Willnow, T. E. and Herz, J. (1994) *J. Cell Sci.* **107,** 719-726.

67. Wood, L. D., Halvorsen, T. L., Dhar, S., Baur, J. A., Pandita, R. K., Wright, W. E., Hande, M. P., Calaf, G., Hei, T. K., Levine, F., Shay, J. W., Wang, J. J. Y., and Pandita, T. K. (2001) *Oncogene* **20,** 278-288.

68. Xie, C., Burns, D. K., Turley, S. D., and Dietschy, J. M. (2000) *J. Neuropathol. Exp. Neurol.* **59,** 1106-1117.

69. Xie, C., Lund, E. G., Turley, S. D., Russell, D. W., and Dietschy, J. M. (2003) *J. Lipid Res.* **44,** 1780-1789.

70. Xu, S., Benoff, B., Liou, H.-L., Lobel, P., and Stock, A. M. (2007) *J. Biol. Chem.* **282,** 23525-23531.